GEORGIA INSTITUTE OF TECHNOLOGY OFFICE OF CONTRACT ADMINISTRATION

PROJECT ADMINISTRATION DATA SHEET

[X] ORIGINAL [ ] REVISION NO. _____

Project No./(Center No.) E-25-623 (R6327-0A0) GTRC/~~GIT~~ DATE 6 / 17 /87

Project Director: D. McDowell School/~~Lab~~ ME

Sponsor: Martin Marietta Energy Systems, Inc.

Oak Ridge

Agreement No.: Subcontract No. 19X-SA631C

Award Period: From 6/1/87 To 9/30/87 (Performance) 9/30/87 Reports

Sponsor Amount:	New With This Change	Total to Date
Contract Value: $		$ 23,000
Funded: $		$ 23,000

Cost Sharing No./(Center No.) _____ Cost Sharing: $ _____

Title: Creep Dominated, Anisotropic Continuum Damage

ADMINISTRATIVE DATA OCA Contact John B. Schonk x4-4820

1) Sponsor Technical Contact:

2) Sponsor Issuing Office:

F.H. Hopper
Subcontract Administrator
Martin Marietta Energy Systems
P.O. Box M
Oak Ridge, TN 37831
615/576-0251

Military Security Classification: _____
(or) Company/Industrial Proprietary: _____

ONR Resident Rep. is ACO: _____ Yes X No
Defense Priority Rating: DPAS

RESTRICTIONS

See Attached _____ Supplemental Information Sheet for Additional Requirements.

Travel: Foreign travel must have prior approval — Contact OCA in each case. Domestic travel requires sponsor approval where total will exceed greater of $500 or 125% of approved proposal budget category.

Equipment: Title vests with Tech if under $5,000 and prior approval is obtained.

COMMENTS:

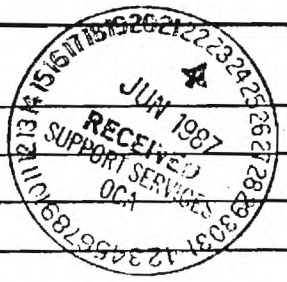

SPONSOR'S I.D. NO. 02.240.001.87.R04

COPIES TO:

Project Director
Research Administrative Network
Research Property Management
Accounting
Procurement/GTRI Supply Services
Research Security Services
Contract Support Div.(OCA)(2) Pat
Research Communications
GTRC
Library
Project File
Other _____

EORGIA INSTITUTE OF TECHNOLOGY OFFICE OF CONTRACT ADMINISTRATION

SPONSORED PROJECT TERMINATION/CLOSEOUT SHEET

SRP993
2-X-B
N-X-B

Date 1/27/88

oject No. E-25-623 School/~~Lab~~ ME

cludes Subproject No.(s) N/A

oject Director(s) D. L. McDowell GTRC / ~~GIT~~

onsor Oak Ridge National Lab Martin Marietta

tle Further Developments in Creep-Dominated, ~~Anisotripic~~ Anisotropic Continuum Damage Theory

fective Completion Date: 9/30/87 (Performance) 9/30/87 (Reports)

ant/Contract Closeout Actions Remaining:

- [ ] None
- [x] Final Invoice or Final Fiscal Report
- [x] Closing Documents
- [x] Final Report of Inventions Questionaire sent to P. I.
- [x] Govt. Property Inventory & Related Certificate
- [ ] Classified Material Certificate
- [ ] Other

ntinues Project No. Continued by Project No.

PIES TO:

oject Director
search Administrative Network
search Property Management
counting
ocurement/GTRI Supply Services
search ~~Security~~ Services
ports Coordinator (OCA)
gal Services

Library
GTRC
Research Communications (2)
Project File Duane Hutchison
Other Angela DuBose
Russ Embry

RM OCA 69.285

AUGUST 13, 1987

PROGRESS REPORT

Subcontract No. 19X-SA631C
Georgia Tech # E-25-623

Submitted to

MARTIN MARIETTA ENERGY SYSTEMS, INC.
Technical Contact: Dr. J. Blass

CREEP-DOMINATED, ANISOTROPIC CONTINUUM DAMAGE

D.L. McDowell
Principal Investigator
George W. Woodruff School of Mechanical Engineering
Georgia Institute of Technology
Atlanta, GA 30332

AUGUST 13, 1987

PROGRESS REPORT

Subcontract No. 19X-SA631C
Georgia Tech # E-25-623

Submitted to

MARTIN MARIETTA ENERGY SYSTEMS, INC.
Technical Contact: Dr. J. Blass

CREEP-DOMINATED, ANISOTROPIC CONTINUUM DAMAGE

D.L. McDowell
Principal Investigator
George W. Woodruff School of Mechanical Engineering
Georgia Institute of Technology
Atlanta, GA 30332

INTRODUCTION

The problem of high temperature creep damage in initially isotropic, polycrystalline metals has received considerable attention. Fundamentally, two distinct approaches have emerged which seek to address the evolution of damage at different size scales. The first approach, traditionally encompassing time-fraction rules and remaining life curves is directed toward description of creep-rupture phenomena under variable stress loading histories. The second approach, the "micromechanical" treatment, seeks to derive expressions for nucleation and/or growth of voids on grain boundaries with suitable prescription of rupture criteria.

This work is concerned with a continuum approach for modeling of physical grain boundary damage under multiaxial, nonproportional, creep-dominated loading histories. Such histories necessitate description of the anisotropic nature of creep damage accumulation since the rupture time is greatly affected by damage anisotropy. In this work, a general framework for continuum creep damage evolution is presented which extends the work of Murakami and Ohno [1-2], Trampczynski et al. [3-4], and Leckie and Onat [5-6].

A basic model for anisotropic creep damage has been developed with support from Martin Marietta subcontracts 19B-07802C and 19X-55966C and grants from the U.S. National Science Foundation. The goals of this funding period are to build on this prior work to include more sophistication and generality in the model, in addition to "exercising" the model with correlation of the nonproportional creep damage response of a more highly anisotropically damaging material.

In this progress report, a more refined version of the anisotropic creep damage model is presented. This latest version includes the specification of an even rank tensor of arbitrary magnitude to model the actual creep damage distribution, alternate definitions for the damage effect tensor, an algorithm for efficient

computation of the mean value of damage on the unit sphere, and incorporation of the retardation effect of compressive biaxial principal stress ratios directly in a modified form of an isochronous stress definition originally attributed to Huddleston [19]. The relationship of the current framework to other major continuum damage approaches, including both substantial and perhaps subtle differences, is developed to a greater extent than previously done. Correlations are presented for several nonproportional creep-dominated loading histories for copper at 250°C in addition to type 304 stainless steel at 593°C; hence, the work statement requirements regarding correlations for copper have been completed. Other tasks are underway. Comments are made regarding progress in incorporating the following effects into the current anisotropic continuum damage approach:

(a) aging effects,
(b) framework for interaction between fatigue damage and creep damage, and
(c) more general cavity growth mechanisms.

CREEP DAMAGE GROWTH LAW

In this work, we adopt the notion that a spatial distribution of grain boundary cavitation and triple-point cracking may be represented as a continuum quantity. Since creep damage is a bulk phenomenon, such a description is quite reasonable as confirmed by results of homogenization theory [7]. Precedental works of Kachanov [8] and Rabotnov [9] are noted among many others.

In the approach taken by Murakami and Ohno [1-2], a symmetric second rank damage rate tensor was assumed. This results, of course, in a second rank tensor damage distribution regardless of the nonproportionality of the applied loading

history. Experiments conducted by Trampczynski, Hayhurst and Leckie [3-4], however, reveal that the creep damage distribution for some materials is highly dependent on principal stress orientation; a second rank tensor representation of physical damage is inadequate. Krajcinovic [10-11] suggests that the directional distribution of physical damage is most appropriately modeled as a dual vector; such a vector can represent, for example, the discontinuity in loading/unloading stiffness exhibited by cracked brittle materials by virtue of crack closure. Leckie and Onat [5-6] suggest stronger conditions, based on damaged material symmetry arguments, which require that a vectorial distribution of damage on the unit sphere be even with respect to $\underset{\sim}{n}$, i.e.

$$\omega(\underset{\sim}{n}) = \omega(-\underset{\sim}{n}) \tag{1}$$

where $\underset{\sim}{n}$ is a unit vector normal to the unit sphere and $\omega(\underset{\sim}{n})$ is the distribution of damage. If the damage is manifested as an array of cracks, for example, ω may be defined as the area fraction of cracks associated with crack face unit normal vector $\underset{\sim}{n}$ [12]. Leckie and Onat have shown that $\omega(\underset{\sim}{n})$ may be represented by an expansion of even rank symmetric tensors.

In this work, we adopt the symmetry arguments of Leckie and Onat. For grain boundary creep damage, we assume that the orientation and magnitude of damage is defined by the unit normal vector and damaged area fraction of each grain boundary facet, i.e.

$$\omega(\underset{\sim}{n}) = \frac{1}{S_g(\underset{\sim}{n})} \int_V dS_{gd}(\underset{\sim}{n}) \tag{2}$$

where $S_g(\underset{\sim}{n})$ is the total grain boundary facet area in volume V with unit normal vector $\underset{\sim}{n}$, and $dS_{gd}(\underset{\sim}{n})$ is the differential damaged grain boundary facet area

associated with unit vector $\underset{\sim}{n}$. The form given in equation (2) permits experimental estimation of $\omega(\underset{\sim}{n})$ from macroscopically homogeneously deformed specimens; for a continuum representation, we may think of the volume of integration as passing to an infinitesimal, i.e. $V \to \delta V$.

Following the development of Leckie and Onat [5-6], we may define the damage distribution $\omega(\underset{\sim}{n})$ in terms of a set $\underset{\sim}{\Gamma}$ of even rank, irreducible tensors obtained from the distribution of damage on the unit sphere. The effect of the current state of damage on damage rate is introduced via stress intensification associated with loss of load bearing area by defect formation and distribution, defect stress concentration, and defect interaction. Effective stress $\underset{\sim}{S}$ may be expressed as a second rank tensor function of Cauchy stress $\underset{\sim}{\sigma}$ and a fourth rank operator $\underset{\sim}{M}(\underset{\sim}{\Gamma})$, i.e.

$$\underset{\sim}{S} = \hat{\underset{\sim}{S}}(\underset{\sim}{M}(\underset{\sim}{\Gamma}), \underset{\sim}{\sigma}) \tag{3}$$

Regarding practical application of such an approach, we may select a "minimal" set $\underset{\sim}{\Gamma}$ based on acceptable approximation of the damage accumulation processes and the rupture criterion. For proportional loading, $\underset{\sim}{\Gamma}$ of rank two may be a sufficient approximation for anisotropic material damage. For nonproportional loading, however, the appropriate rank of $\underset{\sim}{\Gamma}$ depends on both the nonproportionality of the loading history and the nature of the damage distribution.

In this work, we make the simplifying assumption that the principal axes of the Cauchy stress and effective stress coincide, which may be true for proportional loading even up to large cavity volume fractions. However, for nonproportional loading such an assumption suggests a limitation to relatively small cavity volume fractions to ensure that the

rotation of the effective stress with respect to the Cauchy stress is suitably small. With this assumption we may express $\underset{\sim}{M}$ in the principal stress coordinate frame as

$$M_{ijkl}(\underset{\sim}{\Gamma}) = \phi_{ij}(\underset{\sim}{\Gamma})\ \delta_{ik}\delta_{jl} \quad \text{(no sum on i and j)} \tag{4}$$

with

$$\underset{\sim}{\phi} = \sum_{j=1}^{3} \Omega^{(j)}\ \underset{\sim}{n}^{(j)} \otimes \underset{\sim}{n}^{(j)} \tag{5}$$

where $\underset{\sim}{\phi}$ is the damage effect tensor with principal components $\Omega^{(j)}$ and eigenvectors $\underset{\sim}{n}^{(j)}$ collinear with those of $\underset{\sim}{\sigma}$. We do not attempt herein to make a direct connection between the definition of $\underset{\sim}{\phi}$ and loss of cross-sectional area in the Cauchy tetrahedron as do Murakami and Ohno [1-2], recognizing that the actual damage distribution is not in general represented by a second rank tensor; rather, $\underset{\sim}{\phi}$ is viewed as an approximation of the intensification effect of grain boundary damage on the current principal stresses and hence influences damage rate.

In this work, we consider only infinitesimal strains and small rotations. Furthermore, the cavity volume fraction is assumed small so that the assumption of equivalence of the principal coordinate frames for effective and Cauchy stresses may be approximately made. Such an assumption is not as physically restrictive as it might seem in view of the typically small cavity volume fraction up to the rupture event. This does not imply that the damage distribution is isotropic, but that the damage rate is tensorially dictated by the current principal directions of $\underset{\sim}{\sigma}$. This results in an anisotropic damage distribution for proportional or nonproportional loading. Density changes associated with damage are neglected, although they may be included as discussed by Chaboche [13]. Isothermal conditions are assumed. We define the growth rate of ω as a function of $\underset{\sim}{\phi}$ and $\underset{\sim}{\sigma}$ in the following simple way:

$$\dot{\omega}(\underset{\sim}{n}) = \xi(\sigma^*) \left[\eta\, \chi^{(1)} \left\{\Omega^{(1)}\right\}^{l(\sigma^*)} + \right. \tag{6}$$

$$\left. (1-\eta) \sum_{j=1}^{3} \chi^{(j)} \left\{\Omega^{(j)}\right\}^{l(\sigma^*)} \left\{ \underset{\sim}{n} \cdot \underset{\sim}{n}^{(j)} \otimes \underset{\sim}{n}^{(j)} \cdot \underset{\sim}{n} \right\} \left\{ \underset{\sim}{n} \cdot \underset{\sim}{n}^{(j)} \right\}^{2P} \right]$$

$$= \dot{\omega}(\underset{\sim}{n})_{\text{isotropic}} + \dot{\omega}(\underset{\sim}{n})_{\text{anisotropic}}$$

which corresponds to the magnitude in direction $\underset{\sim}{n}$ (obtained by 2(P+1) contractions with $\underset{\sim}{n}$) of the symmetric, anisotropic damage rate tensor $\dot{\underset{\sim}{\Gamma}}$ of rank 2(P+1), i.e.

$$\dot{\underset{\sim}{\Gamma}} = \xi(\sigma^*) \left[\eta\, \chi^{(1)} \left\{\Omega^{(1)}\right\}^{l(\sigma^*)} \overset{P+1}{\underset{i=1}{\otimes}} \underset{\sim}{I} + \right. \tag{7}$$

$$\left. (1-\eta) \sum_{j=1}^{3} \chi^{(j)} \left\{\Omega^{(j)}\right\}^{l(\sigma^*)} \overset{2(P+1)}{\underset{i=1}{\otimes}} \left\{\underset{\sim}{n}^{(j)}\right\} \right]$$

where ξ and l are functions of the isochronous stress σ^* (surface of constant rupture time), $\underset{\sim}{n}^{(j)}$ is the unit vector in the j^{th} principal stress direction, σ_j, $\underset{\sim}{n}^{(j)} \cdot \underset{\sim}{n} = n_k(j) n_k$, P is an integer representative of the order of the anisotropic damage distribution, and η is the fraction of damage rate in the $\underset{\sim}{n}^{(1)}$ direction which is isotropic; η is bounded by $0 \leq \eta \leq 1$ and may also be a function of σ^* as discussed later. The value of P is either zero or a positive integer. $\underset{\sim}{I}$ is the identity tensor. The $\Omega^{(j)}$ are the principal components of the damage effect tensor $\underset{\sim}{\phi}$. Factor $\chi^{(j)}$ excludes contribution of compressive principal stresses to the damage rate, i.e.

$$\chi^{(j)} = \langle \underset{\sim}{n}^{(j)} \cdot \frac{\underset{\sim}{\sigma}}{|\sigma_j|} \cdot \underset{\sim}{n}^{(j)} \rangle \qquad (8)$$

where σ_j are the ordered principal stresses with $\sigma_1 \geq \sigma_2 \geq \sigma_3$, and the Macauley bracket $\langle F \rangle = F$ if $F > 0$; $\langle F \rangle = 0$ otherwise. The scalar product of two second rank tensors $\underset{\sim}{A}$ and $\underset{\sim}{C}$ is defined by $(\underset{\sim}{A}:\underset{\sim}{C}) = (A_{ij}C_{ji})^{1/2}$, and the outer product is denoted by $\otimes$; outer products repeated multipicatively (P+1) and 2(P+1) times are inferred by the summation on $\otimes$ in equation (7).

Several forms may be proposed for $\Omega^{(j)}$. One possibility is that the anisotropic damage rate in principal stress direction $\underset{\sim}{n}^{(j)}$ depends only on the extent of damage in that direction, $w(\underset{\sim}{n}^{(j)})$, i.e.

$$\Omega^{(j)} = \frac{1}{1 - w(\underset{\sim}{n}^{(j)})} \qquad (9)$$

which is a direct anisotropic generalization of the Kachanov-Rabotnov damage approach [14]. Another possibility is that the anisotropic damage rate in the $\underset{\sim}{n}^{(j)}$ direction also depends on η. Such dependence would introduce a significant departure from the spirit of equation (9) only if η is a function of σ^*. We may choose to allow $\Omega^{(j)}$ to depend on $\eta w(\underset{\sim}{n}^{(j)})$, recognizing that this quantity provides a lower bound on the damage oriented orthogonal to the $\underset{\sim}{n}^{(j)}$ direction. A simple way to introduce nonlinear dependence on η is by defining a symmetric, second rank tensor $\underset{\sim}{\zeta}^{(j)}$ defined uniquely by each $w(\underset{\sim}{n}^{(j)})$, in analogy to the definition proposed by Murakami and Ohno [1], as

$$\underset{\sim}{\zeta}^{(j)} = [\ \underset{\sim}{I} - \underset{\sim}{\Pi}(\underset{\sim}{n}^{(j)})\ ]^{-1} \qquad (10)$$

where $\underset{\sim}{\Pi}$ is defined by

$$\underset{\sim}{\Pi}(\underset{\sim}{n}^{(j)}) = \omega(\underset{\sim}{n}^{(j)}) \; [\eta + (1 - \eta) \; \underset{\sim}{n}^{(j)} \otimes \underset{\sim}{n}^{(j)}] \tag{11}$$

The $\underset{\sim}{\phi}$ components in this case are expressed as $\Omega^{(j)} = (\underset{\sim}{\varsigma}^{(j)} : \underset{\sim}{\varsigma}^{(j)})^{1/2}$, i.e.

$$\Omega^{(j)} = \left[\frac{1}{(1 - \omega(\underset{\sim}{n}^{(j)}))^2} + \frac{2}{(1 - \eta\omega(\underset{\sim}{n}^{(j)}))^2} \right]^{1/2} \tag{12}$$

Essentially, this equation assumes that the stress intensification effect associated with each of the damage values $\omega(\underset{\sim}{n}^{(j)})$ is represented by a symmetric, second rank tensor defined by $\omega(\underset{\sim}{n}^{(j)})$, but dependent on η. The scalar multiplier $\Omega^{(j)}$ directly affects evolution of the ω distribution, as seen in equation (6). It should be noted that for isotropic hardening, the damage rate equation assumes the classical Kachanov-Rabotnov form. It is assumed in equation (6) that the evolution of the isotropic component of the ω distribution is dictated by the effect of the damage in the tensile principal stress directions; the isotropic component of damage exists because of constraints between contiguous grains which are affected by relative orientation, extent of grain boundary sliding, etc. As reflected in the isochronous stress, the dilatational and distortional stress invariants affect the rate of creep damage accumulation in addition to the tensile principal stresses.

It is necessary to introduce a specific definition for the isochronous stress. As discussed by Hayhurst et al. [3-4] and Lemaitre and Chaboche [15-18], the isochronous stress is a level surface in stress space denoting equivalent rupture times; it is a function of the maximum principal stress, the second invariant of deviatoric stress, and the

hydrostatic stress. Based on the rather extensive experimental work of Huddleston [19], who considered several materials and various biaxiality ratios, the isochronous stress is defined as

$$\sigma^* = \frac{3}{2} S_1 \left(\frac{2}{3} \frac{\sigma_e}{S_1} \right)^a \exp\left[b\{1 + f(J_1)\langle -J_1/|J_1|\rangle\}\left(\frac{J_1}{S_s} - 1\right) \right] \tag{13}$$

where

$$S_1 = \sigma_1 - \frac{1}{3} \sigma_{kk} \tag{14}$$

$$\sigma_e = \left[(3/2)\underset{\sim}{s} : \underset{\sim}{s} \right]^{1/2} \tag{15}$$

$$\underset{\sim}{s} = \underset{\sim}{\sigma} - \frac{1}{3} \sigma_{kk} \underset{\sim}{I} \tag{16}$$

$$S_s = \left[\sigma_1^2 + \sigma_2^2 + \sigma_3^2 \right]^{1/2} \tag{17}$$

$$J_1 = \sigma_{kk} \tag{18}$$

It should be noted that this form of the isochronous stress is a slightly altered form of that proposed by Huddleston. Very little data were available in the biaxial regime with an in-plane compressive principal stress of greater magnitude than the tensile stress, i.e. a negative J_1. The approach offered by Huddleston is hence modified by inclusion of the term $(1+f(J_1)\langle -J_1/|J_1|\rangle)$, which must be experimentally determined. Further discussion of this term appears in a later section.

This form of the isochronous stress has been rather thoroughly supported by a variety of biaxial creep experiments on tubular specimens of type 304 stainless steel at 593°C at ORNL, including axial tension, equi-biaxial tension (axial

tension and pressure), internal pressure, torsion, axial tension and torsion, and axial compression and torsion. It should be noted that this form of σ^* was verified for loading magnitudes which would be expected to lead to matrix power law creep governed grain boundary damage accumulation.

It is important to examine the role of exponent P in governing the anisotropy of the damage distribution. P = 0 only if the actual damage distribution $\omega(\underset{\sim}{n})$ takes the form of a symmetric second rank tensor. This is approximately the case for type 304 stainless steel at 593°C as will be discussed later. For an isotropically damaging material with $\eta = 1$, the second term in equations (6)-(7) does not apply since the anisotropic component of the damage rate is zero. The results of Trampczynski et al. [3-4] for copper indicate a high degree of anisotropy, and hence a larger value of P.

Obviously, the integrated damage distribution $\omega(\underset{\sim}{n})$ will depend on whether the loading history is proportional or nonproportional. Rotation of the principal stress eigenvectors will in general result in multiple "peaks" in the damage distribution with respect to a fixed material coordinate system. From a practical viewpoint, depending on the rank of the tensorial damage distribution, it may be desirable to express the distribution either precisely in terms of tensor components or approximately in terms of ω values at a discrete number of points on the unit sphere. In the latter case, an interpolation algorithm may be necessary to estimate the ω value in any arbitrary direction. The former representation is desirable for second and perhaps even fourth rank damage tensors, while the latter would seem the only practical route for distributions of higher rank.

Omission of the functional dependence of 1 on σ^* in equations (6)-(7) would imply that time fraction and damage (for proportional loading) are uniquely related, which does not allow description of multiple isochronous stress level sequence effects (nonlinear damage accumulation) [16-18] if the rupture criterion

is stress-independent. In this paper, we will be concerned with correlation of experiments performed at constant isochronous stress and hence do not require explicit stress level-dependence of l, but such dependence offers no particular difficulty. In fact, it was included in the final report under 1986 subcontract 19X-55966C. This dependence is physically necessitated by the stress level-dependence of cavity growth mechanisms as reflected in void growth mechanisms maps [20-22], and is supported by experiments cited by Chaboche et al. [16-17] in which the measured damage growth is retarded as a function of time fraction t/t_R as the isochronous stress level increases. The deleterious effects of low-high stress level sequences and the accumulation of greater creep damage under low stress than high stress conditions at the same time fraction are well-documented [23]. In view of the stress-dependence of cavity growth mechanisms (c.f. [20-22]) and the associated differences in void aspect ratios and constraints in regimes of diffusion-dominated versus matrix power law creep-dominated void growth, it may be necessary to admit dependence of the anisotropy of the damage distribution on stress, i.e. $P = P(\sigma^*)$ and $\eta = \eta(\sigma^*)$.

If the microstructure is unstable and aging effects such as precipitation or coarsening exist, it is necessary to include these effects via description of precipitation/coarsening kinetics. The function $\xi(\sigma^*)$ in equations (6)-(7) is based on the assumption of a fixed number of void nucleation sites and a stable microstructure. As discussed by Leckie and Onat [5-6], a separate evolution equation may be introduced for void nucleation rate. Certainly, void nucleation rate may be associated with intersections of slip bands with grain boundaries and with the precipitation of grain boundary carbides, so that inelastic rate of deformation and diffusion kinetics must both be considered. In this study, we will present correlation with isothermal creep histories at only a constant isochronous stress level for each material such that aging effects are implicitly embedded in

the constants and parameters of the evolution equations for damage and creep deformation. For histories involving significant changes in isochronous stress or temperature, consideration must be given to explicit state variables representing, for example, precipitate size and spacing. Aging is potentially an important consideration for predicting long term rupture performance based on short term tests, and is considered in further detail later in this report.

Another key element of the damage formulation is the rupture criterion. Previous discussion has assumed that ω_{max} = constant at rupture. It is clear from previous work [5-6,23] that the extent of creep damage just prior to the final rupture event depends on stress level. If a stress level-dependent rupture criteria is adopted, then the damage at rupture is not constant and the time fraction at any given damage level, even for constant l, depends on the isochronous stress for proportional loading. A stress level-dependent rupture criterion is more difficult to implement since experimental investigation of the damage distribution at different stress levels is quite involved. Existing data are somewhat sketchy and incomplete. The logical approximation to the physically more precise stress level-dependent rupture criterion is the first approach, i.e. the assumption of a constant damage at failure. This approximation is most likely suitable, even for variable load histories, since the damage growth is highly nonlinear only near the final rupture event. Therefore, from a practical viewpoint, the use of a constant damage at rupture is likely to be sufficient, especially in view of the inherent scatter in creep rupture tests. Hence, the rupture criterion

$$\omega_{max} = \max_{\text{all } \underset{\sim}{n}} \omega(\underset{\sim}{n}) = 1 \tag{19}$$

is selected in this work. It should be noted, however, that the definition of

damage offered in equation (2) in conjunction with equation (19) does not imply that the area fraction of cavitated grain boundaries is unity at rupture; the area fraction of cavitated segments normal to $\underset{\sim}{n}$ is unity. For a highly anisotropically damaging material, the total area fraction of cavitated grain boundaries may be quite low. It can be shown, for example, that the area fraction of damaged grain boundary segments upon satisfaction of equation (19) for uniaxial loading is expressed as the mean value of $\omega(\underset{\sim}{n})$ over the unit sphere as

$$f_h = \frac{2(P + 1)\eta + 1}{2P + 3} \tag{20}$$

For example, for $\eta = 0$ and $P = 1$ ($\underset{\sim}{\Gamma}$ of rank four), $f_h = 0.2$ at rupture. If the damage is isotropic, $\eta = 1$ and $f_h = 1$ at rupture. If $\underset{\sim}{\Gamma}$ is second rank, $P = 0$ and $f_h = (2\eta + 1)/3$, i.e. the hydrostatic component of $\underset{\sim}{\Gamma}$.

Finally, it should be noted that under conditions of finite strain, the damage distribution must evolve in reference to a material coordinate frame, necessitating an appropriate finite strain formulation [1-2,13] and consideration of material density changes [13,24].

CORRELATION WITH NONPROPORTIONAL CREEP HISTORIES

It is necessary to implement the foregoing damage formulation in a viscoplastic constitutive framework of desired sophistication and accuracy. In this section, we will first discuss the selected form of the coupling with a rather general viscoplastic model framework. Then we will specialize to unified creep-plasticity and power-law creep constitutive laws for comparison of high temperature, nonproportional creep rupture experiments conducted on type 304 stainless steel and

pure copper, respectively. The level of anisotropy of creep damage in these two materials is markedly different.

The constitutive model for rate-dependent deviatoric inelasticity must be coupled with the damage distribution just presented. An isothermal framework for achieving this coupling for small cavity volume fractions is as follows:

viscoplastic flow rule:
$$\dot{\underset{\sim}{\epsilon}}^{n} = f(\underset{\sim}{s}D,\ \underset{\sim}{\alpha}D,\ \kappa) \tag{21}$$

hardening rules:

kinematic:
$$\dot{\underset{\sim}{\alpha}}D = H_{\alpha}(\underset{\sim}{s}D,\ \underset{\sim}{\alpha}D,\ K^{*})\ ||\dot{\underset{\sim}{\epsilon}}^{n}||\ \underset{\sim}{\nu} - R_{\alpha}(\underset{\sim}{\alpha}D)\ \underset{\sim}{\alpha}D \tag{22}$$

isotropic:
$$\dot{\kappa} = G_{\kappa}(\underset{\sim}{s}D,\ \underset{\sim}{\alpha}D,\ \kappa)\ ||\dot{\underset{\sim}{\epsilon}}^{n}|| - R_{\kappa}(\kappa) \tag{23}$$

$$\dot{K}^{*} = G_{R^{*}}(\underset{\sim}{s}D,\ \underset{\sim}{\alpha}D,\ K^{*})\ ||\dot{\underset{\sim}{\epsilon}}^{n}|| - R_{K^{*}}(K^{*}) \tag{24}$$

Here deviatoric stress $\underset{\sim}{s} = \underset{\sim}{\sigma} - (\sigma_{kk}/3)\underset{\sim}{I}$, and backstress $\underset{\sim}{\alpha}$ is deviatoric. The inelastic strain $\underset{\sim}{\epsilon}^{n}$ includes both conventional creep and plastic strain as in other unified theories. The backstress reflects, in a general sense, directional internal stress fields associated with dislocation entanglements at both thermal and athermal barriers. Scalar state variables K^{*} and κ introduce strain hardening/softening effects in the backstress evolution and flow rules, respectively. Equations (21)-(24) include a hardening/recovery format typical of existing unified creep-plasticity approaches (c.f. [25-32]). Additionally, the directional index $\underset{\sim}{\nu}$ may be selected to correspond to a hardening/dynamic recovery format in the first term for $\dot{\underset{\sim}{\alpha}}$, as shown by Rousellier and Chaboche [33-34].

Note that the effect of damage is reflected by a multiplicative factor D and the product $\underset{\sim}{s}D$, for example, can be thought of as an effective stress for the viscoplastic deformation. As stated by Leckie [5-6] and viewed herein as a

tentative approximation, experiments show that the influence of the damage tensor on the creep rate is isotropic and monotonically increasing, even into the tertiary regime. This has been demonstrated even for materials which damage in a highly anisotropic manner [6]. In detailed experiments on intentionally perforated specimens, Murakami [2] has shown that the influence of cavity volume fraction on stress-strain response is isotropic for cavity fractions up to a few percent, a typical range for engineering alloys up to rupture. These results, of course, are necessary to admit scalar D to couple damage with the deformation response; obviously, D must be related to the mean value of the ω distribution, i.e.

$$D = \hat{D}(\Psi) \tag{25}$$

where Ψ is defined by

$$\Psi = \frac{1}{4\pi} \int_{A_u} \omega(\underset{\sim}{n})\, dA \tag{26}$$

Note that the effect of damage on the tertiary creep rate will remain unaltered upon rotation of the principal stress axes with this formulation as is experimentally observed [3-6].

A very useful recursion formula may be derived (see Appendix) by considering the mean value over the unit sphere of the damage rate distribution, i.e.

$$\dot{\Psi} = \eta\, \dot{\omega}(\underset{\sim}{n}^{(1)}) + \sum_{j=1}^{3} \frac{1}{(2P+3)} \left[\dot{\omega}(\underset{\sim}{n}^{(j)}) - \eta\, \dot{\omega}(\underset{\sim}{n}^{(1)}) \right] \tag{27}$$

with the initial (undamaged) condition $\Psi(0) = 0$, where

$$\dot{\omega}(\underset{\sim}{n}^{(j)}) = \xi(\sigma^*) \left[\eta \, \chi^{(1)} \left\{ \Omega^{(1)} \right\}^{l(\sigma^*)} + (1-\eta) \, \chi^{(j)} \left\{ \Omega^{(j)} \right\}^{l(\sigma^*)} \right] \qquad (28)$$

In the more general case of larger cavity volume fractions [2], we must define an appropriate effective stress $\underset{\sim}{S}^c$ derived from an operation of a fourth rank tensor $\underset{\sim}{I}(\underset{\sim}{\phi})$ on the applied stress

$$\underset{\sim}{S}^c = \frac{1}{2} \left\{ \underset{\sim}{I} : \underset{\sim}{\sigma} + (\underset{\sim}{I} : \underset{\sim}{\sigma})^T \right\} \qquad (29)$$

where $\underset{\sim}{I}(\underset{\sim}{\phi})$ may be expressed in terms of $\underset{\sim}{\phi}$ and its scalar invariants vis-à-vis the representation theorem for isotropic tensor functions [35]; the constants in this representation may be selected to fit experimental results. In addition, an effective backstress $\underset{\sim}{\alpha}^c$ must be analogously defined through a fourth rank tensor transformation; such a representation would obviously be quite complex, providing strong impetus for the aforementioned assumption of the isotropy of the damage effect on creep deformation. As pointed out by Chaboche, inclusion of damage in the viscoplastic potential would result in an additional damage coefficient which leads to volumetric inelastic strain. It should be noted that $\underset{\sim}{S}^c$ and $\underset{\sim}{\alpha}^c$ would replace $D\underset{\sim}{s}$ and $D\underset{\sim}{\alpha}$ in equations (21)-(24) in the case of large cavity fractions.

It should be mentioned that the elastic compliance is also affected by the presence of creep damage, although an explicit form for this dependence is not presented in this work. Let T be absolute temperature. Assuming the Helmholtz free energy density can be decomposed into elastic and viscous components [11,13],

$$\psi = \psi^e(\underset{\sim}{\epsilon}^e, \underset{\sim}{\Gamma}, T) + \psi^v(\underset{\sim}{\alpha}, \kappa, K^*, \underset{\sim}{\Gamma}, T) \qquad (30)$$

along with $\underset{\sim}{\epsilon} = \underset{\sim}{\epsilon}^{e} + \underset{\sim}{\epsilon}^{n}$ leads to the thermoelastic relation

$$\underset{\sim}{\sigma} = \rho \frac{\partial \psi}{\partial \underset{\sim}{\epsilon}^{e}} \tag{31}$$

which obviously depends on the damage distribution through $\underset{\sim}{\Gamma}$.

The coupling of damage with two significantly different viscoplastic formulations is discussed next.

A. Rate-Dependent Bounding Surface Formulation: Type 304 Stainless Steel at 593°C

For the sake of completeness, experiments conducted at ORNL during the last contract period are again reported, along with the correlations of the anisotropic continuum damage theory.

For multiaxial cyclic plasticity, it has previously been demonstrated that a bounding surface approach [36-41] provides very good correlation of nonproportional deformation behavior. Since such behavior is of concern to nonproportional cyclic histories, a recently introduced [42] strain-hardening model based on a rate-dependent bounding surface with a Mroz translation rule for backstress is adopted. Key features of this theory include isotropic hardening reflected through growth of the bounding surface rather than a scalar parameter in the flow rule, and rate-dependence of the backstress evolution even at high strain rates. These features contrast with conventional unified creep-plasticity models (c.f. [25-32]). Rate-dependence is reflected primarily through bounding surface dependence on overstress, strain-hardening is reflected through growth of the bounding surface, and smooth yielding response is obtained through use of the Mroz distance vector in

the backstress hardening rate coefficient.

Briefly, the damage-coupled bounding surface model can be stated in multiaxial form as

$$\dot{\underset{\sim}{\epsilon}}^{n} = \frac{3}{2} K \langle \bar{\sigma} D - K_o \rangle^{n} \exp(Z \langle \bar{\sigma} D - K_o \rangle^{n+1}) \ (\underset{\sim}{s} - \underset{\sim}{\alpha})/\bar{\sigma} \tag{32}$$

where

$$\bar{\sigma} = [(3/2)(\underset{\sim}{s} - \underset{\sim}{\alpha}):(\underset{\sim}{s} - \underset{\sim}{\alpha})]^{1/2} = \sqrt{3/2} \ ||\underset{\sim}{s} - \underset{\sim}{\alpha}|| \tag{33}$$

$$\bar{\alpha} = [(3/2) \ \underset{\sim}{\alpha} : \underset{\sim}{\alpha}]^{1/2} \tag{34}$$

Here deviatoric stress $\underset{\sim}{s} = \underset{\sim}{\sigma} - (\sigma_{kk}/3)\underset{\sim}{I}$, backstress $\underset{\sim}{\alpha}$ is deviatoric, and we have defined $\kappa = K_o$ = constant. The inelastic strain $\underset{\sim}{\epsilon}^{n}$ includes both conventional creep and plastic strain as in other unified theories. The effective overstress and backstress are denoted as $\bar{\sigma}$ and $\bar{\alpha}$, respectively. The exponential term was proposed by Nouailhas [43] for description of high strain rate events.

The competition between hardening and static thermal recovery terms in the backstress rate equation is introduced in this bounding surface formulation in the following way:

$$\dot{\underset{\sim}{\alpha}} D = H(\bar{\alpha} D, \delta) ||\dot{\underset{\sim}{\epsilon}}^{n}|| \underset{\sim}{\nu} - R(\bar{\alpha} D) \underset{\sim}{\alpha} D \tag{35}$$

where

$$H(\bar{\alpha} D, \delta) = \beta_o + \beta_1 \exp(-\beta_4 \langle 1 - \beta_3 \left(\frac{\delta}{R^*}\right) \rangle^{\beta_5}) + \beta_2 \exp(-\beta_6 \bar{\alpha}^* D) \tag{36}$$

$$\delta = \sqrt{3/2} \ || \ \sqrt{2/3} \ R^* \underset{\sim}{N} - \underset{\sim}{s}|| \quad , \quad \underset{\sim}{N} = (\underset{\sim}{s} - \underset{\sim}{\alpha})/||\underset{\sim}{s} - \underset{\sim}{\alpha}|| \tag{37}$$

$$\bar{\alpha}^* = (R^* - \delta - \bar{\sigma}) \tag{38}$$

$$R(\bar{\alpha}D) = \beta_7 \exp(-\beta_8 \bar{\alpha}D) \ (\bar{\alpha}D)^{\beta_9} \tag{39}$$

It should be noted that in this particular formulation with the bounding surface fixed at the origin, the restriction $\delta > 0$ is enforced at a constant strain rate to avoid contact of the stress point with the bounding surface. This is achieved by driving the exponential term effectively to zero at a non-zero δ/R^* ratio. If the bounding surface were allowed to translate, this restriction would not apply; such a generalization is currently being carried out.

The specific form for $D(\Psi)$ selected for this model is

$$D(\Psi) = 1 + C \ \Psi^m \tag{40}$$

The radius of the bounding surface, R^*, evolves with accumulated plastic strain (creep hardening) and responds through the effective overstress to changes in inelastic strain rate to reflect the rate-dependence of the asymptotic state of $\underset{\sim}{\alpha}$, i.e.

$$R^* = \beta_{10} \ \rho \ [1 + \beta_{12} \ \bar{\sigma}^{\beta_{13}}] \tag{41}$$

where

$$\dot{\rho} = \beta_{11} \ (\rho_{mf} - \rho) \ \sqrt{2/3} \ ||\dot{\underset{\sim}{\epsilon}}^n|| \tag{42}$$

with initial condition $\rho(0) = \rho_0$. As seen in equation (41), this formulation clearly exhibits both viscous overstress and backstress effects, motivated by experiments which reveal a rate-dependent dislocation structures even at high strain rates.

The directional index for the backstress hardening rate is a rate-dependent

Mroz form

$$\underset{\sim}{\nu} = \left[\frac{\sqrt{2/3}\, R^{*}\, \underset{\sim}{N} - \underset{\sim}{s}}{\sqrt{2/3}\, \delta} \right] \tag{43}$$

The bounding surface and the surface of constant dimension K_o which prescribes elastic response are shown in Fig. 1 along with the vector $\underset{\sim}{\nu}$ in deviatoric stress space. It should be noted that the damage effect D is applied to R^* in addition to tensorial stress quantities since R^* is related to the saturated or asymptotic value of stress [44].

In this formulation, $K, K_o, Z, n, C, m, \beta_o, \beta_1, \beta_2, \beta_3, \beta_4, \beta_5, \beta_6, \beta_7, \beta_8, \beta_9, \beta_{10}, \beta_{11}, \beta_{12}, \beta_{13}$, and ρ_{mf} are isothermal material constants. Non-isothermal generalization can be achieved primarily by invoking temperature dependence of the backstress recovery term [28] and some of the constants, although this is not necessary in the current isothermal work. Note that K_o does not evolve, resulting in a domination of the inelastic response by evolution of the backstress. This feature allows the overstress tensor to properly model inelastic strain rate direction for rapidly changing nonproportional loading directions or for a departure from a previous loading path for which steady state creep conditions were reached as discussed by McDowell [42] and Lowe and Miller [45-46].

The hardening function which governs smooth transition from a very "stiff" region of backstress rate to an asymptotic response is the second term in equation (36) where the Mroz distance vector is normalized by bounding surface radius. Constants $\beta_1, \beta_4, \beta_5$, and β_3 govern this transition and are selected to match a monotonic, strain-controlled uniaxial test at a single strain rate in addition to a cyclic, strain-controlled uniaxial test at a single strain rate. The cyclic test is used primarily to determine β_3, which ensures that the normalization will be

satisfactory for both monotonic and cyclic behavior. Constant β_0 describes asymptotic response and constants β_2 and β_6 are employed in a second-order term to model the backstress level dependence of hardening rate observed experimentally when hardening dominates recovery. Constants ρ_{mf} and β_{11} introduce strain hardening into the model and can be determined either from a uniaxial monotonic or cyclic test. Constants β_{10},β_{12}, and β_{13} are determined from flow stress/strain rate sensitivity data at the temperature of interest; since strain rate sensitivity of R^* is directly related to that of stress in this model, these constants can be determined in a straightforward manner after the constants in the flow rule have been defined to fit a range of desired (observed) backstress behavior obtained from "dip" tests, multiaxial creep or cyclic plasticity experiments involving a sudden change in inelastic strain rate direction, etc. Constants C and m are determined by matching the integrated inelastic strain rate behavior with tertiary creep data.

It should be noted that this rate-dependent bounding surface work can be further generalized by inclusion of translation of the bounding surface. Work in progress at Georgia Tech has revealed the advantages of doing so.

Interrupted creep tests are generally necessary to assess exponent l at a given isochronous stress level; l can also be determined in an approximate way by periodically unloading from the creep curve [15-18] or by matching the integrated damage-coupled creep equations (32)-(43) with observed onset of tertiary response assuming m = 1 in equation (40). The value m = 1 arises from the Murakami study [2] mentioned earlier. Stress exponent k is easily identified as the slope of the $\log(t_R)$ vs. $\log(\sigma)$ curve obtained from uniaxial tests. Isotropic damage fraction η is identified as the ratio of the transverse damage to the longitudinal damage in a uniaxial test, and is identified by quantitative metallographic techniques described elsewhere [42].

At the isochronous stress level of this study, cavity growth is governed by

matrix power law creep. Hence, we define

$$\xi(\sigma^*) = B \left[\sigma^* \right]^k \tag{44}$$

Once k is known, coefficent B can be found at the isochronous stress level associated with l by integrating and matching rupture times from uniaxial tests with the assumed rupture criterion $\omega_{max} = 1$.

Tension-torsion tests were conducted at ORNL on thin-walled tubular specimens of type 304 stainless steel (ORNL Ref. heat 9T2796) at 593°C. The specimens were annealed in argon at 1093°C for 30 minutes, and were subsequently air cooled at >100°C/min to room temperature. Refer to Huddleston [19] for further experimental details.

For an isochronous stress of 176.1 MPa at 593°C, the constants are $B = 2.71 \times 10^{-28}$ sec^{-1} and l = 4.8. Units of stress and damage rate are MPa and sec^{-1}, respectively. Constants independent of isochronous stress include k = 8.5551 and $\eta = 0.61$. Quantitative evaluation of the grain boundary damage distribution for these biaxial experiments revealed that the damage distribution is suitably described by a second rank tensor [42] which sets P = 0. Exponent l was estimated by matching the tertiary response of uniaxial tests with the integrated damage-coupled creep equations.

The details may be found elsewhere [42] regarding the determination of the constants for the rate-dependent bounding surface model for type 304 stainless steel at room temperature. In summary, the material constants at 593°C for the damage-coupled creep-plasticity model are:

$K = 5 \times 10^{-48}$	$\beta_5 = 1.25$	$\beta_{12} = 0.225$
$K_o = 13.8$	$\beta_6 = 0.0196$	$\beta_{13} = 1.91$
$n = 30$	$\beta_7 = 1.552 \times 10^{-19}$	$\rho_{mf} = 517$
$\beta_o = 1104$	$\beta_8 = -0.0207$	$\rho_o = 145$
$\beta_1 = 6.9 \times 10^6$	$\beta_9 = 5.088$	$C = 0.32$
$\beta_2 = 1044$	$\beta_{10} = 0.00361$	$m = 1$
$\beta_3 = 1.18$	$\beta_{11} = 7.0$	$Z = 0$
$\beta_4 = 23.16$		

where the units of stress are in MPa and time in sec.

The coordinate system employed for the stress analysis of the tubular specimens is shown in Fig. 2. Model predictions and experimental data for three different biaxial creep experiments are shown in Figs. 3-5. In these figures, inelastic axial and tensorial shear strain components are plotted versus time in addition to the axial and shear stress history. It is noted that the rupture time is generally well-predicted as is the inelastic strain upon initial loading and subsequent secondary and tertiary creep rates. The inelastic strain and rupture behavior is well-predicted for proportionally loaded specimen GT-1. The rupture time for specimen GT-4A is somewhat overpredicted for a simple nonproportional loading history, though the strain at rupture and the tertiary character are in reasonable agreement. The correlation obtained for GT-6, a somewhat complex creep-dominated cyclic loading history, is quite good. In all these experiments, the isochronous stress was held constant at 176.15 MPa and the principal stress directions were rotated at some point(s) in the loading history as shown in the figures.

B. Simple Power Law Creep: Pure Copper at 250°C

Trampczynski et al. [3-4] have conducted nonproportional loading experiments on commercially pure copper thin-walled tubular specimens at 250°C and have found in this case that damage is highly anisotropic, i.e. $\eta \simeq 0$. Both by metallurgical examination and by comparison of rupture times with uniaxial and proportional specimens at the same isochronous stress level, they concluded that damage accumulation in copper could be treated as highly decoupled with respect to several discrete loading directions in a nonproportional sequence history. It should be noted that Murakami and Ohno have applied their second rank tensor model to this data set as an approximation, although the physical damage distribution in this case is not accurately represented by a second rank tensor.

The grain boundary metallographs [3] indicate that the appropriate representation of grain boundary cracking at rupture in these specimens is fully anisotropic, $\eta = 0$, and that the deviation of damaged cavity facet normals about the maximum principal stress direction(s) is extremely small, i.e. $P > 0$. Since the maximum principal stress governs the fully anisotropic damage response in this case, $a = b = 0$ in the general isochronous stress form, i.e.

$$\sigma^* = \frac{3}{2} S_1 \tag{45}$$

For axial torsional loading of a thin-walled tube, $\sigma^* = \sigma_1$. The anisotropic damage rate equation may be written in this case as

$$\dot{\omega}(\underset{\sim}{n}) = \xi(\sigma^*) \sum_{j=1}^{3} \left\{\Omega^{(j)}\right\}^{l(\sigma^*)} \chi^{(j)} \left\{ \underset{\sim}{n}\cdot\underset{\sim}{n}^{(j)} \otimes \underset{\sim}{n}^{(j)}\cdot\underset{\sim}{n} \right\} \left\{ \underset{\sim}{n}\cdot\underset{\sim}{n}^{(j)} \right\}^{2P} \tag{46}$$

where again the cavity growth is dominated by matrix power law creep,

so that $\xi(\sigma^*)$ is defined as in equation (44). Since only one principal stress is tensile for this particular biaxial loading configuration,

$$\dot{\omega}(\underset{\sim}{n}) = B\ (\sigma_1)^k \left\{\Omega^{(1)}\right\}^{l(\sigma^*)} \chi^{(1)} \left\{ \underset{\sim}{n}\cdot\underset{\sim}{n}^{(1)} \otimes \underset{\sim}{n}^{(1)}\cdot\underset{\sim}{n} \right\} \left\{ \underset{\sim}{n}\cdot\underset{\sim}{n}^{(1)} \right\}^{2P} \tag{47}$$

$$\underset{\approx}{\zeta}^{(1)} = \left\{ \underset{\sim}{I} - \underset{\sim}{n}^{(1)} \otimes \underset{\sim}{n}^{(1)}\ \omega(\underset{\sim}{n}^{(1)}) \right\}^{-1} \tag{48}$$

$$\Omega^{(1)} = \left[\underset{\approx}{\zeta}^{(1)} : \underset{\approx}{\zeta}^{(1)} \right]^{1/2} = \left[\left[\frac{1}{1 - \omega(\underset{\sim}{n}^{(1)})} \right]^2 + 2 \right]^{1/2} \tag{49}$$

For copper, we choose to consider a less sophisticated constitutive model for the creep deformation. The coupling with damage for power law creep is given by

$$\dot{\underset{\sim}{\epsilon}}^n = \frac{3}{2} \left[\frac{\sigma_e D}{A} \right]^n \frac{\underset{\sim}{s}}{\sigma_e} \tag{50}$$

where D in this case is selected as

$$D = \left[1 + C\ \Psi^m\right]^{1/n} \tag{51}$$

although the form given earlier could also be used.

From Trampczynski et al. [3], n = 6.95. From Murakami and Ohno [1] and Trampczynski [3], k = 5.52 and l = 5.6. At the isochronous stress level to be considered in this study, a mean rupture time of 315 hours is expected for uniaxial creep conditions at 250°C. The constants A = 195, B = 1.913×10^{-14}, C = 3.0, and m = 6.0 were selected to provide the best fit to the secondary and tertiary response of the nonproportional biaxial history shown in Fig. 6 with the additional constraint that t_R = 315 hours for any proportional tension-torsion loading path. It should be noted that the units of stress and time are MPa and hours,

respectively, for the above set of constants. In this sense, the general shape of the tertiary response achieved by the theory shown in Fig. 6 is not truly predicted, although the rupture time is.

The value of P was selected as a significantly large integer to result in significant decoupling of the bimodal peaks of the damage distribution resulting from an occasional $33.7^{\bullet}$ rotation of the applied maximum principal stress as discussed by Trampczynski et al. [3]. As P increases, the damage distribution assumes a more highly anisotropic, directional character; as a consequence, the predicted rupture life increases for nonproportional loading histories. In the experiments on copper conducted by Trampczynski et al. [3], two maximum principal stress orientations were alternatively enforced at an angle of $\pm 16.87^{\bullet}$ from the tube longitudinal direction. Hence, the tensile principal stress was periodically rotated within the plane of the specimen wall via change of the sign of the applied torque, though the principal stress magnitude was held fixed at 46.8 MPa.

In this work P = 6 was selected to ensure little interaction of the damage accumulated in the two directions, as physically observed. The experimental and theoretical results are compared in Figs. 6-7 for two nonproportional loading histories. In these plots, the engineering creep shear strain is plotted rather than the tensorial creep shear strain. Note the correlation offered by the theory, which exhibits the same general trends as the second rank tensor approach of Murakami and Ohno [1-2]. In these figures, the inelastic strain upon initial loading and the primary strain during the first loading event are eliminated from the presentation of the experimental data since the power law creep equation does not consider these components. No attempt was made, however, to eliminate the transient inelastic strains which occur at each subsequent loading reversal. This accounts for much of the error in creep strain evident in Fig. 7 for the complex loading history. This disagreement would not exist with an appropriately

sophisticated inelastic strain rate law, such as the one offered in the previous section. The life is reasonably well-correlated for both histories.

C. Compressive Biaxial Stress Ratios: Type 304 Stainless Steel at 593°C

Experiments were conducted at ORNL in 1986 in association with subcontract 19X-55966C in which a significant biaxial compressive stress ratio was present during all or part of the total rupture life of the thin-walled tubular specimens. The retardation of the creep damage rate associated with this type of loading was originally accounted for by multiplying the damage rate by the ratio of the maximum principal stress to minumum principal stress [42]. Such an approach, however, was not particularly meaningful from a physical viewpoint. It is desirable instead to include the effect through dependence of the isochronous stress σ^* on J_1 as described in equation (13). Huddleston's original formulation for σ^* was based on scant data in the negative J_1 regime. We show here that only a slight perturbation of his original formulation is necessary in the compressive biaxial stress ratio regime to acceptably describe the behavior of type 304 stainless steel at 593°C.

Using Huddleston's data [19] for a compressive biaxial stress ratio of -1.15 and the results of a proportional, constant load creep experiment performed under subcontract 19X-55966C (specimen GT-9) with a compressive biaxial stress ratio of -2.62 and a rupture time of 2952 hours, we can determine the constants in a power law expression

$$f(J_1) = C_1 \langle -J_1 \rangle^{C_2} \tag{52}$$

by integrating the preceding damage rate formulation and matching the rupture times of these two experiments (with $\dot{J}_1$ = constant). This results in the values C_1 =

0.00434 and C_2 = 0.635. To see the influence of this modification on Huddleston's original formulation, a plot of both formulations appear for the same isochronous stress level, normalized to the uniaxial case, in Fig. 8. Note that the Rankine criterion is also plotted for reference. Clearly, the two formulations are nearly indistinguishable in the plot, even in the third quadrant, although they predict significantly different rupture times for negative J_1.

OTHER WORK IN PROGRESS

(A) Aging Effects:

If the microstructure is unstable and aging effects such as precipitation or coarsening exist, it may be necessary to include these effects via description of precipitation/coarsening kinetics. This is true particularly for variable stress and/or temperature loading histories for which aging effects cannot be implicitly embedded in a set of isothermal, isostress material constants. Type 304 stainless steel exhibits aging in the form of precipitation and growth of $M_{23}C_6$ carbides on grain boundaries, which may serve as void nucleation sites. Data regarding aging phenomena and associated effects on rupture life are often quite conflicting, however, with significant variability depending on heat treatment, processing, etc. Furthermore, little quantitative information exists regarding the mechanics representation of aging.

The function $\xi(\sigma^*)$ in equations (6)-(7) is based on the assumption of a fixed number of void nucleation sites and a stable microstructure. As discussed by Leckie and Onat [5], a separate evolution equation may be introduced for void nucleation rate. The nucleation rate may be dependent on inelastic strain rate.

Certainly, the void nucleation rate may be associated with intersections of slip bands with grain boundaries and with the precipitation of grain boundary carbides, so that inelastic rate of deformation and diffusion kinetics must both be considered.

Aging effects may be incorportated by adopting formulation which employs time-dependent coefficients in the damage rate and inelastic strain rate equations, as motivated by the work of Cho and Findley [47-48]. In their work, the various inelastic strain components were made to depend on power law functions of aging time. Such an approach is phenomenologically based and may achieve acceptable correlation for variable stress and temperature histories. It may be desirable from a micromechanical viewpoint, however, to incorporate aging effects via evolution of a state variable or a set of state variables which represent physically distinct mechanisms. Mean precipitate size and spacing, for example, are logical candidate state variables for systems which exhibit unstable precipitation.

Obviously, aging is a diffusion-dependent phenomenon and should follow an Arrhenius dependence on absolute temperature. However, the nature of the possible coupling between aging rate and inelastic deformation, when such coupling exists, is not well-defined. The following framework is tentatively suggested for incorporation of aging effects in the damage rate equation:

$$\dot{\underset{\sim}{\Gamma}} = \xi(\sigma^*, \varsigma_i) \left[\eta \, \chi^{(1)} \left\{ \Omega^{(1)} \right\}^{l(\sigma^*)} \bigotimes_{i=1}^{P+1} \underset{\sim}{I} + (1-\eta) \sum_{j=1}^{3} \chi^{(j)} \left\{ \Omega^{(j)} \right\}^{l(\sigma^*)} \bigotimes_{i=1}^{2(P+1)} \left\{ \underset{\sim}{n}^{(j)} \right\} \right] \tag{53}$$

where ς_i for $i = 1,2,\ldots,M_\varsigma$ is a set of aging variables with rates specified by

$$\dot{\varsigma}_i = A_i \left[\bar{\varsigma}_i - \varsigma_i \right] \exp(-Q_i/kT) \qquad (54)$$

$\bar{\varsigma}_i$ is the potential value of ς_i reached at long times, Q_i is the activation energy for the growth process of the i^{th} variable, k is Boltzmann's constant, and T is absolute temperature.

This type of approach collapses to that proposed by Cho and Findley if a single state variable is employed, i.e. $M_\varsigma = 1$, and the influence of ς on damage rate coefficent ξ is multiplicative, i.e.

$$\xi(\sigma^*,\varsigma) = \hat{\xi}(\sigma^*) \{-\ln[(\bar{\varsigma} - \varsigma)/(\bar{\varsigma} - \varsigma_0)]A_i^{-1}\exp(Q_i/kT)\}^{N_\varsigma} \qquad (55)$$

where ς_0 is the initial value of ς and N_ς is a power law exponent. The reader may show by integration of equation (54) that the quantity within the curly brackets in equation (55) is merely time. Hence, equation (55) is a power law accountance for aging time. The purpose of writing it in the manner shown is to introduce an illustrative case where the state variable and aging time approaches are equivalent.

A simple form of the state variable approach or even the power law dependence on aging time in equation (55) should be sufficient for most alloys of interest, at least across a relatively small range of operating stresses and temperatures.

(B) Framework for Creep-Fatigue Interaction:

Numerous creep-fatigue approaches have been offered in the literature. Almost all of these approaches focus on uniaxial loading or treat multiaxial creep-fatigue damage as isotropic. In this work, we have generalized a continuum creep damage model for the case of multiaxial nonproportional loading. Though multiaxial fatigue formulations exist for proportional loading [49-50], no well-accepted theory exists for nonproportional loading. Hence, we can couch the interaction between creep and fatigue (and environment if necessary) at several different levels of sophistication.

The first approach is to use a uniaxial form of a fatigue damage rate equation. Lemaitre, Chaboche and associates have contributed significantly to the development of continuum fatigue damage approaches (c.f. [51), but we do not feel that fatigue damage is aptly modeled as a continuum quantity. Rather, it is typified by a non-uniform distribution of microcracks even in uniaxial loading. For the relatively ductile class of materials generally considered for high temperature applications in the power generation industry, e.g. type 304 stainless steel, the damage rate approach proposed by Majumdar and Maiya [52] is very appealing. Since it is a rate approach, it is a logical companion for the continuum creep damage approach already presented. Following Majumdar and Maiya, the creep damage-coupled microcrack growth rate can be expressed as

$$\frac{1}{a}\frac{da}{dt} = \left[\begin{array}{c} T \\ C \end{array}\right] (1 + \alpha \ln(\Psi/\Psi_o)) \, (\bar{\epsilon}_a^n)^{Z_1} \, ||\dot{\underset{\sim}{\epsilon}}^n||^{Z_2} \qquad (56)$$

where Ψ is defined in equation (26) and

a = current microcrack length

$\bar{\epsilon}_a^n$ = effective inelastic strain amplitude

T, C are coefficients for tensile and compressive stress, respectively, and

T, C, z_1, z_2 and α are temperature, environment, and microstructural dependent material parameters.

The quantity Ψ_o is a threshold limit for the mean value of creep damage for interaction with fatigue damage to occur. Essentially, this formulation implies that voids nucleating and growing ahead of a propagating fatigue microcrack will accelerate the growth via coalescence ahead of the crack tip. Failure is defined either by equation (19) in creep or by attainment of a critical crack length, whichever occurs first. Note that the fatigue damage does not influence the creep damage rate, since creep damage is a bulk phenomenon in contrast to fatigue damage.

This approach has been successfully applied to creep-fatigue lifetime prediction of the austenitic stainless steels [52] and Cr-Mo-V steels [53].

Further work should address the incorporation of multiaxial fatigue effects into the damage rate approach, at least for proportional cyclic loading. Though certain stress- and strain-based dependencies of fatigue life can be expressed for the multiaxial nonproportional loading case, the framing of a thoroughly general, accurate approach must await the completion of significantly more experimental work.

(C) More General Cavity Growth Mechanisms:

It is in general desirable to generalize the creep damage rate equation (6) to conform to the relevant operative mechanisms for cavity growth at a given temperature and isochronous stress level. For example, cavity growth mechanism

maps have been constructed for some materials (c.f. [21] to delineate this temperature and stress dependence. At stresses typical of applications but lower than those usually employed in laboratory experiments, for example, it may be necessary to account for coupled grain boundary diffusion-power law creep [20-22] mechanisms. For this study, however, the isochronous stress level selected is within the domain of power law creep. Hence, a power law dependence of damage growth rate on isochronous stress appears in equation (44).

There are fundamentally two distinct approaches for accounting for stress- and temperature-dependent cavity growth mechanisms. Let us discuss here an isothermal case only, in keeping with the format of the theory already presented. In the first approach, one may refer to a cavity growth mechanism map to determine which regime is applicable, then adjust the parameters in $\xi(\sigma^*)$ and the functional form of $\Omega^{(j)}$ to phenomenologically account for the influence of cavity growth mechanism on damage rate and, hence, rupture time. The work of Cocks and Ashby [22] serves as a useful guide for perhaps a more micromechanically-based approach for generalization to other cavity growth regimes. In their work, the actual form of the dependence on the stress and current level of damage depends on the operative cavity growth mechanism. Furthermore, they compare the approach with that of a Kachanov continuum damage model, thereby establishing a means of incorporation of their ideas in the current framework when creep damage is predominately in the form of voids. Discussion of these comparisons can be found in reports written under Martin Marietta subcontracts 19B-07802C and 19X-55966C. The application of specific forms in the context of the present model is one of the goals of the current work statement.

Drawing from the work of Raj, Ashby and Cocks, it may be possible to generalize predominately uniaxial, isotropic concepts of void nucleation and growth rates in terms of the present anisotropic model.

It should also be mentioned that there are some materials for which dislocation debris arrangement and attendant voids in the vicinity of barriers are associated with creep rupture [54] rather than classical void growth. For such materials, it may be necessary to tie the creep damage rate more intimately to cumulative creep deformation rather than cavity growth associated with normal stresses. In this case, according to Leckie [50], it may be desirable to interpret the damage variable or tensor in terms of the immobile dislocation density at barriers rather than an area fraction of voids on grain boundaries. It is likely that such creep damage mechanisms would require dependence on the inelastic strain, rather than isochronous stress, and perhaps the details of the stress state.

CONCLUSIONS

The work during the current funding period is serving to further enhance the anisotropic creep damage approach developed in earlier contract work. A damage distribution with even symmetry has been introduced on the unit sphere which evolves in rate form as a symmetric tensor of rank necessary to match physically measured damage distributions. The approach is motivated by the treatment of even rank tensor distributions forwarded by Leckie and Onat [5-6], and contains as a subset the specific tensorial definitions of damage adopted in the anisotropic theories of Chaboche (rank four) [13,18,24] and Murakami and Ohno [1-2] (rank two).

A general form of coupling with damage has been suggested for an internal variable inelasticity framework and specific forms have been investigated for type 304 stainless steel at 593°C and pure copper at 250°C with the assumption of small cavity volume fractions. Good correlation of rupture time, secondary creep, and tertiary creep has been obtained for proportional and nonproportional, isothermal, constant isochronous nominal stress loading histories for both mildly and highly

anisotropically creep damaging materials. A recursion formula has been derived for the evolution of the mean value of damage on the unit sphere which offers computational simplification. A modification of Huddleston's isochronous stress has been introduced for more accurate correlation of compressive biaxial principal stress ratios.

Work in progress regarding aging effects, creep-fatigue interaction, and more general cavity growth laws has also been discussed.

REFERENCES

1. Murakami, S., and Ohno, N., "A Continuum Theory of Creep and Creep Damage," Creep in Structures, IUTAM, 1980, pp. 422-444 (Eds. Ponter and Hayhurst).
2. Murakami, S., "Notion of Continuum Damage Mechanics and its Application to Anisotropic Creep Damage Theory," ASME J. of Engineering Materials and Technology, Vol. 105, April 1983, pp. 99-105.
3. Trampczynski, W. A., Hayhurst, D.R., and Leckie, F.A., "Creep Rupture of Copper and Aluminum Under Non-Proportional Loading," J. Mech. Phys. Solids, Vol. 29, No. 5/6, 1981, pp. 353-374.
4. Trampczynski, W. A., and Hayhurst, D.R., "Creep Deformation and Rupture Under Non-Proportional Loading," Creep in Structures, IUTAM, Eds. Ponter and Hayhurst, 1980, pp. 388-405.
5. Leckie, F. A., and Onat, E. T., "Tensorial Nature of Damage Measuring Internal Variables," Physical Non-Linearities in Structural Analysis, IUTAM, 1980, pp. 140-155 (Eds. Hult and Lemaitre).
6. Leckie, F. A., "The Constitutive Equations for High Temperatures and Their Relationship to Design," Proc. Int. Conf. on Constitutive Laws for Engineering Materials, Eds. Desai and Gallagher, Univ. of Arizona, Tucson, Jan. 1983, p. 93.
7. Duvaut, C., "Analyse Fonctionnelle - Mèchanique des Milieu Continus-Homogènèisation", Theoretical and Applied Mechanics, North-Holland, Amsterdam, 1976.
8. Kachanov, L., Fundamental of Fracture Mechanics, Nauka, Moscow, 1974.
9. Rabotnov, Y. N., Creep Problems in Structural Members, Amsterdam, North Holland Publishing Co., 1969.
10. Krajcinovic, D., "Creep of Structures - A Continuous Damage Mechanics Approach," J. Structural Mechanics, 11(1), 1983, pp. 1-11.
11. Krajcinovic, D., and Fonseka, G.U., "The Continuous Damage Theory of Brittle Materials," Parts 1 and 2, ASME J. Appl. Mech., Vol. 48, 1981, pp. 809-824.
12. Costin, L. S., and Stone, C. M., "Implementation of a Finite Element Damage Model for Rock," in Constitutive Laws for Engr. Materials: Theory and Applications, Vol. II, Eds. Desai, Krempl, Kiousis and Kundu, Tucson, Arizona, USA, 1987, pp. 829-840.

13. Chaboche, J. L., "Continuum Damage Mechanics: Present State and Future Trends," ONERA T.P. n°1986-53, Séminaire International sur l'Approche Locale de la Rupture, Moret-sur-Loing, June 3-5, 1986.
14. Chow, C. L., and Wang, J., "An Anisotropic Theory of Elasticity for Continuum Damage Mechanics," Int. J. Fracture, 33, 1987, pp. 3-16.
15. Chaboche, J. L., "Continuous Damage Mechanics - A Tool to Describe Phenomena Before Crack Initiation," Nuclear Engr. and Design, Vol. 64, 1981, pp. 233-247.
16. Lemaitre, J., and Chaboche, J. L., "Aspect Phénoménologique de la Rupture par Endommagement," J. de Mécanique Appliquée, Vol. 2, No. 3, 1978, pp. 317-365.
17. Lemaitre, J., and Chaboche, J. L., "A Non-Linear Model of Creep-Fatigue Damage Cumulation and Interaction," Mechanics of Visco-Plastic Media and Bodies, Ed. Jan Hult, Springer, Berlin, 1975, pp. 297-301.
18. Chaboche, J. L., "Le Concept de Contrainte Effective Appliqué a l'élasticité et a la Viscoplasticité en Présence d'un Endommagement Anisotrope," Coll. Euromech. 115, Grenoble, 1979 (CNRS, 1982).
19. Huddleston, R. L., "An Improved Multiaxial Creep-Rupture Strength Criterion," ASME J. Pressure Vessels and Piping, Paper 84-PVP-106, 1984.
20. Miller, D. A., and Langdon, T. G., "Independent and Sequential Cavity Growth Mechanisms," Scripta Metallurgica, Vol. 14, 1980, pp. 143-148.
21. Svensson, L. E., and Dunlop, G. L., "Mechanisms for the Growth of Intergranular Creep Cavities," Creep in Structures, IUTAM, 1980, pp. 445-462 (Eds. Ponter and Hayhurst).
22. Cocks, A.C.F., and Ashby, M.F., "On Creep Fracture by Void Growth," J. Progress in Materials Science, Vol. 27, 1981, pp. 189-245.
23. Woodford, D.A., "Creep Damage and the Remaining Life Concept," ASME J. Engr. Materials and Technology, Vol. 101, Oct. 1979, pp. 311-316.
24. Chaboche, J. L., "Anisotropic Creep Damage in the Framework of Continuum Damage Mechanics," Nucl. Engr. Des., 79, 1984, pp. 309-319.
25. Pugh, C. E., and Robinson, D.N., "Some Trends in Constitutive Equation Model Development for High-Temperature Behavior Model Development for High-Temperature Behavior of Fast-Reactor Structural Alloys," Nuc. Engr. and Design, Vol. 48, 1978, pp. 269-276.

26. Krieg, R. D., Swearengen, J. C., and Rohde, R. W., "A Physically-Based Internal Variable Model for Rate-Dependent Plasticity," Inelastic Behavior of Pressure Vessel and Piping Components (Eds. Chang and Krempl), PVP-PB-028, ASME, 1978, pp. 15-28.
27. Lagneborg, R., "A Modified Recovery-Creep Model and its Evaluation," Metal Science Journal, Vol. 6, 1972, pp. 127-133.
28. Miller, A., "An Inelastic Constitutive Model for Monotonic, Cyclic, and Creep Deformation," ASME J. of Engineering Materials and Technology, Vol. 98, 1976, pp. 97-113.
29. Ponter, A.R.S., and Leckie, F.A., "Constitutive Relationships for the Time-Dependent Deformation of Metals," J. Eng. Mat. and Technology, Trans. ASME, Volume 98, 1976.
30. Hart, E.W., "Constitutive Relations for Non-Elastic Deformations of Metals," J. Eng. Mat. and Technology, Trans. ASME, Volume 98, 1976.
31. Chan, K.S., Bodner, S.R., Walker, K.P., and Lindholm, U.S., "A Survey of Unified Constitutive Theories," Proc. 2nd Symp. on Nonlinear Constitutive Relations for High Temperature Applications, NASA Lewis Research Center, June 13-15, 1984.
32. Walker, K. P., "Research and Development Program for Nonlinear Structural Modeling with Advanced Time-Temperature Dependent Constitutive Relationships," NASA Report CR-165533, NASA Lewis RC, Nov. 1981.
33. Chaboche, J. L., and Rousselier, G., "On the Plastic and Viscoplastic Constitutive Equations- Part I: Rules Developed With Internal Variable Concept," ASME J. Pressure Vessel Technology, Vol. 105, 1983, pp. 153-158.
34. Chaboche, J. L., and Rousselier, G., "On the Plastic and Viscoplastic Constitutive Equations- Part II: Application of Internal Variable Concepts to the 316 Stainless Steel," ASME J. Pressure Vessel Technology, Vol. 105, 1983, pp. 159-164.
35. Wang, C. C., "A New Representation Theorem for Isotropic Functions: An Answer to Professor G. F. Smith's Criticism of My Paper on Representations for Isotropic Functions," Arch. Rat. Mech. Anal., Vol. 36, 1970, pp. 198-223.
36. Dafalias, Y.F., and Popov, E.P., "A Model of Nonlinearly Hardening Materials for Complex Loading," Acta Mechanica, Vol. 21, 1975, pp. 173-192.

37. Dafalias, Y.F., "The Concept and Application of the Bounding Surface in Plasticity Theory," Physical Non-Linearities in Structural Analysis, Eds. J. Hult and J. Lemaitre, IUTAM Symposium, Senlis, France, Springer Verlag, 1981, pp. 56-63.
38. Tseng, N.T., and Lee, G.C., "Simple Plasticity Model of the Two-Surface Type," ASCE Journal of Engineering Mechanics, Vol. 109, No. 3, June 1983, pp. 795-810.
39. Mroz, Z., "An Attempt to Describe the Behaviour of Metals Under Cyclic Loads Using a More General Workhardening Model," Acta Mechanica, Vol. 7, 1967, pp. 199-212.
40. McDowell, D. L., "A Two Surface Model for Transient Nonproportional Cyclic Plasticity: Part 1," ASME J. Applied Mechanics paper No. 85-APM-9, 1985.
41. McDowell, D. L., "A Two Surface Model for Transient Nonproportional Cyclic Plasticity: Part 2," ASME J. Applied Mechanics Paper No. 85-APM-10, 1985.
42. McDowell, D. L., Ho, K. I., and Stalley, J., "An Anisotropic, Damage-Coupled Viscoplastic Model for Creep-Dominated Cyclic Loading," presented at Third Int. Symp. on Nonlinear Fracture Mech., Knoxville, TN, Nov. 1986.
43. Nouailhas, D., "A Viscoplastic Modelling Applied to Stainless Steel Behavior, " in Constitutive Laws for Engr. Materials: Theory and Applications, Vol. II, Eds. Desai, Krempl, Kiousis and Kundu, Tucson, Arizona, USA, 1987, pp. 717-724.
44. McDowell, D. L., and Moosbrugger, J. C., "A Rate-Dependent Bounding Surface Model," work in progress, 1987.
45. Lowe, T. C., and Miller, A. K., "Improved Constitutive Equations for Modeling Strain Softening- Part I: Conceptual Development," ASME J. Engr. Materials and Technology, Vol. 106, 1984, pp. 337-342.
46. Lowe, T. C., and Miller, A. K., "Improved Constitutive Equations for Modeling Strain Softening- Part II: Predictions for Aluminum," ASME J. Engr. Materials and Technology, Vol. 106, 1984, pp. 343-348.
47. Cho, U.W., and Findley, W.N., "Creep and Creep Recovery of 304 Stainless Steel at Low Stresses with Effects of Aging on Creep and Plastic Strains," ASME J. Appl. Mech., Vol. 48, 1981, pp. 785-790.

48. Cho, U.W., and Findley, W.N., "Creep and Plastic Strains of 304 Stainless Steel at 593°C Under Step Stress Changes, Considering Aging," ASME J. Appl. Mech., Vol. 49, 1982, pp. 297-304.
49. Brown, M.W., and Miller, K.J., Low-Cycle Fatigue and Life Prediction, ASTM STP 770, ASTM, 1982, pp. 482-499.
50. Lohr, R.D., and Ellison, E.G., Fatigue of Engineering Materials and Structures, Vol. 3, 1980, pp. 1-17.
51. Lemaitre, J., and Plumtree, A., "Application of Damage Concepts to Predict Creep-Fatigue Failures," ASME J. Engr. Matls. Tech., Vol. 101, 1979, pp. 284-292.
52. Majumdar, S., and Maiya, P.S., "A Mechanistic Model for Time-Dependent Fatigue," ASME J. Engr. Matls. Tech., Vol. 102, 1980, pp. 159-167.
53. Priest, R.H., and Ellison, E.G., "An Assessment of Life Analysis Techniques for Fatigue-Creep Situations," Res Mechanica, Vol. 4, 1982, pp. 127-150.
54. Leckie, F.A., "Modelling of High-Temperature Microstructural Damage," presented at the 1987 ASME Applied Mech., Bioengr. and Fluids Engr. Conf., Cincinnati, OH, June 1987.

APPENDIX

In this appendix, the derivation leading to equation (27) is detailed. Consider first the case of a finite number, e.g. two, principal stress orientations in a given loading history. Also suppose that the damage is purely anisotropic, i.e. $\eta = 0$. For such cases in which a finite number of primary loading configurations are known a priori, we may analytically carry out the determination of Ψ. Define the two maximum principal stress directions as

$$\underset{\sim}{n}_{I}^{(1)} = a_I \, \underset{\sim}{e}_1 + b_I \, \underset{\sim}{e}_2 \tag{A1}$$

$$\underset{\sim}{n}_{II}^{(1)} = a_{II} \, \underset{\sim}{e}_1 + b_{II} \, \underset{\sim}{e}_2 \tag{A2}$$

where $\underset{\sim}{e}_1$ and $\underset{\sim}{e}_2$ are orthogonal unit vectors in the tube longitudinal and circumferential directions, respectively, as shown in Figure 2. Since $\eta = 0$, we may write $\omega(\underset{\sim}{n})$ as

$$\omega(\underset{\sim}{n}) = \underset{\sim}{n} \cdot [\, \omega(\underset{\sim}{n}_{I}^{(1)}) \, (\underset{\sim}{n} \cdot \underset{\sim}{n}_{I}^{(1)})^{2P} \, \underset{\sim}{n}_{I}^{(1)} \otimes \underset{\sim}{n}_{I}^{(1)} + \omega(\underset{\sim}{n}_{II}^{(1)}) \, (\underset{\sim}{n} \cdot \underset{\sim}{n}_{II}^{(1)})^{2P} \, \underset{\sim}{n}_{II}^{(1)} \otimes \underset{\sim}{n}_{II}^{(1)} \,] \cdot \underset{\sim}{n} \tag{A3}$$

and $\omega(\underset{\sim}{n}_{\varsigma}^{(1)})$ is given for ς = I, II by integration of equation (6) when the principal stress is in the ς orientation, i.e.

$$\dot{\omega}(\underset{\sim}{n}_{\varsigma}^{(1)}) = B\ (\sigma_1)^k \left[2 + \frac{1}{\left[1 - \omega(\underset{\sim}{n}_{\varsigma}^{(1)})\right]^2} \right]^{1/2} \qquad \text{(A4)}$$

The mean value of $\omega(\underset{\sim}{n})$ may be determined by a formal integration over the unit sphere carried out in spherical coordinates θ and ϕ (radius = 1) as

$$\Psi = \frac{2}{4\pi} \int_0^{2\pi} \int_0^{\pi/2} \omega(\hat{\underset{\sim}{n}}(\theta,\phi))\ \sin\phi\ d\phi\ d\theta \qquad \text{(A5)}$$

where $\underset{\sim}{n} = \hat{\underset{\sim}{n}}(\theta,\phi) = \cos\phi\ \underset{\sim}{e}_1 + \sin\phi\ \cos\theta\ \underset{\sim}{e}_2 + \sin\phi\ \sin\theta\ \underset{\sim}{e}_3$

Here, θ is taken positive counterclockwise from the positive $\underset{\sim}{e}_2$ direction to the projection of $\underset{\sim}{n}$ on the $\underset{\sim}{e}_2$- $\underset{\sim}{e}_3$ plane and ϕ is the angle between the $\underset{\sim}{n}$ and $\underset{\sim}{e}_1$ directions. By substitution of the two damage distributions indicated in equation (A4),

$$\Psi = \frac{1}{2\pi} \int_0^{2\pi} \int_0^{\pi/2} \sum_{\varsigma=1}^{2} W_{\varsigma}\ \sin\phi\ d\phi d\theta \qquad \text{(A6)}$$

where

$$W_{\varsigma} = \omega(\underset{\sim}{n}_{\varsigma}^{(1)})\ [a_{\varsigma}\cos\phi + b_{\varsigma}\sin\phi\cos\theta]^{2(P+1)} \quad , \qquad \text{(A7)}$$

we arrive, with the benefit of the identity $(a_{\varsigma}^2 + b_{\varsigma}^2) = 1$, at the simple recursion relation

$$\Psi(P) = (2P + 3)^{-1} \left[\omega(\underset{\sim}{n}_I^{(1)}) + \omega(\underset{\sim}{n}_{II}^{(1)}) \right] \qquad (A8)$$

which precludes the need for numerical integration to determine Ψ for any P in this case. It is interesting to note that if P = 0, the two ω distributions are each equivalent to that of a symmetric second rank tensor, and $\Psi(0)$ is simply the sum of the hydrostatic components of each tensor.

A great computational aid is offered if a general rate expression may be found for Ψ, the mean value of $\omega(\underset{\sim}{n})$ over the unit sphere. In particular, such an expression would eliminate the need to perform numerical integration at each time step over the surface of the unit sphere. In addition, the resolution of the discrete representation of $\omega(\underset{\sim}{n})$ on the unit sphere could be dramatically coarsened since the accuracy of numerical integration for Ψ would not be an issue; the discretization of the unit sphere (i.e. the finite number N of $\omega(\underset{\sim}{n}_N)$ values) would be left to consideration of the accuracy of the damage growth equation only.

This generalization is readily achieved by noting that the recursion formula stated in equation (8) may be generalized by the superposition of an arbitrary number of anisotropic damage distributions for which $\eta = 0$, i.e.

$$\Psi(P) = (2P + 3)^{-1} \left[\omega(\underset{\sim}{n}_I^{(j)}) + \omega(\underset{\sim}{n}_{II}^{(j)}) + \ldots \right] \qquad (A9)$$

Recognizing that this relation applies to the anisotropic component of the damage rate distribution given in equation (6) and that the isotropic component of the distribution is equivalent to its mean value over the unit sphere, we may write the general expression which appears in equation (27).

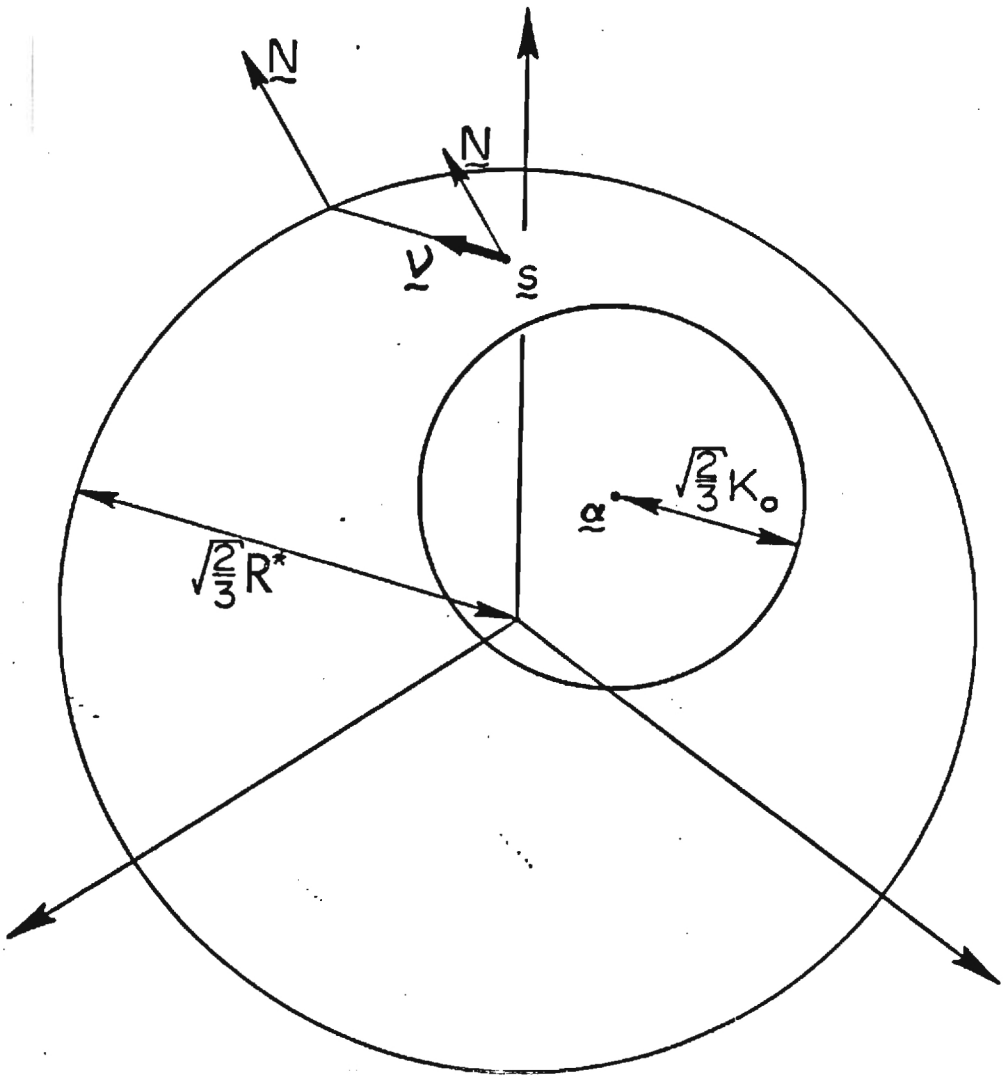

FIG. 1- Bounding and loading surfaces in deviatoric stress space.

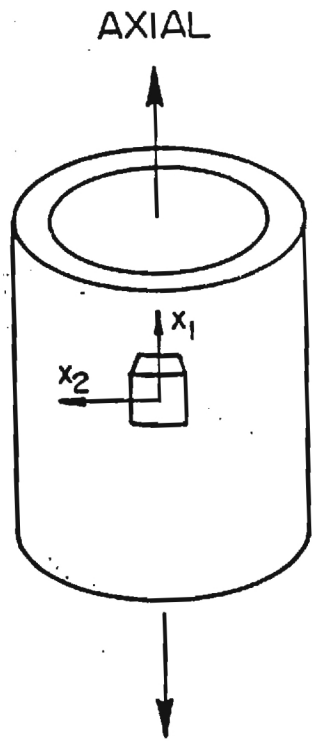

FIG. 2- Coordinate system for the thin-walled tubular tension torsion specimen; x_1 and x_2 are the axial and circumferential coordinates, respectively, at the specimen mid-plane.

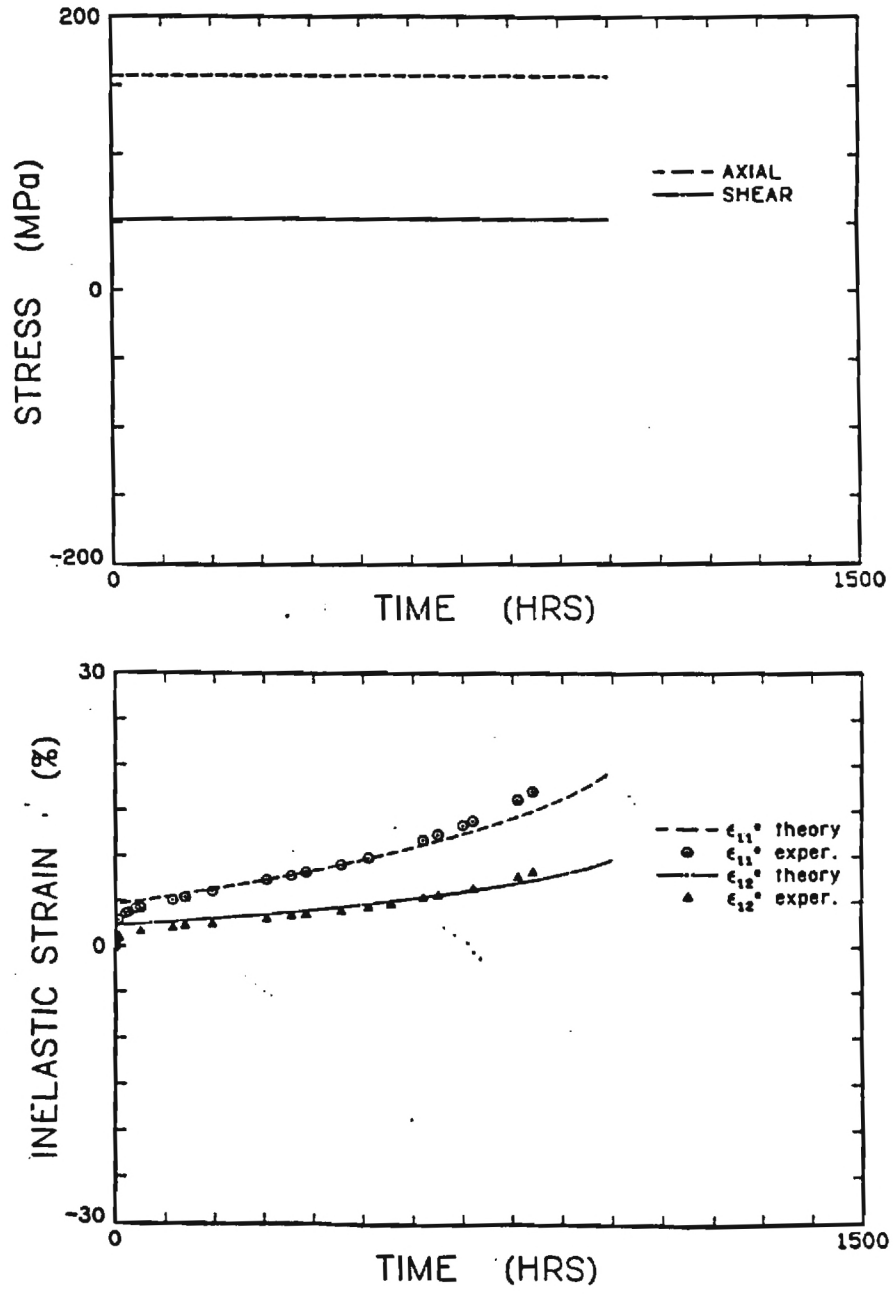

FIG. 3- Type 304 stainless steel at 593°C: applied biaxial nominal stress history (top) and predicted versus experimental inelastic strains (bottom) for specimen GT-1. Actual and predicted rupture times are 892 hr and 998 hr, respectively.

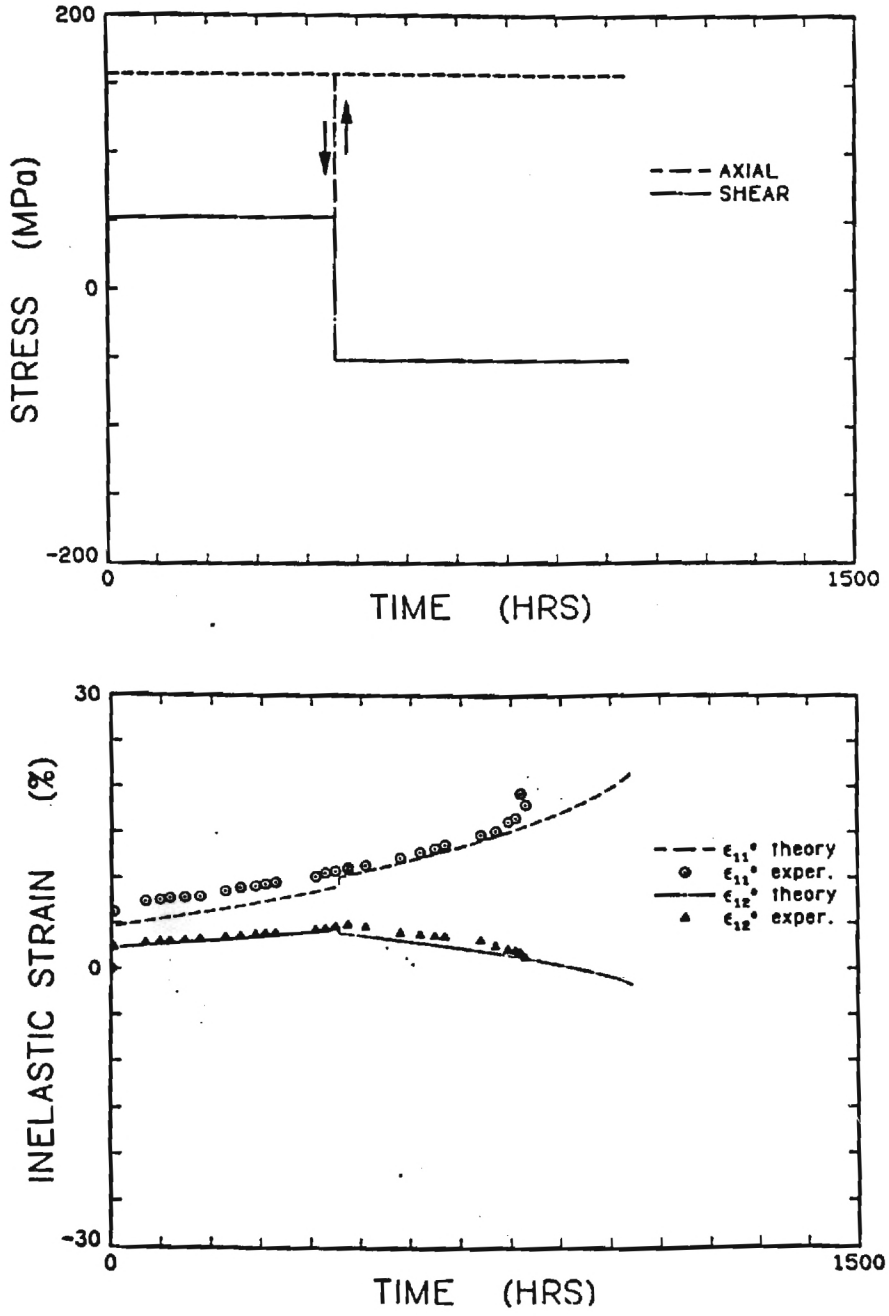

FIG. 4- Type 304 stainless steel at 593°C: applied biaxial nominal stress history (top) and predicted versus experimental inelastic strains (bottom) for specimen GT-4A. Actual and predicted rupture times are 851 hr and 1043 hr, respectively.

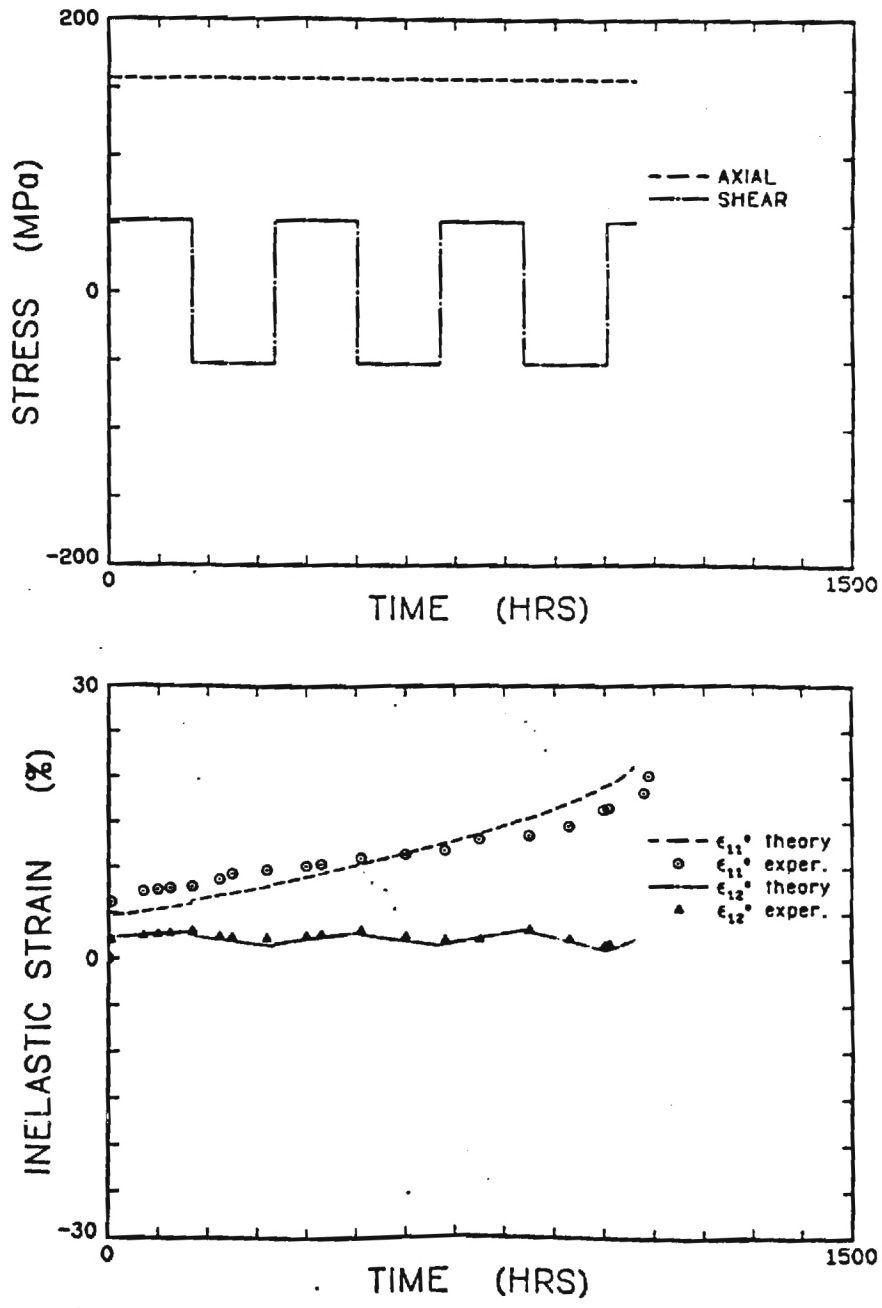

FIG. 5- Type 304 stainless steel at 593°C: applied biaxial nominal stress history (top) and predicted versus experimental inelastic strains (bottom) for specimen GT-6. Actual and predicted rupture times are 1088 hr and 1060 hr, respectively.

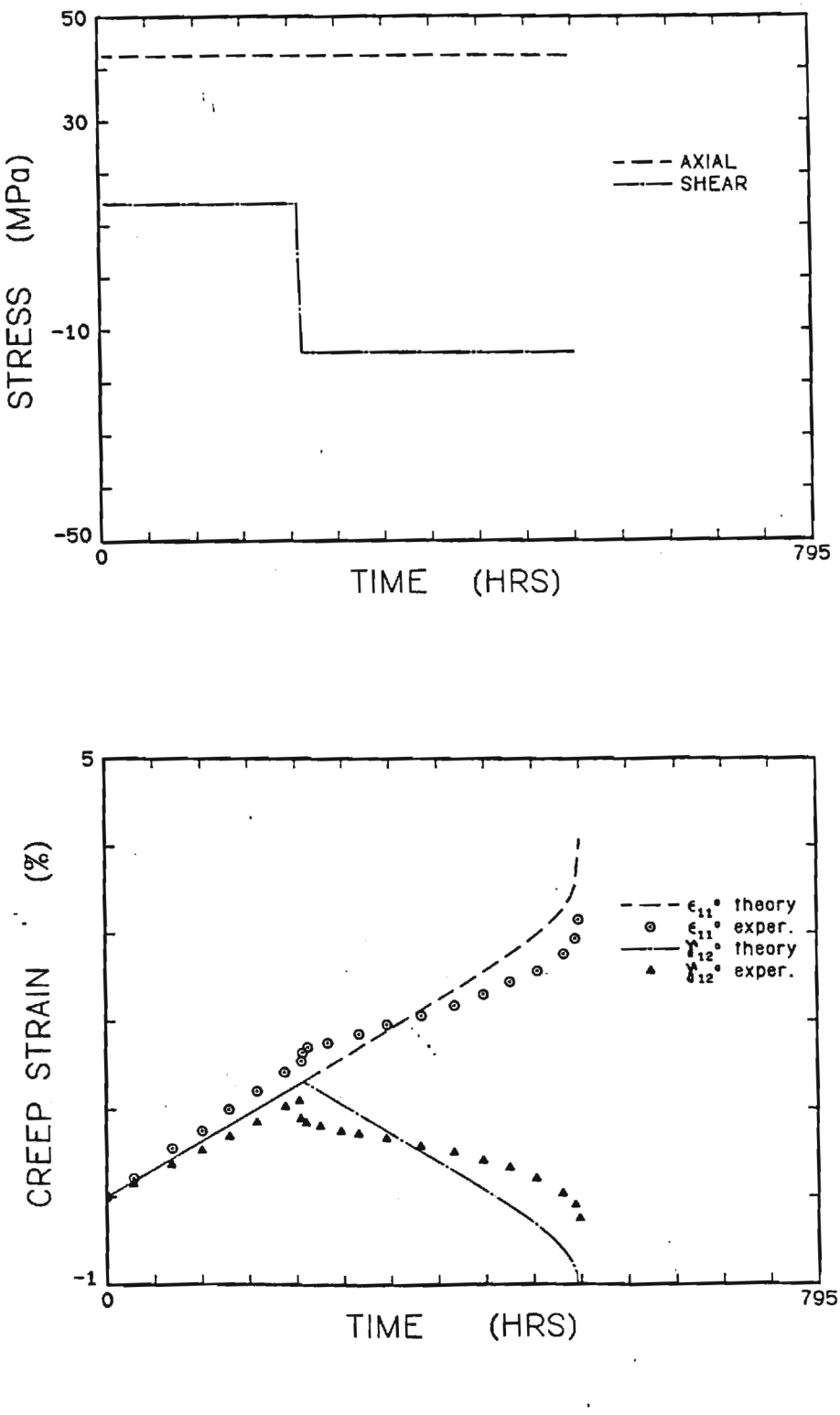

FIG. 6- Copper at 250°C: applied biaxial nominal stress history (top) and predicted versus experimental [3] creep strains (bottom) for a history with a single reversal.

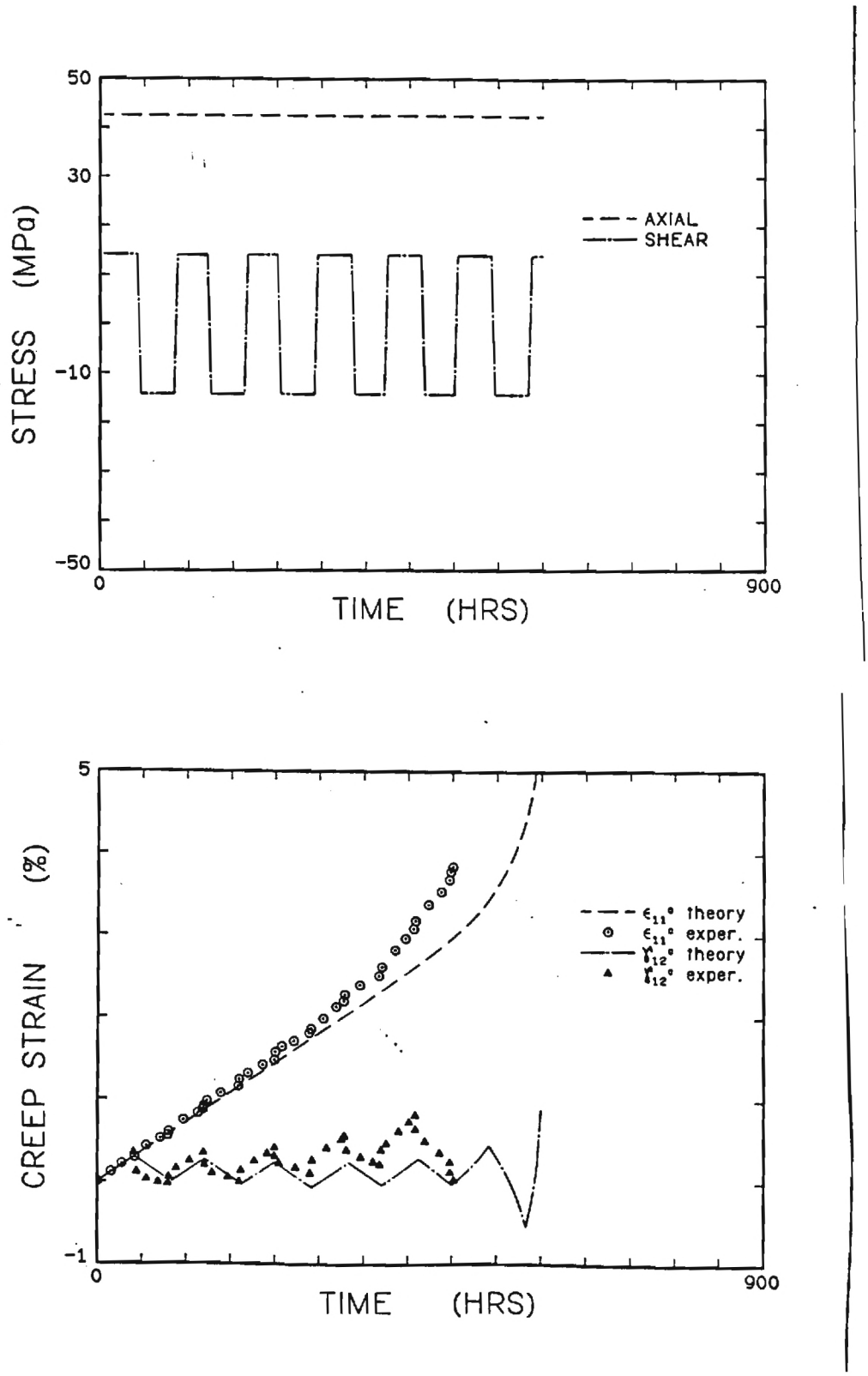

FIG. 7- Copper at 250°C: applied biaxial nominal stress history (top) and predicted versus experimental [3] creep strains (bottom) for a history with multiple reversals.

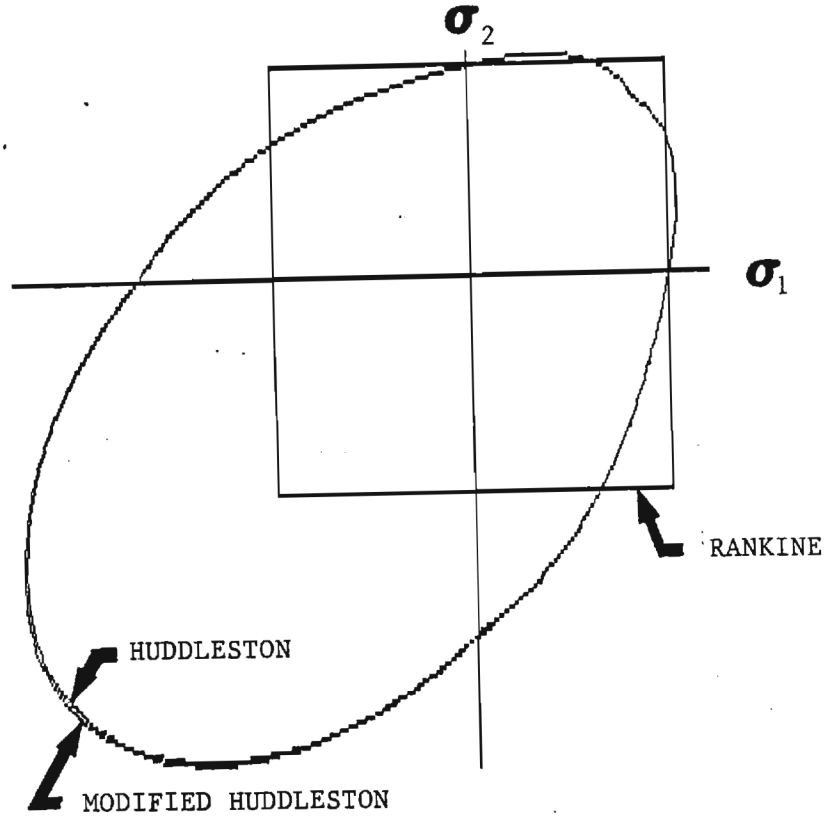

FIG. 8- Normalized plots of the isochronous stress surface of Huddleston [19] and the current formulation for type 304 stainless steel at 593°C in the biaxial σ_1-σ_2 space (σ_3 = 0).

FINAL REPORT
GTRI Project Number E-25-623

CREEP-DOMINATED, ANISOTROPIC CONTINUUM DAMAGE

By
D.L. McDowell
Principal Investigator
George W. Woodruff School of Mechanical Engineering
Georgia Institute of Technology

Submitted to
MARTIN MARIETTA ENERGY SYSTEMS, INC.
Technical Contact: Dr. J. Blass

Under
Subcontract No. 19X-SA631C

September 30, 1987

GEORGIA INSTITUTE OF TECHNOLOGY
A UNIT OF THE UNIVERSITY SYSTEM OF GEORGIA
THE GEORGE W. WOODRUFF SCHOOL OF MECHANICAL ENGINEERING
ATLANTA, GEORGIA 30332

1987

SEPTEMBER 30, 1987

FINAL REPORT

Subcontract No. 19X-SA631C
Georgia Tech # E-25-623

Submitted to

MARTIN MARIETTA ENERGY SYSTEMS, INC.
Technical Contact: Dr. J. Blass

CREEP-DOMINATED, ANISOTROPIC CONTINUUM DAMAGE

D.L. McDowell
Principal Investigator
George W. Woodruff School of Mechanical Engineering
Georgia Institute of Technology
Atlanta, GA 30332

INTRODUCTION

The problem of high temperature creep damage in initially isotropic, polycrystalline metals has received considerable attention. Fundamentally, two distinct approaches have emerged which seek to address the evolution of damage at different size scales. The first approach, traditionally encompassing time-fraction rules and remaining life curves is directed toward description of creep-rupture phenomena under variable stress loading histories. The second approach, the "micromechanical" treatment, seeks to derive expressions for nucleation and/or growth of voids on grain boundaries with suitable prescription of rupture criteria.

This work is concerned with a continuum approach for modeling of physical grain boundary damage under multiaxial, nonproportional, creep-dominated loading histories. Such histories necessitate description of the anisotropic nature of creep damage accumulation since the rupture time is greatly affected by damage anisotropy. In this work, a general framework for continuum creep damage evolution is presented which extends the work of Murakami and Ohno [1-2], Trampczynski et al. [3-4], and Leckie and Onat [5-6].

A basic model for anisotropic creep damage has been developed with support from Martin Marietta subcontracts 19B-07802C and 19X-55966C and grants from the U.S. National Science Foundation. The goals of the current funding period were to build on this prior work, including more sophistication and generality in the model, in addition to "exercising" the model with correlation of the nonproportional creep damage response of a more highly anisotropically damaging material.

In this final project report, a more refined version of the anisotropic creep damage model is presented. This latest version includes the specification of an even rank tensor of arbitrary magnitude to model the actual creep damage distribution, alternate definitions for the damage effect tensor, an algorithm for efficient computation of the mean value of damage on the unit sphere, and

incorporation of the retardation effect of compressive biaxial principal stress ratios directly in a modified form of an isochronous stress definition originally attributed to Huddleston [19]. The relationship of the current framework to other major continuum damage approaches, including both substantial and perhaps subtle differences, is developed to a greater extent than previously done. Correlations are presented for several nonproportional creep-dominated loading histories for copper at 250°C in addition to type 304 stainless steel at 593°C; hence, the work statement requirements regarding correlations for copper have been completed.

Specific ways to include the following effects in the current anisotropic continuum damage approach are outlined and discussed:

(a) aging effects,
(b) framework for interaction between fatigue damage and creep damage, and
(c) more general cavity growth mechanisms.

CREEP DAMAGE GROWTH LAW

In this work, we adopt the notion that a spatial distribution of grain boundary cavitation and triple-point cracking may be represented as a continuum quantity. Since creep damage is a bulk phenomenon, such a description is quite reasonable as confirmed by results of homogenization theory [7]. Precedental works of Kachanov [8] and Rabotnov [9] are noted among many others.

In the approach taken by Murakami and Ohno [1-2], a symmetric second rank damage rate tensor was assumed. This results, of course, in a second rank tensor damage distribution regardless of the nonproportionality of the applied loading

history. Experiments conducted by Trampczynski, Hayhurst and Leckie [3-4], however, reveal that the creep damage distribution for some materials is highly dependent on principal stress orientation; a second rank tensor representation of physical damage is inadequate. Krajcinovic [10-11] suggests that the directional distribution of physical damage is most appropriately modeled as a dual vector; such a vector can represent, for example, the discontinuity in loading/unloading stiffness exhibited by cracked brittle materials by virtue of crack closure. Leckie and Onat [5-6] suggest stronger conditions, based on damaged material symmetry arguments, which require that a vectorial distribution of damage on the unit sphere be even with respect to $\underset{\sim}{n}$, i.e.

$$\omega(\underset{\sim}{n}) = \omega(-\underset{\sim}{n}) \tag{1}$$

where $\underset{\sim}{n}$ is a unit vector normal to the unit sphere and $\omega(\underset{\sim}{n})$ is the distribution of damage. If the damage is manifested as an array of cracks, for example, ω may be defined as the area fraction of cracks associated with crack face unit normal vector $\underset{\sim}{n}$ [12]. Leckie and Onat have shown that $\omega(\underset{\sim}{n})$ may be represented by an expansion of even rank symmetric tensors.

In this work, we adopt the symmetry arguments of Leckie and Onat. For grain boundary creep damage, we assume that the orientation and magnitude of damage is defined by the unit normal vector and damaged area fraction of each grain boundary facet, i.e.

$$\omega(\underset{\sim}{n}) = \frac{1}{S_g(\underset{\sim}{n})} \int_V dS_{gd}(\underset{\sim}{n}) \tag{2}$$

where $S_g(\underset{\sim}{n})$ is the total grain boundary facet area in volume V with unit normal vector $\underset{\sim}{n}$, and $dS_{gd}(\underset{\sim}{n})$ is the differential damaged grain boundary facet area

associated with unit vector $\underset{\sim}{n}$. The form given in equation (2) permits experimental estimation of $\omega(\underset{\sim}{n})$ from macroscopically homogeneously deformed specimens; for a continuum representation, we may think of the volume of integration as passing to an infinitesimal, i.e. $V \to \delta V$.

Following the development of Leckie and Onat [5-6], we may define the damage distribution $\omega(\underset{\sim}{n})$ in terms of a set $\underset{\sim}{\Gamma}$ of even rank, irreducible tensors obtained from the distribution of damage on the unit sphere. The effect of the current state of damage on damage rate is introduced via stress intensification associated with loss of load bearing area by defect formation and distribution, defect stress concentration, and defect interaction. Effective stress $\underset{\sim}{S}$ may be expressed as a second rank tensor function of Cauchy stress $\underset{\sim}{\sigma}$ and a fourth rank operator $\underset{\sim}{M}(\underset{\sim}{\Gamma})$, i.e.

$$\underset{\sim}{S} = \hat{\underset{\sim}{S}}(\underset{\sim}{M}(\underset{\sim}{\Gamma}), \underset{\sim}{\sigma}) \tag{3}$$

Regarding practical application of such an approach, we may select a "minimal" set $\underset{\sim}{\Gamma}$ based on acceptable approximation of the damage accumulation processes and the rupture criterion. For proportional loading, $\underset{\sim}{\Gamma}$ of rank two may be a sufficient approximation for anisotropic material damage. For nonproportional loading, however, the appropriate rank of $\underset{\sim}{\Gamma}$ depends on both the nonproportionality of the loading history and the nature of the damage distribution.

In this work, we make the simplifying assumption that the principal axes of the Cauchy stress and effective stress coincide, which may be true for proportional loading even up to large cavity volume fractions. However, for nonproportional loading such an assumption suggests a limitation to relatively small cavity volume fractions to ensure that the

rotation of the effective stress with respect to the Cauchy stress is suitably small. With this assumption we may express $\underset{\sim}{M}$ in the principal stress coordinate frame as

$$M_{ijkl}(\underset{\sim}{\Gamma}) = \phi_{ij}(\underset{\sim}{\Gamma})\ \delta_{ik}\delta_{jl} \quad \text{(no sum on i and j)} \tag{4}$$

with

$$\underset{\sim}{\phi} = \sum_{j=1}^{3} \Omega^{(j)}\ \underset{\sim}{n}^{(j)} \otimes \underset{\sim}{n}^{(j)} \tag{5}$$

where $\underset{\sim}{\phi}$ is the damage effect tensor with principal components $\Omega^{(j)}$ and eigenvectors $\underset{\sim}{n}^{(j)}$ collinear with those of $\underset{\sim}{\sigma}$. We do not attempt herein to make a direct connection between the definition of $\underset{\sim}{\phi}$ and loss of cross-sectional area in the Cauchy tetrahedron as do Murakami and Ohno [1-2], recognizing that the actual damage distribution is not in general represented by a second rank tensor; rather, $\underset{\sim}{\phi}$ is viewed as an approximation of the intensification effect of grain boundary damage on the current principal stresses and hence influences damage rate.

In this work, we consider only infinitesimal strains and small rotations. Furthermore, the cavity volume fraction is assumed small so that the assumption of equivalence of the principal coordinate frames for effective and Cauchy stresses may be approximately made. Such an assumption is not as physically restrictive as it might seem in view of the typically small cavity volume fraction up to the rupture event. This does not imply that the damage distribution is isotropic, but that the damage rate is tensorially dictated by the current principal directions of $\underset{\sim}{\sigma}$. This results in an anisotropic damage distribution for proportional or nonproportional loading. Density changes associated with damage are neglected, although they may be included as discussed by Chaboche [13]. Isothermal conditions are assumed. We define the growth rate of ω as a function of $\underset{\sim}{\phi}$ and $\underset{\sim}{\sigma}$ in the following simple way:

$$\dot{\omega}(\underset{\sim}{n}) = \xi(\sigma^*) \left[\eta\, \chi^{(1)} \left\{\Omega^{(1)}\right\}^{l(\sigma^*)} + \right. \tag{6}$$

$$\left. (1-\eta) \sum_{j=1}^{3} \chi^{(j)} \left\{\Omega^{(j)}\right\}^{l(\sigma^*)} \left\{ \underset{\sim}{n} \cdot \underset{\sim}{n}^{(j)} \otimes \underset{\sim}{n}^{(j)} \cdot \underset{\sim}{n} \right\} \left\{ \underset{\sim}{n} \cdot \underset{\sim}{n}^{(j)} \right\}^{2P} \right]$$

$$= \dot{\omega}(\underset{\sim}{n})_{\text{isotropic}} + \dot{\omega}(\underset{\sim}{n})_{\text{anisotropic}}$$

which corresponds to the magnitude in direction $\underset{\sim}{n}$ (obtained by 2(P+1) contractions with $\underset{\sim}{n}$) of the symmetric, anisotropic damage rate tensor $\dot{\underset{\sim}{\Gamma}}$ of rank 2(P+1), i.e.

$$\dot{\underset{\sim}{\Gamma}} = \xi(\sigma^*) \left[\eta\, \chi^{(1)} \left\{\Omega^{(1)}\right\}^{l(\sigma^*)} \bigotimes_{i=1}^{P+1} \underset{\sim}{I} + \right. \tag{7}$$

$$\left. (1-\eta) \sum_{j=1}^{3} \chi^{(j)} \left\{\Omega^{(j)}\right\}^{l(\sigma^*)} \bigotimes_{i=1}^{2(P+1)} \left\{\underset{\sim}{n}^{(j)}\right\} \right]$$

where ξ and l are functions of the isochronous stress σ^* (surface of constant rupture time), $\underset{\sim}{n}^{(j)}$ is the unit vector in the j^{th} principal stress direction, σ_j, $\underset{\sim}{n}^{(j)} \cdot \underset{\sim}{n} = n_k{}^{(j)} n_k$, P is an integer representative of the order of the anisotropic damage distribution, and η is the fraction of damage rate in the $\underset{\sim}{n}^{(1)}$ direction which is isotropic; η is bounded by $0 \leq \eta \leq 1$ and may also be a function of σ^* as discussed later. The value of P is either zero or a positive integer. $\underset{\sim}{I}$ is the identity tensor. The $\Omega^{(j)}$ are the principal components of the damage effect tensor $\underset{\sim}{\phi}$. Factor $\chi^{(j)}$ excludes contribution of compressive principal stresses to the damage rate, i.e.

$$\chi^{(j)} = \langle \underset{\sim}{n}^{(j)} \cdot \frac{\underset{\sim}{\sigma}}{|\sigma_j|} \cdot \underset{\sim}{n}^{(j)} \rangle \qquad (8)$$

where σ_j are the ordered principal stresses with $\sigma_1 \geq \sigma_2 \geq \sigma_3$, and the Macauley bracket $\langle F \rangle = F$ if $F > 0$; $\langle F \rangle = 0$ otherwise. The scalar product of two second rank tensors $\underset{\sim}{A}$ and $\underset{\sim}{C}$ is defined by $(\underset{\sim}{A}:\underset{\sim}{C}) = (A_{ij}C_{ji})^{1/2}$, and the outer product is denoted by $\otimes$; outer products repeated multipicatively (P+1) and 2(P+1) times are inferred by the summation on $\otimes$ in equation (7).

Several forms may be proposed for $\Omega^{(j)}$. One possibility is that the anisotropic damage rate in principal stress direction $\underset{\sim}{n}^{(j)}$ depends only on the extent of damage in that direction, $w(\underset{\sim}{n}^{(j)})$, i.e.

$$\Omega^{(j)} = \frac{1}{1 - w(\underset{\sim}{n}^{(j)})} \qquad (9)$$

which is a direct anisotropic generalization of the Kachanov-Rabotnov damage approach [14]. Another possibility is that the anisotropic damage rate in the $\underset{\sim}{n}^{(j)}$ direction also depends on η. Such dependence would introduce a significant departure from the spirit of equation (9) only if η is a function of σ^*. We may choose to allow $\Omega^{(j)}$ to depend on $\eta w(\underset{\sim}{n}^{(j)})$, recognizing that this quantity provides a lower bound on the damage oriented orthogonal to the $\underset{\sim}{n}^{(j)}$ direction. A simple way to introduce nonlinear dependence on η is by defining a symmetric, second rank tensor $\underset{\approx}{\zeta}^{(j)}$ defined uniquely by each $w(\underset{\sim}{n}^{(j)})$, in analogy to the definition proposed by Murakami and Ohno [1], as

$$\underset{\approx}{\zeta}^{(j)} = [\ \underset{\sim}{I} - \underset{\approx}{\Pi}(\underset{\sim}{n}^{(j)})\ ]^{-1} \qquad (10)$$

where $\underset{\sim}{\Pi}$ is defined by

$$\underset{\sim}{\Pi}(\underset{\sim}{n}^{(j)}) = \omega(\underset{\sim}{n}^{(j)}) \; [\eta + (1 - \eta) \; \underset{\sim}{n}^{(j)} \otimes \underset{\sim}{n}^{(j)}] \tag{11}$$

The $\underset{\sim}{\phi}$ components in this case are expressed as $\Omega^{(j)} = (\underset{\sim}{\zeta}^{(j)} : \underset{\sim}{\zeta}^{(j)})^{1/2}$, i.e.

$$\Omega^{(j)} = \left[\frac{1}{(1 - \omega(\underset{\sim}{n}^{(j)}))^2} + \frac{2}{(1 - \eta\omega(\underset{\sim}{n}^{(j)}))^2} \right]^{1/2} \tag{12}$$

Essentially, this equation assumes that the stress intensification effect associated with each of the damage values $\omega(\underset{\sim}{n}^{(j)})$ is represented by a symmetric, second rank tensor defined by $\omega(\underset{\sim}{n}^{(j)})$, but dependent on η. The scalar multiplier $\Omega^{(j)}$ directly affects evolution of the ω distribution, as seen in equation (6). It should be noted that for isotropic hardening, the damage rate equation assumes the classical Kachanov-Rabotnov form. It is assumed in equation (6) that the evolution of the isotropic component of the ω distribution is dictated by the effect of the damage in the tensile principal stress directions; the isotropic component of damage exists because of constraints between contiguous grains which are affected by relative orientation, extent of grain boundary sliding, etc. As reflected in the isochronous stress, the dilatational and distortional stress invariants affect the rate of creep damage accumulation in addition to the tensile principal stresses.

It is necessary to introduce a specific definition for the isochronous stress. As discussed by Hayhurst et al. [3-4] and Lemaitre and Chaboche [15-18], the isochronous stress is a level surface in stress space denoting equivalent rupture times; it is a function of the maximum principal stress, the second invariant of deviatoric stress, and the

hydrostatic stress. Based on the rather extensive experimental work of Huddleston [19], who considered several materials and various biaxiality ratios, the isochronous stress is defined as

$$\sigma^* = \frac{3}{2} S_1 \left(\frac{2}{3} \frac{\sigma_e}{S_1} \right)^a \exp\left[b\{1 + f(J_1)\langle -J_1/|J_1|\rangle\}\left(\frac{J_1}{S_s} - 1\right) \right] \tag{13}$$

where

$$S_1 = \sigma_1 - \frac{1}{3} \sigma_{kk} \tag{14}$$

$$\sigma_e = \left[(3/2)\underset{\sim}{s} : \underset{\sim}{s} \right]^{1/2} \tag{15}$$

$$\underset{\sim}{s} = \underset{\sim}{\sigma} - \frac{1}{3} \sigma_{kk} \underset{\sim}{I} \tag{16}$$

$$S_s = \left[\sigma_1^2 + \sigma_2^2 + \sigma_3^2 \right]^{1/2} \tag{17}$$

$$J_1 = \sigma_{kk} \tag{18}$$

It should be noted that this form of the isochronous stress is a slightly altered form of that proposed by Huddleston. Very little data were available in the biaxial regime with an in-plane compressive principal stress of greater magnitude than the tensile stress, i.e. a negative J_1. The approach offered by Huddleston is hence modified by inclusion of the term $(1+f(J_1)\langle -J_1/|J_1|\rangle)$, which must be experimentally determined. Further discussion of this term appears in a later section.

This form of the isochronous stress has been rather thoroughly supported by a variety of biaxial creep experiments on tubular specimens of type 304 stainless steel at 593°C at ORNL, including axial tension, equi-biaxial tension (axial

tension and pressure), internal pressure, torsion, axial tension and torsion, and axial compression and torsion. It should be noted that this form of σ^* was verified for loading magnitudes which would be expected to lead to matrix power law creep governed grain boundary damage accumulation.

It is important to examine the role of exponent P in governing the anisotropy of the damage distribution. P = 0 only if the actual damage distribution $\omega(\underset{\sim}{n})$ takes the form of a symmetric second rank tensor. This is approximately the case for type 304 stainless steel at 593°C as will be discussed later. For an isotropically damaging material with η = 1, the second term in equations (6)-(7) does not apply since the anisotropic component of the damage rate is zero. The results of Trampczynski et al. [3-4] for copper indicate a high degree of anisotropy, and hence a larger value of P.

Obviously, the integrated damage distribution $\omega(\underset{\sim}{n})$ will depend on whether the loading history is proportional or nonproportional. Rotation of the principal stress eigenvectors will in general result in multiple "peaks" in the damage distribution with respect to a fixed material coordinate system. From a practical viewpoint, depending on the rank of the tensorial damage distribution, it may be desirable to express the distribution either precisely in terms of tensor components or approximately in terms of ω values at a discrete number of points on the unit sphere. In the latter case, an interpolation algorithm may be necessary to estimate the ω value in any arbitrary direction. The former representation is desirable for second and perhaps even fourth rank damage tensors, while the latter would seem the only practical route for distributions of higher rank.

Omission of the functional dependence of 1 on σ^* in equations (6)-(7) would imply that time fraction and damage (for proportional loading) are uniquely related, which does not allow description of multiple isochronous stress level sequence effects (nonlinear damage accumulation) [16-18] if the rupture criterion

is stress-independent. In this paper, we will be concerned with correlation of experiments performed at constant isochronous stress and hence do not require explicit stress level-dependence of l, but such dependence offers no particular difficulty. In fact, it was included in the final report under 1986 subcontract 19X-55966C. This dependence is physically necessitated by the stress level-dependence of cavity growth mechanisms as reflected in void growth mechanisms maps [20-22], and is supported by experiments cited by Chaboche et al. [16-17] in which the measured damage growth is retarded as a function of time fraction t/t_R as the isochronous stress level increases. The deleterious effects of low-high stress level sequences and the accumulation of greater creep damage under low stress than high stress conditions at the same time fraction are well-documented [23]. In view of the stress-dependence of cavity growth mechanisms (c.f. [20-22]) and the associated differences in void aspect ratios and constraints in regimes of diffusion-dominated versus matrix power law creep-dominated void growth, it may be necessary to admit dependence of the anisotropy of the damage distribution on stress, i.e. $P = P(\sigma^*)$ and $\eta = \eta(\sigma^*)$.

If the microstructure is unstable and aging effects such as precipitation or coarsening exist, it is necessary to include these effects via description of precipitation/coarsening kinetics. The function $\xi(\sigma^*)$ in equations (6)-(7) is based on the assumption of a fixed number of void nucleation sites and a stable microstructure. As discussed by Leckie and Onat [5-6], a separate evolution equation may be introduced for void nucleation rate. Certainly, void nucleation rate may be associated with intersections of slip bands with grain boundaries and with the precipitation of grain boundary carbides, so that inelastic rate of deformation and diffusion kinetics must both be considered. In this study, we will present correlation with isothermal creep histories at only a constant isochronous stress level for each material such that aging effects are implicitly embedded in

the constants and parameters of the evolution equations for damage and creep deformation. For histories involving significant changes in isochronous stress or temperature, consideration must be given to explicit state variables representing, for example, precipitate size and spacing. Aging is potentially an important consideration for predicting long term rupture performance based on short term tests, and is considered in further detail later in this report.

Another key element of the damage formulation is the rupture criterion. Previous discussion has assumed that ω_{max} = constant at rupture. It is clear from previous work [5-6,23] that the extent of creep damage just prior to the final rupture event depends on stress level. If a stress level-dependent rupture criteria is adopted, then the damage at rupture is not constant and the time fraction at any given damage level, even for constant λ, depends on the isochronous stress for proportional loading. A stress level-dependent rupture criterion is more difficult to implement since experimental investigation of the damage distribution at different stress levels is quite involved. Existing data are somewhat sketchy and incomplete. The logical approximation to the physically more precise stress level-dependent rupture criterion is the first approach, i.e. the assumption of a constant damage at failure. This approximation is most likely suitable, even for variable load histories, since the damage growth is highly nonlinear only near the final rupture event. Therefore, from a practical viewpoint, the use of a constant damage at rupture is likely to be sufficient, especially in view of the inherent scatter in creep rupture tests. Hence, the rupture criterion

$$\omega_{max} = \max_{\text{all } \underset{\sim}{n}} \omega(\underset{\sim}{n}) = 1 \tag{19}$$

is selected in this work. It should be noted, however, that the definition of

damage offered in equation (2) in conjunction with equation (19) does not imply that the area fraction of cavitated grain boundaries is unity at rupture; the area fraction of cavitated segments normal to $\underset{\sim}{n}$ is unity. For a highly anisotropically damaging material, the total area fraction of cavitated grain boundaries may be quite low. It can be shown, for example, that the area fraction of damaged grain boundary segments upon satisfaction of equation (19) for uniaxial loading is expressed as the mean value of $\omega(\underset{\sim}{n})$ over the unit sphere as

$$f_h = \frac{2(P + 1)\eta + 1}{2P + 3} \tag{20}$$

For example, for $\eta = 0$ and $P = 1$ ($\underset{\sim}{\Gamma}$ of rank four), $f_h = 0.2$ at rupture. If the damage is isotropic, $\eta = 1$ and $f_h = 1$ at rupture. If $\underset{\sim}{\Gamma}$ is second rank, $P = 0$ and $f_h = (2\eta + 1)/3$, i.e. the hydrostatic component of $\underset{\sim}{\Gamma}$.

Finally, it should be noted that under conditions of finite strain, the damage distribution must evolve in reference to a material coordinate frame, necessitating an appropriate finite strain formulation [1-2,13] and consideration of material density changes [13,24].

CORRELATION WITH NONPROPORTIONAL CREEP HISTORIES

It is necessary to implement the foregoing damage formulation in a viscoplastic constitutive framework of desired sophistication and accuracy. In this section, we will first discuss the selected form of the coupling with a rather general viscoplastic model framework. Then we will specialize to unified creep-plasticity and power-law creep constitutive laws for comparison of high temperature, nonproportional creep rupture experiments conducted on type 304 stainless steel and

pure copper, respectively. The level of anisotropy of creep damage in these two materials is markedly different.

The constitutive model for rate-dependent deviatoric inelasticity must be coupled with the damage distribution just presented. An isothermal framework for achieving this coupling for small cavity volume fractions is as follows:

viscoplastic flow rule:
$$\dot{\underset{\sim}{\epsilon}}^{n} = f(\underset{\sim}{s}D,\ \underset{\sim}{\alpha}D,\ \kappa) \tag{21}$$

hardening rules:

kinematic:
$$\dot{\underset{\sim}{\alpha}}D = H_{\alpha}(\underset{\sim}{s}D,\ \underset{\sim}{\alpha}D,\ K^{*})\ ||\dot{\underset{\sim}{\epsilon}}^{n}||\ \underset{\sim}{\nu} - R_{\alpha}(\underset{\sim}{\alpha}D)\ \underset{\sim}{\alpha}D \tag{22}$$

isotropic:
$$\dot{\kappa} = G_{\kappa}(\underset{\sim}{s}D,\ \underset{\sim}{\alpha}D,\ \kappa)\ ||\dot{\underset{\sim}{\epsilon}}^{n}|| - R_{\kappa}(\kappa) \tag{23}$$

$$\dot{K}^{*} = G_{R^{*}}(\underset{\sim}{s}D,\ \underset{\sim}{\alpha}D,\ K^{*})\ ||\dot{\underset{\sim}{\epsilon}}^{n}|| - R_{K^{*}}(K^{*}) \tag{24}$$

Here deviatoric stress $\underset{\sim}{s} = \underset{\sim}{\sigma} - (\sigma_{kk}/3)\underset{\sim}{I}$, and backstress $\underset{\sim}{\alpha}$ is deviatoric. The inelastic strain $\underset{\sim}{\epsilon}^{n}$ includes both conventional creep and plastic strain as in other unified theories. The backstress reflects, in a general sense, directional internal stress fields associated with dislocation entanglements at both thermal and athermal barriers. Scalar state variables K^{*} and κ introduce strain hardening/softening effects in the backstress evolution and flow rules, respectively. Equations (21)-(24) include a hardening/recovery format typical of existing unified creep-plasticity approaches (c.f. [25-32]). Additionally, the directional index $\underset{\sim}{\nu}$ may be selected to correspond to a hardening/dynamic recovery format in the first term for $\dot{\underset{\sim}{\alpha}}$, as shown by Rousellier and Chaboche [33-34].

Note that the effect of damage is reflected by a multiplicative factor D and the product $\underset{\sim}{s}D$, for example, can be thought of as an effective stress for the viscoplastic deformation. As stated by Leckie [5-6] and viewed herein as a

tentative approximation, experiments show that the influence of the damage tensor on the creep rate is isotropic and monotonically increasing, even into the tertiary regime. This has been demonstrated even for materials which damage in a highly anisotropic manner [6]. In detailed experiments on intentionally perforated specimens, Murakami [2] has shown that the influence of cavity volume fraction on stress-strain response is isotropic for cavity fractions up to a few percent, a typical range for engineering alloys up to rupture. These results, of course, are necessary to admit scalar D to couple damage with the deformation response; obviously, D must be related to the mean value of the ω distribution, i.e.

$$D = \hat{D}(\Psi) \tag{25}$$

where Ψ is defined by

$$\Psi = \frac{1}{4\pi} \int_{A_u} \omega(\underset{\sim}{n})\, dA \tag{26}$$

Note that the effect of damage on the tertiary creep rate will remain unaltered upon rotation of the principal stress axes with this formulation as is experimentally observed [3-6].

A very useful recursion formula may be derived (see Appendix) by considering the mean value over the unit sphere of the damage rate distribution, i.e.

$$\dot{\Psi} = \eta\, \dot{\omega}(\underset{\sim}{n}^{(1)}) + \sum_{j=1}^{3} \frac{1}{(2P+3)} \left[\dot{\omega}(\underset{\sim}{n}^{(j)}) - \eta\, \dot{\omega}(\underset{\sim}{n}^{(1)}) \right] \tag{27}$$

with the initial (undamaged) condition $\Psi(0) = 0$, where

$$\dot{\omega}(\underset{\sim}{n}^{(j)}) = \xi(\sigma^*) \left[\eta \chi^{(1)} \left\{\Omega^{(1)}\right\}^{l(\sigma^*)} + (1-\eta) \chi^{(j)} \left\{\Omega^{(j)}\right\}^{l(\sigma^*)} \right] \qquad (28)$$

In the more general case of larger cavity volume fractions [2], we must define an appropriate effective stress $\underset{\sim}{S}^c$ derived from an operation of a fourth rank tensor $\underset{\sim}{\Upsilon}(\underset{\sim}{\phi})$ on the applied stress

$$\underset{\sim}{S}^c = \frac{1}{2} \left\{ \underset{\sim}{\Upsilon} : \underset{\sim}{\sigma} + (\underset{\sim}{\Upsilon} : \underset{\sim}{\sigma})^T \right\} \qquad (29)$$

where $\underset{\sim}{\Upsilon}(\underset{\sim}{\phi})$ may be expressed in terms of $\underset{\sim}{\phi}$ and its scalar invariants vis-à-vis the representation theorem for isotropic tensor functions [35]; the constants in this representation may be selected to fit experimental results. In addition, an effective backstress $\underset{\sim}{\alpha}^c$ must be analogously defined through a fourth rank tensor transformation; such a representation would obviously be quite complex, providing strong impetus for the aforementioned assumption of the isotropy of the damage effect on creep deformation. As pointed out by Chaboche, inclusion of damage in the viscoplastic potential would result in an additional damage coefficient which leads to volumetric inelastic strain. It should be noted that $\underset{\sim}{S}^c$ and $\underset{\sim}{\alpha}^c$ would replace $D\underset{\sim}{s}$ and $D\underset{\sim}{\alpha}$ in equations (21)-(24) in the case of large cavity fractions.

It should be mentioned that the elastic compliance is also affected by the presence of creep damage, although an explicit form for this dependence is not presented in this work. Let T be absolute temperature. Assuming the Helmholtz free energy density can be decomposed into elastic and viscous components [11,13],

$$\psi = \psi^e(\underset{\sim}{\varepsilon}^e, \underset{\sim}{\Gamma}, T) + \psi^v(\underset{\sim}{\alpha}, \kappa, K^*, \underset{\sim}{\Gamma}, T) \qquad (30)$$

along with $\underset{\sim}{\epsilon} = \underset{\sim}{\epsilon}^{e} + \underset{\sim}{\epsilon}^{n}$ leads to the thermoelastic relation

$$\underset{\sim}{\sigma} = \rho \frac{\partial \psi}{\partial \underset{\sim}{\epsilon}^{e}} \tag{31}$$

which obviously depends on the damage distribution through $\underset{\sim}{\Gamma}$.

The coupling of damage with two significantly different viscoplastic formulations is discussed next.

A. Rate-Dependent Bounding Surface Formulation: Type 304 Stainless Steel at 593°C

For the sake of completeness, experiments conducted at ORNL during the last contract period are again reported, along with the correlations of the anisotropic continuum damage theory.

For multiaxial cyclic plasticity, it has previously been demonstrated that a bounding surface approach [36-41] provides very good correlation of nonproportional deformation behavior. Since such behavior is of concern to nonproportional cyclic histories, a recently introduced [42] strain-hardening model based on a rate-dependent bounding surface with a Mroz translation rule for backstress is adopted. Key features of this theory include isotropic hardening reflected through growth of the bounding surface rather than a scalar parameter in the flow rule, and rate-dependence of the backstress evolution even at high strain rates. These features contrast with conventional unified creep-plasticity models (c.f. [25-32]). Rate-dependence is reflected primarily through bounding surface dependence on overstress, strain-hardening is reflected through growth of the bounding surface, and smooth yielding response is obtained through use of the Mroz distance vector in

the backstress hardening rate coefficient.

Briefly, the damage-coupled bounding surface model can be stated in multiaxial form as

$$\dot{\underset{\sim}{\epsilon}}^{n} = \frac{3}{2} K \langle \bar{\sigma} D - K_o \rangle^{n} \exp(Z \langle \bar{\sigma} D - K_o \rangle^{n+1}) \; (\underset{\sim}{s} - \underset{\sim}{\alpha})/\bar{\sigma} \tag{32}$$

where

$$\bar{\sigma} = [(3/2)(\underset{\sim}{s} - \underset{\sim}{\alpha}):(\underset{\sim}{s} - \underset{\sim}{\alpha})]^{1/2} = \sqrt{3/2} \; ||\underset{\sim}{s} - \underset{\sim}{\alpha}|| \tag{33}$$

$$\bar{\alpha} = [(3/2) \; \underset{\sim}{\alpha} : \underset{\sim}{\alpha}]^{1/2} \tag{34}$$

Here deviatoric stress $\underset{\sim}{s} = \underset{\sim}{\sigma} - (\sigma_{kk}/3)\underset{\sim}{I}$, backstress $\underset{\sim}{\alpha}$ is deviatoric, and we have defined $\kappa = K_o$ = constant. The inelastic strain $\underset{\sim}{\epsilon}^{n}$ includes both conventional creep and plastic strain as in other unified theories. The effective overstress and backstress are denoted as $\bar{\sigma}$ and $\bar{\alpha}$, respectively. The exponential term was proposed by Nouailhas [43] for description of high strain rate events.

The competition between hardening and static thermal recovery terms in the backstress rate equation is introduced in this bounding surface formulation in the following way:

$$\dot{\underset{\sim}{\alpha}} D = H(\bar{\alpha} D, \delta) \, ||\dot{\underset{\sim}{\epsilon}}^{n}|| \underset{\sim}{\nu} - R(\bar{\alpha} D) \underset{\sim}{\alpha} D \tag{35}$$

where

$$H(\bar{\alpha} D, \delta) = \beta_o + \beta_1 \exp\left(-\beta_4 \left\langle 1 - \beta_3 \left(\frac{\delta}{R^*}\right) \right\rangle^{\beta_5}\right) + \beta_2 \exp(-\beta_6 \bar{\alpha}^* D) \tag{36}$$

$$\delta = \sqrt{3/2} \; || \; \sqrt{2/3} \; R^* \underset{\sim}{N} - \underset{\sim}{s}|| \quad , \quad \underset{\sim}{N} = (\underset{\sim}{s} - \underset{\sim}{\alpha})/||\underset{\sim}{s} - \underset{\sim}{\alpha}|| \tag{37}$$

$$\bar{\alpha}^* = (R^* - \delta - \bar{\sigma}) \tag{38}$$

$$R(\bar{\alpha}D) = \beta_7 \exp(-\beta_8 \bar{\alpha}D) \ (\bar{\alpha}D)^{\beta_9} \tag{39}$$

It should be noted that in this particular formulation with the bounding surface fixed at the origin, the restriction $\delta > 0$ is enforced at a constant strain rate to avoid contact of the stress point with the bounding surface. This is achieved by driving the exponential term effectively to zero at a non-zero δ/R^* ratio. If the bounding surface were allowed to translate, this restriction would not apply; such a generalization is currently being carried out.

The specific form for $D(\Psi)$ selected for this model is

$$D(\Psi) = 1 + C \ \Psi^m \tag{40}$$

The radius of the bounding surface, R^*, evolves with accumulated plastic strain (creep hardening) and responds through the effective overstress to changes in inelastic strain rate to reflect the rate-dependence of the asymptotic state of $\underset{\sim}{\alpha}$, i.e.

$$R^* = \beta_{10} \ \rho \ [1 + \beta_{12} \ \bar{\sigma}^{\ \beta_{13}}] \tag{41}$$

where

$$\dot{\rho} = \beta_{11} \ (\rho_{mf} - \rho) \ \sqrt{2/3} \ ||\dot{\underset{\sim}{\epsilon}}^n|| \tag{42}$$

with initial condition $\rho(0) = \rho_0$. As seen in equation (41), this formulation clearly exhibits both viscous overstress and backstress effects, motivated by experiments which reveal a rate-dependent dislocation structures even at high strain rates.

The directional index for the backstress hardening rate is a rate-dependent

Mroz form

$$\underset{\sim}{\nu} = \left[\frac{\sqrt{2/3}\, R^{*}\, \underset{\sim}{N} - \underset{\sim}{s}}{\sqrt{2/3}\, \delta} \right] \tag{43}$$

The bounding surface and the surface of constant dimension K_0 which prescribes elastic response are shown in Fig. 1 along with the vector $\underset{\sim}{\nu}$ in deviatoric stress space. It should be noted that the damage effect D is applied to R^* in addition to tensorial stress quantities since R^* is related to the saturated or asymptotic value of stress [44].

In this formulation, $K, K_0, Z, n, C, m, \beta_0, \beta_1, \beta_2, \beta_3, \beta_4, \beta_5, \beta_6, \beta_7, \beta_8, \beta_9, \beta_{10}, \beta_{11}, \beta_{12}, \beta_{13}$, and ρ_{mf} are isothermal material constants. Non-isothermal generalization can be achieved primarily by invoking temperature dependence of the backstress recovery term [28] and some of the constants, although this is not necessary in the current isothermal work. Note that K_0 does not evolve, resulting in a domination of the inelastic response by evolution of the backstress. This feature allows the overstress tensor to properly model inelastic strain rate direction for rapidly changing nonproportional loading directions or for a departure from a previous loading path for which steady state creep conditions were reached as discussed by McDowell [42] and Lowe and Miller [45-46].

The hardening function which governs smooth transition from a very "stiff" region of backstress rate to an asymptotic response is the second term in equation (36) where the Mroz distance vector is normalized by bounding surface radius. Constants $\beta_1, \beta_4, \beta_5$, and β_3 govern this transition and are selected to match a monotonic, strain-controlled uniaxial test at a single strain rate in addition to a cyclic, strain-controlled uniaxial test at a single strain rate. The cyclic test is used primarily to determine β_3, which ensures that the normalization will be

satisfactory for both monotonic and cyclic behavior. Constant β_0 describes asymptotic response and constants β_2 and β_6 are employed in a second-order term to model the backstress level dependence of hardening rate observed experimentally when hardening dominates recovery. Constants ρ_{mf} and β_{11} introduce strain hardening into the model and can be determined either from a uniaxial monotonic or cyclic test. Constants β_{10},β_{12}, and β_{13} are determined from flow stress/strain rate sensitivity data at the temperature of interest; since strain rate sensitivity of R^* is directly related to that of stress in this model, these constants can be determined in a straightforward manner after the constants in the flow rule have been defined to fit a range of desired (observed) backstress behavior obtained from "dip" tests, multiaxial creep or cyclic plasticity experiments involving a sudden change in inelastic strain rate direction, etc. Constants C and m are determined by matching the integrated inelastic strain rate behavior with tertiary creep data.

It should be noted that this rate-dependent bounding surface work can be further generalized by inclusion of translation of the bounding surface. Work in progress at Georgia Tech has revealed the advantages of doing so.

Interrupted creep tests are generally necessary to assess exponent l at a given isochronous stress level; l can also be determined in an approximate way by periodically unloading from the creep curve [15-18] or by matching the integrated damage-coupled creep equations (32)-(43) with observed onset of tertiary response assuming m = 1 in equation (40). The value m = 1 arises from the Murakami study [2] mentioned earlier. Stress exponent k is easily identified as the slope of the $\log(t_R)$ vs. $\log(\sigma)$ curve obtained from uniaxial tests. Isotropic damage fraction η is identified as the ratio of the transverse damage to the longitudinal damage in a uniaxial test, and is identified by quantitative metallographic techniques described elsewhere [42].

At the isochronous stress level of this study, cavity growth is governed by

matrix power law creep. Hence, we define

$$\xi(\sigma^*) = B \left[\sigma^* \right]^k \tag{44}$$

Once k is known, coefficent B can be found at the isochronous stress level associated with l by integrating and matching rupture times from uniaxial tests with the assumed rupture criterion $\omega_{max} = 1$.

Tension-torsion tests were conducted at ORNL on thin-walled tubular specimens of type 304 stainless steel (ORNL Ref. heat 9T2796) at 593°C. The specimens were annealed in argon at 1093°C for 30 minutes, and were subsequently air cooled at >100°C/min to room temperature. Refer to Huddleston [19] for further experimental details.

For an isochronous stress of 176.1 MPa at 593°C, the constants are $B = 2.71 \times 10^{-28}$ sec^{-1} and l = 4.8. Units of stress and damage rate are MPa and sec^{-1}, respectively. Constants independent of isochronous stress include k = 8.5551 and $\eta = 0.61$. Quantitative evaluation of the grain boundary damage distribution for these biaxial experiments revealed that the damage distribution is suitably described by a second rank tensor [42] which sets P = 0. Exponent l was estimated by matching the tertiary response of uniaxial tests with the integrated damage-coupled creep equations.

The details may be found elsewhere [42] regarding the determination of the constants for the rate-dependent bounding surface model for type 304 stainless steel at room temperature. In summary, the material constants at 593°C for the damage-coupled creep-plasticity model are:

$K = 5 \times 10^{-48}$	$\beta_5 = 1.25$	$\beta_{12} = 0.225$
$K_o = 13.8$	$\beta_6 = 0.0196$	$\beta_{13} = 1.91$
$n = 30$	$\beta_7 = 1.552 \times 10^{-19}$	$\rho_{mf} = 517$
$\beta_0 = 1104$	$\beta_8 = -0.0207$	$\rho_o = 145$
$\beta_1 = 6.9 \times 10^6$	$\beta_9 = 5.088$	$C = 0.32$
$\beta_2 = 1044$	$\beta_{10} = 0.00361$	$m = 1$
$\beta_3 = 1.18$	$\beta_{11} = 7.0$	$Z = 0$
$\beta_4 = 23.16$		

where the units of stress are in MPa and time in sec.

The coordinate system employed for the stress analysis of the tubular specimens is shown in Fig. 2. Model predictions and experimental data for three different biaxial creep experiments are shown in Figs. 3-5. In these figures, inelastic axial and tensorial shear strain components are plotted versus time in addition to the axial and shear stress history. It is noted that the rupture time is generally well-predicted as is the inelastic strain upon initial loading and subsequent secondary and tertiary creep rates. The inelastic strain and rupture behavior is well-predicted for proportionally loaded specimen GT-1. The rupture time for specimen GT-4A is somewhat overpredicted for a simple nonproportional loading history, though the strain at rupture and the tertiary character are in reasonable agreement. The correlation obtained for GT-6, a somewhat complex creep-dominated cyclic loading history, is quite good. In all these experiments, the isochronous stress was held constant at 176.15 MPa and the principal stress directions were rotated at some point(s) in the loading history as shown in the figures.

B. Simple Power Law Creep: Pure Copper at 250°C

Trampczynski et al. [3-4] have conducted nonproportional loading experiments on commercially pure copper thin-walled tubular specimens at 250°C and have found in this case that damage is highly anisotropic, i.e. $\eta \simeq 0$. Both by metallurgical examination and by comparison of rupture times with uniaxial and proportional specimens at the same isochronous stress level, they concluded that damage accumulation in copper could be treated as highly decoupled with respect to several discrete loading directions in a nonproportional sequence history. It should be noted that Murakami and Ohno have applied their second rank tensor model to this data set as an approximation, although the physical damage distribution in this case is not accurately represented by a second rank tensor.

The grain boundary metallographs [3] indicate that the appropriate representation of grain boundary cracking at rupture in these specimens is fully anisotropic, $\eta = 0$, and that the deviation of damaged cavity facet normals about the maximum principal stress direction(s) is extremely small, i.e. $P > 0$. Since the maximum principal stress governs the fully anisotropic damage response in this case, $a = b = 0$ in the general isochronous stress form, i.e.

$$\sigma^* = \frac{3}{2} S_1 \tag{45}$$

For axial torsional loading of a thin-walled tube, $\sigma^* = \sigma_1$. The anisotropic damage rate equation may be written in this case as

$$\dot{\omega}(\underset{\sim}{n}) = \xi(\sigma^*) \sum_{j=1}^{3} \left\{\Omega^{(j)}\right\}^{l(\sigma^*)} \chi^{(j)} \left\{ \underset{\sim}{n}\cdot\underset{\sim}{n}^{(j)} \otimes \underset{\sim}{n}^{(j)}\cdot\underset{\sim}{n} \right\} \left\{ \underset{\sim}{n}\cdot\underset{\sim}{n}^{(j)} \right\}^{2P} \tag{46}$$

where again the cavity growth is dominated by matrix power law creep,

so that $\xi(\sigma^*)$ is defined as in equation (44). Since only one principal stress is tensile for this particular biaxial loading configuration,

$$\dot{\omega}(\underset{\sim}{n}) = B\,(\sigma_1)^k \left\{\Omega^{(1)}\right\}^{l(\sigma^*)} \chi^{(1)} \left\{ \underset{\sim}{n}\cdot\underset{\sim}{n}^{(1)} \otimes \underset{\sim}{n}^{(1)}\cdot\underset{\sim}{n} \right\} \left\{ \underset{\sim}{n}\cdot\underset{\sim}{n}^{(1)} \right\}^{2P} \tag{47}$$

$$\underset{\approx}{\zeta}^{(1)} = \left\{ \underset{\sim}{I} - \underset{\sim}{n}^{(1)} \otimes \underset{\sim}{n}^{(1)}\, \omega(\underset{\sim}{n}^{(1)}) \right\}^{-1} \tag{48}$$

$$\Omega^{(1)} = \left[\underset{\approx}{\zeta}^{(1)} : \underset{\approx}{\zeta}^{(1)} \right]^{1/2} = \left[\left[\frac{1}{1 - \omega(\underset{\sim}{n}^{(1)})} \right]^2 + 2 \right]^{1/2} \tag{49}$$

For copper, we choose to consider a less sophisticated constitutive model for the creep deformation. The coupling with damage for power law creep is given by

$$\dot{\underset{\sim}{\epsilon}}^{n} = \frac{3}{2} \left[\frac{\sigma_e D}{A} \right]^n \frac{\underset{\sim}{s}}{\sigma_e} \tag{50}$$

where D in this case is selected as

$$D = \left[1 + C\,\Psi^m\right]^{1/n} \tag{51}$$

although the form given earlier could also be used.

From Trampczynski et al. [3], n = 6.95. From Murakami and Ohno [1] and Trampczynski [3], k = 5.52 and l = 5.6. At the isochronous stress level to be considered in this study, a mean rupture time of 315 hours is expected for uniaxial creep conditions at 250°C. The constants A = 195, B = 1.913×10^{-14}, C = 3.0, and m = 6.0 were selected to provide the best fit to the secondary and tertiary response of the nonproportional biaxial history shown in Fig. 6 with the additional constraint that t_R = 315 hours for any proportional tension-torsion loading path. It should be noted that the units of stress and time are MPa and hours,

respectively, for the above set of constants. In this sense, the general shape of the tertiary response achieved by the theory shown in Fig. 6 is not truly predicted, although the rupture time is.

The value of P was selected as a significantly large integer to result in significant decoupling of the bimodal peaks of the damage distribution resulting from an occasional 33.7° rotation of the applied maximum principal stress as discussed by Trampczynski et al. [3]. As P increases, the damage distribution assumes a more highly anisotropic, directional character; as a consequence, the predicted rupture life increases for nonproportional loading histories. In the experiments on copper conducted by Trampczynski et al. [3], two maximum principal stress orientations were alternatively enforced at an angle of ±16.87° from the tube longitudinal direction. Hence, the tensile principal stress was periodically rotated within the plane of the specimen wall via change of the sign of the applied torque, though the principal stress magnitude was held fixed at 46.8 MPa.

In this work P = 6 was selected to ensure little interaction of the damage accumulated in the two directions, as physically observed. The experimental and theoretical results are compared in Figs. 6-7 for two nonproportional loading histories. In these plots, the engineering creep shear strain is plotted rather than the tensorial creep shear strain. Note the correlation offered by the theory, which exhibits the same general trends as the second rank tensor approach of Murakami and Ohno [1-2]. In these figures, the inelastic strain upon initial loading and the primary strain during the first loading event are eliminated from the presentation of the experimental data since the power law creep equation does not consider these components. No attempt was made, however, to eliminate the transient inelastic strains which occur at each subsequent loading reversal. This accounts for much of the error in creep strain evident in Fig. 7 for the complex loading history. This disagreement would not exist with an appropriately

sophisticated inelastic strain rate law, such as the one offered in the previous section. The life is reasonably well-correlated for both histories.

C. Compressive Biaxial Stress Ratios: Type 304 Stainless Steel at 593°C

Experiments were conducted at ORNL in 1986 in association with subcontract 19X-55966C in which a significant biaxial compressive stress ratio was present during all or part of the total rupture life of the thin-walled tubular specimens. The retardation of the creep damage rate associated with this type of loading was originally accounted for by multiplying the damage rate by the ratio of the maximum principal stress to minumum principal stress [42]. Such an approach, however, was not particularly meaningful from a physical viewpoint. It is desirable instead to include the effect through dependence of the isochronous stress σ^* on J_1 as described in equation (13). Huddleston's original formulation for σ^* was based on scant data in the negative J_1 regime. We show here that only a slight perturbation of his original formulation is necessary in the compressive biaxial stress ratio regime to acceptably describe the behavior of type 304 stainless steel at 593°C.

Using Huddleston's data [19] for a compressive biaxial stress ratio of -1.15 and the results of a proportional, constant load creep experiment performed under subcontract 19X-55966C (specimen GT-9) with a compressive biaxial stress ratio of -2.62 and a rupture time of 2952 hours, we can determine the constants in a power law expression

$$f(J_1) = C_1 \langle -J_1 \rangle^{C_2} \qquad (52)$$

by integrating the preceding damage rate formulation and matching the rupture times of these two experiments (with $\dot{1}$ = constant). This results in the values C_1 =

0.00434 and C_2 = 0.635. To see the influence of this modification on Huddleston's original formulation, a plot of both formulations appear for the same isochronous stress level, normalized to the uniaxial case, in Fig. 8. Note that the Rankine criterion is also plotted for reference. Clearly, the two formulations are nearly indistinguishable in the plot, even in the third quadrant, although they predict significantly different rupture times for negative J_1.

MODEL EXTENSIONS

(A) Aging Effects:

If the microstructure is unstable and aging effects such as precipitation or coarsening exist, it may be necessary to include these effects explicitly via description of precipitation/coarsening kinetics. This is true particularly for variable stress and/or temperature loading histories for which aging effects cannot be implicitly embedded in a set of isothermal, isostress material constants. Aging of type 304 stainless steel is manifested in the form of precipitation and growth of $M_{23}C_6$ carbides on grain boundaries, which may serve as void nucleation sites. Data regarding aging phenomena and associated effects on rupture life are often quite conflicting, however, with significant variability depending on heat treatment, processing, etc. Furthermore, little quantitative information exists regarding the mechanics representation of aging.

The function $\xi(\sigma^*)$ in equations (6)-(7) is based on the assumption of a fixed number of void nucleation sites and a stable microstructure. As discussed by Leckie and Onat [5], a separate evolution equation may be introduced for void

nucleation rate. The nucleation rate may be dependent on inelastic strain rate. Certainly, the void nucleation rate may be associated with intersections of slip bands with grain boundaries and with the precipitation of grain boundary carbides, so that inelastic rate of deformation and diffusion kinetics must both be considered.

Aging effects may be incorporated by adopting a formulation which employs time-dependent coefficients in the damage rate and inelastic strain rate equations, as motivated by the work of Cho and Findley [47-48]. In their work, the various inelastic strain components were made to depend on power law functions of aging time. Such an approach is phenomenologically based and may achieve acceptable correlation for variable stress and temperature histories. It may be desirable from a micromechanical viewpoint, however, to incorporate aging effects via evolution of a state variable or a set of state variables which represent physically distinct mechanisms. Mean precipitate size and spacing, for example, are logical candidate state variables for systems which exhibit unstable precipitation.

Obviously, aging is a diffusion-dependent phenomenon and should follow an Arrhenius dependence on absolute temperature. However, the nature of the possible coupling between aging rate and inelastic deformation, when such coupling exists, is not well-defined. If it is reasonably assumed that the rate of aging is somehow linked to cavity nucleation rate, one may embed aging effects in the damage rate equation. The following general framework is proposed for incorporation of aging effects in the damage rate equation:

$$\dot{\underset{\sim}{\Gamma}} = \xi(\sigma^*, \varsigma_i) \left[\eta \chi^{(1)} \left\{ \Omega^{(1)} \right\}^{l(\sigma^*)} \bigotimes_{i=1}^{P+1} \underset{\sim}{I} + \right. \tag{53}$$

$$\left. (1 - \eta) \sum_{j=1}^{3} \chi^{(j)} \left\{ \Omega^{(j)} \right\}^{l(\sigma^*)} \bigotimes_{i=1}^{2(P+1)} \left\{ \underset{\sim}{n}^{(j)} \right\} \right]$$

where ς_i for $i = 1,2,\ldots,M_\varsigma$ is a set of aging variables with rates specified by

$$\dot{\varsigma}_i = A_i \left[\bar{\varsigma}_i - \varsigma_i \right] \exp(-Q_i/kT) \tag{54}$$

$\bar{\varsigma}_i$ is the potential value of ς_i reached at long times, Q_i is the activation energy for the growth process of the i^{th} variable, k is Boltzmann's constant, and T is absolute temperature [55].

This type of approach collapses to that proposed by Cho and Findley [47-48] if a single state variable is employed, i.e. $M_\varsigma = 1$, and the influence of ς on damage rate coefficent ξ is multiplicative, i.e.

$$\xi(\sigma^*, \varsigma) = \hat{\xi}(\sigma^*) \left\{ -\ln[(\bar{\varsigma} - \varsigma)/(\bar{\varsigma} - \varsigma_0)] A_1^{-1} \exp(Q_1/kT) \right\}^{N_\varsigma} \tag{55}$$

where ς_0 is the initial value of ς and N_ς is a power law exponent. The reader may show by integration of equation (54) that the quantity within the curly brackets in equation (55) is merely time. Hence, equation (55) is a power law accountance for aging time. The purpose of writing it in the manner shown is to introduce an illustrative case where the state variable and aging time approaches are equivalent.

A simple form of the state variable approach or even the power law dependence on aging time in equation (55) should be sufficient for most alloys of interest, at least across a relatively small range of operating stresses and temperatures.

For type 304 stainless steel, $M_{23}C_6$ precipitation takes place in a temperature range from about 500°C to 950°C (932°F to 1742°F). It should be noted that exposure times in operating components will in general be much longer than in laboratory tests. Hence, even a slightly unstable microstructure may result in different creep-rupture properties in the operating component with the same initial heat treatment. One specific way to include carbide growth effects is through a multiplicative influence on the driving force, i.e.

$$\xi(\sigma^*, \varsigma) = \hat{\xi}(\sigma^*)\ Q(\varsigma_i) \tag{56}$$

where ς_i relate to, for example, carbide size and number of carbides. The function $Q(\varsigma_i)$ can reflect the void initiation-growth process through appropriate definition of ς_i and the corresponding evolution equation(s).

By reviewing Ashby and Raj's work [55], it may be suggested that a variable Ω represents the area fraction of grain boundary occupied by carbide precipitate and is derived from a set of two substate variables N_C and A_C which represent the number and size of carbides, respectively. By analogy to the nucleation and growth of voids, the rate of Ω depends on two physical processes, the rate of nucleation of new carbides, $\dot{N}_C$ (per unit area per second), and their rate of growth, $\dot{A}_C$ (area increase per carbide per second); $\dot{\Omega}$ is determined by properly combining these two qunatities.

Suppose at time $t = \tau$ the nucleation rate is $\dot{N}_C(\tau)$. Then the number of nuclei appearing in an increment of time $\delta\tau$ is $\dot{N}_C(\tau)\delta\tau$. At some later time t_f, each of

these has grown to an area expressed by

$$\int_{t=\tau}^{t=t_f} \dot{A}_c(t-\tau)\, d\tau \tag{57}$$

This means that the area fraction of boundary occupied by the nuclei that appeared at time τ is

$$\dot{N}_c(\tau)\ \delta\tau \int_{t=\tau}^{t=t_f} \dot{A}_c(t-\tau)\, dt \tag{58}$$

and the total area fraction covered by all carbides at the final time, t_f, is computed by convolution, i.e.

$$\Omega(t_f) = \int_{\tau=0}^{\tau=t_f} \dot{N}_c(\tau)\ \{\int_{t=\tau}^{t=t_f} \dot{A}_c(t-\tau)\, dt\}\, d\tau \tag{59}$$

Hence, Ω contains the history of nucleation an growth of grain boundary carbides; it should be noted that N_c and A_c can be employed as the pertinent set of internal variables if carbide size and spacing effects must be retained independently.

A suggested constitutive equation for nucleation rate $\dot{N}_c$ is

$$\dot{N}_c = K_c\ (N_{max} - N_c)\ \exp(-\frac{Q_1}{kT}) \tag{60}$$

where N_{max} is the total number of potential carbide nucleation sites, K_c is a material constant, and Q_1 is the activation energy of nucleation.

In addition to $\dot{N}_c$, we use the following growth rate $\dot{A}_c$ (coarsening equation)

proposed by Ashby and Raj [55]

$$\dot{A}_c = \left(\frac{C\sigma^*}{kT}\right)^{\alpha} t^{-\beta} \qquad (61)$$

where C is a material constant; Ashby and Raj suggest the values $\alpha = 2/3$ and $\beta = 1/3$ on the basis of physical arguments.

(B) Framework for Creep-Fatigue Interaction:

Numerous creep-fatigue approaches have been offered in the literature. Almost all of these approaches focus on uniaxial loading or treat multiaxial creep-fatigue damage as isotropic. In this work, we have generalized a continuum creep damage model for the case of multiaxial nonproportional loading. Though multiaxial fatigue formulations exist for proportional loading [49-50], no well-accepted theory exists for nonproportional loading. Hence, we can couch the interaction between creep and fatigue (and environment if necessary) at several different levels of sophistication.

The first approach is to use a uniaxial form of a fatigue damage rate equation. Lemaitre, Chaboche and associates have contributed significantly to the development of continuum fatigue damage approaches (c.f. [51]), but we do not believe that fatigue damage is aptly modeled as a continuum quantity. Rather, it is typified by a nonuniform spatial distribution of microcracks even in uniaxial loading. For the relatively ductile class of materials generally considered for high temperature applications in the power generation industry, e.g. type 304 stainless steel, the damage rate approach proposed by Majumdar and Maiya [52] is

very appealing. Since it is a rate approach, it is a logical companion for the continuum creep damage approach already presented. Following Majumdar and Maiya, the creep damage-coupled microcrack growth rate can be expressed as

$$\frac{1}{a}\frac{da}{dt} = \begin{bmatrix} T \\ C \end{bmatrix} (1 + \alpha \ln(\Psi/\Psi_o)) \, (\bar{\epsilon}_a^n)^{z_1} \, ||\dot{\underset{\sim}{\epsilon}}^n||^{z_2} \qquad (62)$$

where Ψ is defined in equation (26), and

a = current microcrack length

$\bar{\epsilon}_a^n$ = effective inelastic strain amplitude

T, C are coefficients for tensile and compressive stress, respectively, and

T, C, z_1, z_2 and α are temperature, environment, and microstructural dependent material parameters.

The quantity Ψ_o is a threshold limit for the mean value of creep damage at which interaction with fatigue damage may occur. Essentially, this formulation implies that voids nucleating and growing ahead of a propagating fatigue microcrack will accelerate the growth via coalescence ahead of the crack tip. Failure is defined either by equation (19) in creep or by attainment of a critical crack length, whichever occurs first. Note that the fatigue damage does not influence the creep damage rate, since creep damage is a bulk phenomenon in contrast to fatigue damage.

This approach has been successfully applied to creep-fatigue lifetime prediction of the austenitic stainless steels [52] and Cr-Mo-V steels [53].

The next level of sophistication at which a fatigue damage rate equation may be written includes the effect of multiaxial strain state on microcrack propagation. For example, it is now widely known [49-50,56-57] that critical plane theories

based on the maximum range of shear strain and the mean strain or stress across these planes correlates with fatigue crack initiation under combined stress states much more accurately than theories based on effective strain amplitudes. Hence, we may write the damage rate equation as

$$\frac{1}{a}\frac{da}{dt} = \begin{bmatrix} T \\ C \end{bmatrix} (1 + \alpha \ln(\Psi/\Psi_o)) \, (\epsilon^*)^{z_1} \, ||\dot{\underset{\sim}{\epsilon}}^n||^{z_2} \tag{63}$$

where Ψ, as before, is defined in equation (26), and

$$\epsilon^* = \frac{\Delta\gamma^*}{2} + z_3 \, \Delta\epsilon^* \tag{64}$$

is a combination of the inelastic shear strain range on a "critical" plane, $\Delta\gamma^*$, and the normal strain range across this plane, $\Delta\epsilon^*$. If the critical plane is defined as that corresponding to the maximum range of inelastic shear strain (e.g. [49,56]), then

$$\frac{\Delta\gamma^*}{2} = \max_{\text{all } \underset{\sim}{n}} \frac{\Delta\gamma}{2} = \frac{\Delta\gamma(\underset{\sim}{n}^*)}{2} \tag{65}$$

$$\Delta\epsilon^* = \Delta(\underset{\sim}{n}^* \cdot \underset{\sim}{\epsilon}^n \cdot \underset{\sim}{n}^*) \tag{66}$$

where $\underset{\sim}{n}^*$ is the unit vector normal to the plane(s) of maximum inelastic shear strain range.

Rather than selecting $\Delta\epsilon^*$ as a modifying influence, it may be more appropriate to use the stress range and/or mean stress normal to the plane of maximum inelastic shear strain range. Similar critical plane approaches exist which differentiate fatigue crack initiation on the basis of orientation of the critical plane(s) with respect to the surface. It should be noted that this sort of critical plane

approach, in any form, has been verified to a significant extent only for proportional loading; more experimental work is necessary to characterize fatigue under nonproportional cyclic loading.

At the highest level of complexity, a fatigue damage tensor could be constructed which would inherently include the orientation and length of microcracks. Obviously, though, the interaction rules for fatigue and creep damage rates would be difficult to assess in an anisotropic context; furthermore, the notion of fatigue damage as a continuum quantity is suspect in most cases since it is surface localized. An exception might be microcrack propagation along heavily cavitated internal grain boundaries.

(C) More General Cavity Growth Mechanisms:

It is in general desirable to generalize the creep damage rate equation (6) to conform with the relevant operative mechanisms for cavity growth at a given temperature and isochronous stress level. For example, cavity growth mechanism maps have been constructed for some materials (c.f. [21]) to delineate this temperature and stress dependence. At stresses typical of applications but lower than those usually employed in laboratory experiments, for example, it may be necessary to account for coupled grain boundary diffusion-power law creep [20-22] mechanisms. For this study, however, the isochronous stress level selected is within the domain of power law creep. Hence, a power law dependence of damage growth rate on isochronous stress appears in equation (44).

There are fundamentally two distinct approaches for accounting for stress- and temperature-dependent cavity growth mechanisms. Let us discuss here the isothermal case only, in keeping with the format of the theory already presented. In the

first approach, one may refer to a cavity growth mechanism map to determine which regime is applicable, then adjust the parameters in $\xi(\sigma^*)$ and the functional form of $\Omega^{(j)}$ to phenomenologically account for the influence of cavity growth mechanism on damage rate and, hence, rupture time. The work of Cocks and Ashby [22] serves as a useful guide for perhaps a more micromechanically-based approach for generalization to other cavity growth regimes. In their work, the actual form of the dependence on the stress and current level of damage depends on the operative cavity growth mechanism. Furthermore, they compare the approach with that of a Kachanov continuum damage model, thereby establishing a means of incorporation of their ideas in the current framework when creep damage is predominately in the form of voids. Discussion of these comparisons can be found in reports written under Martin Marietta subcontracts 19B-07802C and 19X-55966C.

Drawing from the work of Raj, Ashby and Cocks, it may be possible to generalize predominately uniaxial, isotropic concepts of void nucleation and growth rates in terms of the present anisotropic model.

It should also be mentioned that there are some materials for which dislocation debris arrangement and attendant voids in the vicinity of barriers are associated with creep rupture rather than classical void growth. For such materials, it may be necessary to tie the creep damage rate more intimately to cumulative creep deformation rather than cavity growth associated with normal stresses. In this case, according to Leckie [54], it may be desirable to interpret the damage variable or tensor in terms of the immobile dislocation density at barriers rather than an area fraction of voids on grain boundaries. It is likely that such creep damage mechanisms would require dependence on the inelastic strain, rather than isochronous stress, and perhaps details of the stress state.

As previously mentioned, the formulation of the damage rate coefficient in

equation (44) is based on the assumption of a single cavity growth mechanism, cavity growth on grain boundaries governed by power law creep of the matrix. It is well known, however, that the cavity growth mechanisms, and hence rate of growth, are both temperature and stress level dependent. The micro-mechanical viewpoint has been very useful in assesing the grain boundary void growth rate under constrained and unconstrained conditions as a function of macroscopically applied stress and creep strain rate [20-22,55].

Cocks and Ashby [22] showed that the growth of voids can be controlled by boundary diffusion, by surface diffusion, by power law creep, or by a coupling between diffusion and power law creep. Voids usually grow by diffusion when they are small, but matrix power law creep takes over as the dominant growth mechanism as they become larger: this coupling of mechanisms must be taken into account in calculating damage. In this case, the driving force for damage growth should reflect the linear dependence of diffusive void growth rate on stress as well as the nonlinear stress dependence associated with matrix power law creep. Boundary diffusion generally predominates surface diffusion owing to higher diffusivity along grain boundaries. A possible general form for the damage evolution equation would be

$$\begin{aligned}\dot{\underset{\sim}{\Gamma}} = B[(\sigma^*)^k g_1] \Bigg[\eta\, \chi^{(1)} \left\{\Omega^{(1)}\right\}^{l(\sigma^*)} \bigotimes_{i=1}^{P+1} \underset{\sim}{I} + \\ (1-\eta) \sum_{j=1}^{3} \chi^{(j)} \left\{\Omega^{(j)}\right\}^{l(\sigma^*)} \bigotimes_{i=1}^{2(P+1)} \left\{\underset{\sim}{n}^{(j)}\right\} \Bigg] \\ + A[\sigma_1 g_2] \Bigg[\eta_d \chi^{(1)} \bigotimes_{i=1}^{P+1} \underset{\sim}{I} + \end{aligned} \tag{67}$$

$$(1 - \eta_d) \sum_{j=1}^{3} \chi^{(j)} \overset{2(P+1)}{\underset{i=1}{\otimes}} \left\{ \underset{\sim}{n}^{(j)} \right\} \Bigg]$$

where

$$g_1 = \hat{g}_1(\sigma^*, \Omega^{(j)})$$

$$g_2 = \hat{g}_2(\sigma^*, \Omega^{(j)})$$

Here, g_1 and g_2 are represent the fuctional dependence of damage rate on stress and damage for the power law creep and boundary diffusion cases, respectively. The parameters B, k and A must of course vary in accordance with the stress-temperature regimes on a cavity growth mechanism map. Factors η and η_d pertain to the fraction of isotropic damage for power law matrix creep and boundary diffusion dominated cavity growth, respectively. Next we consider explicit forms for g_1 and g_2.

(i) Boundary Diffusion

When growth is controlled by boundary diffusion alone, matter diffuses out of the growing voids and plates onto the grain boundary. The void remains spherical because surface diffusion rapidly redistributes matter within it. By reviewing Cocks and Ashby's work, the isotropic damage rate equation is shown to be

$$\dot{\psi} = \dot{\epsilon}_o \frac{\phi_o}{\psi^{1/2} \ln(1/\psi)} \left[\frac{\sigma_1}{\sigma_o} \right] \tag{68}$$

where ψ is a scalar damage parameter, $\dot{\epsilon}_o$ and σ_o are material constants, and ϕ_o depends on grain boundary diffusivity, i.e.

$$\phi_o = \frac{2D_b \delta_b V \sigma_o}{kTL^3 \dot{\epsilon}_o} \tag{69}$$

where D_b is the grain boundary diffusion coefficient, δ_b is the grain boundary thickness, V is the atomic volume and 2L is the center-to-center void spacing. Note that the other components of local stress field (σ_2,σ_3) have no significant influence on void growth by this mechanism. In equation (69), k is Boltzmann's constant.

When ψ approaches unity, we may write

$$\psi^{1/2} \ln(1/\psi) \simeq (1 - \psi) \tag{70}$$

and the damage rate equation becomes

$$\dot{\psi} = A \sigma_1 \left[\frac{1}{1 - \psi}\right] \tag{71}$$

(ii) Coupled Case

Coupling boundary diffusion with power law creep, we can express the functions g_1 and g_2 as

$$g_1 = 1 \tag{72}$$

$$g_2 = \frac{\phi_o'}{\Psi^{1/2} \ln(1/\Psi)} \tag{73}$$

where

$$\phi_o' = \frac{D_b \delta_b}{L^3} \tag{74}$$

and the ratio (A/B) depends on position on the cavity growth mechanism map. In equation (73), Ψ is defined as in equation (26). When the stress level is high, for example, $A > B$. The opposite is true for high temperature and low stress levels.

Note that exactly the same concept holds when void growth is governed by both surface diffusion and power law matrix creep. Although the diffusion equation is approximate, the coupled damage rate equation is inherently a more complete description than only power law matrix creep (e.g. $g_2 = 0$) over a wide range of stress and temperature levels.

As a final remark, it should be emphasized that the damage rate equation approach has essentially concentrated on the growth of grain boundary voids, and the void nucleation process has not been explicitly treated. Equation (53) employs the tacit assumption that void nucleation is included via introduction of state variables for aging. However, if the actual cavity nucleation rate, $\dot{N}_V$, were known, one could convolute the integration in time, i.e.

$$\underset{\sim}{\Gamma}(t_f) = \int_{\tau=0}^{t_f} \dot{N}_V(\tau) \left[\int_{t=\tau}^{t_f} \xi[\sigma^*(t-\tau), \Omega^{(j)}(t-\tau)]\{ \ldots \}\, dt \right] d\tau \tag{75}$$

In this case, constitutive equations must be introduced for $\dot{N}_V$, e.g.

$$\dot{N}_v = f_c(N_c, A_c)\ \dot{N}_c + f_\epsilon(||\dot{\underset{\sim}{\epsilon}}^n||, N_c, A_c)\ ||\dot{\underset{\sim}{\epsilon}}^n|| \qquad (76)$$

such that both carbide nucleation and slip band intersection with grain boundaries and/or carbides contribute to the void nucleation rate. Of course, the parameters of coefficient function ξ would have to be determined by performing the integration of equation (75) and comparing with experiments once equation (76) is specified.

CONCLUSIONS

The work performed in the current funding period has served to further enhance the anisotropic creep damage approach developed in earlier contract work. A damage distribution with even symmetry has been introduced on the unit sphere which evolves in rate form as a symmetric tensor of rank necessary to match physically measured damage distributions. The approach is motivated by the treatment of even rank tensor distributions forwarded by Leckie and Onat [5-6], and contains as a subset the specific tensorial definitions of damage adopted in the anisotropic theories of Chaboche (rank four) [13,18,24] and Murakami and Ohno [1-2] (rank two).

A general form of coupling with damage has been suggested for an internal variable inelasticity framework and specific forms have been investigated for type 304 stainless steel at 593°C and pure copper at 250°C with the assumption of small cavity volume fractions. Good correlation of rupture time, secondary creep, and tertiary creep has been obtained for proportional and nonproportional, isothermal, constant isochronous nominal stress loading histories for both mildly and highly anisotropically creep damaging materials. A formula has been derived for the

evolution of the mean value of damage on the unit sphere which offers computational simplification. A modification of Huddleston's isochronous stress has been introduced for more accurate correlation of compressive biaxial principal stress ratios.

A state variable approach has been offered for inclusion of aging effects; the approach effectively reduces to a time hardening formulation for special choices of the internal variable(s), but has the flexibility to include additional complexity.

A coupling of the anisotropic creep damage approach with a fatigue damage rate equation has been proposed, along with a multiaxial generalization of the strain-based fatigue approach which has been validated for proportional strain cycling.

Finally, the distinct processes of matrix power law creep and boundary diffusion governed cavity growth have both been included as driving forces for damage growth, the relative contribution of each process dependent on the current stress-temperature regime on a cavity growth mechanism map.

REFERENCES

1. Murakami, S., and Ohno, N., "A Continuum Theory of Creep and Creep Damage," Creep in Structures, IUTAM, 1980, pp. 422-444 (Eds. Ponter and Hayhurst).
2. Murakami, S., "Notion of Continuum Damage Mechanics and its Application to Anisotropic Creep Damage Theory," ASME J. of Engineering Materials and Technology, Vol. 105, April 1983, pp. 99-105.
3. Trampczynski, W. A., Hayhurst, D.R., and Leckie, F.A., "Creep Rupture of Copper and Aluminum Under Non-Proportional Loading," J. Mech. Phys. Solids, Vol. 29, No. 5/6, 1981, pp. 353-374.
4. Trampczynski, W. A., and Hayhurst, D.R., "Creep Deformation and Rupture Under Non-Proportional Loading," Creep in Structures, IUTAM, Eds. Ponter and Hayhurst, 1980, pp. 388-405.
5. Leckie, F. A., and Onat, E. T., "Tensorial Nature of Damage Measuring Internal Variables," Physical Non-Linearities in Structural Analysis, IUTAM, 1980, pp. 140-155 (Eds. Hult and Lemaitre).
6. Leckie, F. A., "The Constitutive Equations for High Temperatures and Their Relationship to Design," Proc. Int. Conf. on Constitutive Laws for Engineering Materials, Eds. Desai and Gallagher, Univ. of Arizona, Tucson, Jan. 1983, p. 93.
7. Duvaut, C., "Analyse Fonctionnelle - Mèchanique des Milieu Continus-Homogénéisation", Theoretical and Applied Mechanics, North-Holland, Amsterdam, 1976.
8. Kachanov, L., Fundamental of Fracture Mechanics, Nauka, Moscow, 1974.
9. Rabotnov, Y. N., Creep Problems in Structural Members, Amsterdam, North Holland Publishing Co., 1969.
10. Krajcinovic, D., "Creep of Structures - A Continuous Damage Mechanics Approach," J. Structural Mechanics, 11(1), 1983, pp. 1-11.
11. Krajcinovic, D., and Fonseka, G.U., "The Continuous Damage Theory of Brittle Materials," Parts 1 and 2, ASME J. Appl. Mech., Vol. 48, 1981, pp. 809-824.

12. Costin, L. S., and Stone, C. M., "Implementation of a Finite Element Damage Model for Rock," in Constitutive Laws for Engr. Materials: Theory and Applications, Vol. II, Eds. Desai, Krempl, Kiousis and Kundu, Tucson, Arizona, USA, 1987, pp. 829-840.
13. Chaboche, J. L., "Continuum Damage Mechanics: Present State and Future Trends," ONERA T.P. n°1986-53, Séminaire International sur l'Approche Locale de la Rupture, Moret-sur-Loing, June 3-5, 1986.
14. Chow, C. L., and Wang, J., "An Anisotropic Theory of Elasticity for Continuum Damage Mechanics," Int. J. Fracture, 33, 1987, pp. 3-16.
15. Chaboche, J. L., "Continuous Damage Mechanics - A Tool to Describe Phenomena Before Crack Initiation," Nuclear Engr. and Design, Vol. 64, 1981, pp. 233-247.
16. Lemaitre, J., and Chaboche, J. L., "Aspect Phénoménologique de la Rupture par Endommagement," J. de Mécanique Appliquée, Vol. 2, No. 3, 1978, pp. 317-365.
17. Lemaitre, J., and Chaboche, J. L., "A Non-Linear Model of Creep-Fatigue Damage Cumulation and Interaction," Mechanics of Visco-Plastic Media and Bodies, Ed. Jan Hult, Springer, Berlin, 1975, pp. 297-301.
18. Chaboche, J. L., "Le Concept de Contrainte Effective Appliqué a l'élasticité et a la Viscoplasticité en Présence d'un Endommagement Anisotrope," Coll. Euromech. 115, Grenoble, 1979 (CNRS, 1982).
19. Huddleston, R. L., "An Improved Multiaxial Creep-Rupture Strength Criterion," ASME J. Pressure Vessels and Piping, Paper 84-PVP-106, 1984.
20. Miller, D. A., and Langdon, T. G., "Independent and Sequential Cavity Growth Mechanisms," Scripta Metallurgica, Vol. 14, 1980, pp. 143-148.
21. Svensson, L. E., and Dunlop, G. L., "Mechanisms for the Growth of Intergranular Creep Cavities," Creep in Structures, IUTAM, 1980, pp. 445-462 (Eds. Ponter and Hayhurst).
22. Cocks, A.C.F., and Ashby, M.F., "On Creep Fracture by Void Growth," J. Progress in Materials Science, Vol. 27, 1981, pp. 189-245.
23. Woodford, D.A., "Creep Damage and the Remaining Life Concept," ASME J. Engr. Materials and Technology, Vol. 101, Oct. 1979, pp. 311-316.

24. Chaboche, J. L., "Anisotropic Creep Damage in the Framework of Continuum Damage Mechanics," Nucl. Engr. Des., 79, 1984, pp. 309-319.
25. Pugh, C. E., and Robinson, D.N., "Some Trends in Constitutive Equation Model Development for High-Temperature Behavior Model Development for High-Temperature Behavior of Fast-Reactor Structural Alloys," Nuc. Engr. and Design, Vol. 48, 1978, pp. 269-276.
26. Krieg, R. D., Swearengen, J. C., and Rohde, R. W., "A Physically-Based Internal Variable Model for Rate-Dependent Plasticity," Inelastic Behavior of Pressure Vessel and Piping Components (Eds. Chang and Krempl), PVP-PB-028, ASME, 1978, pp. 15-28.
27. Lagneborg, R., "A Modified Recovery-Creep Model and its Evaluation," Metal Science Journal, Vol. 6, 1972, pp. 127-133.
28. Miller, A., "An Inelastic Constitutive Model for Monotonic, Cyclic, and Creep Deformation," ASME J. of Engineering Materials and Technology, Vol. 98, 1976, pp. 97-113.
29. Ponter, A.R.S., and Leckie, F.A., "Constitutive Relationships for the Time-Dependent Deformation of Metals," J. Eng. Mat. and Technology, Trans. ASME, Volume 98, 1976.
30. Hart, E.W., "Constitutive Relations for Non-Elastic Deformations of Metals," J. Eng. Mat. and Technology, Trans. ASME, Volume 98, 1976.
31. Chan, K.S., Bodner, S.R., Walker, K.P., and Lindholm, U.S., "A Survey of Unified Constitutive Theories," Proc. 2nd Symp. on Nonlinear Constitutive Relations for High Temperature Applications, NASA Lewis Research Center, June 13-15, 1984.
32. Walker, K. P., "Research and Development Program for Nonlinear Structural Modeling with Advanced Time-Temperature Dependent Constitutive Relationships," NASA Report CR-165533, NASA Lewis RC, Nov. 1981.
33. Chaboche, J. L., and Rousselier, G., "On the Plastic and Viscoplastic Constitutive Equations- Part I: Rules Developed With Internal Variable Concept," ASME J. Pressure Vessel Technology, Vol. 105, 1983, pp. 153-158.
34. Chaboche, J. L., and Rousselier, G., "On the Plastic and Viscoplastic Constitutive Equations- Part II: Application of Internal Variable Concepts to the 316 Stainless Steel," ASME J. Pressure Vessel Technology, Vol. 105, 1983, pp. 159-164.

35. Wang, C. C., "A New Representation Theorem for Isotropic Functions: An Answer to Professor G. F. Smith's Criticism of My Paper on Representations for Isotropic Functions," Arch. Rat. Mech. Anal., Vol. 36, 1970, pp. 198-223.
36. Dafalias, Y.F., and Popov, E.P., "A Model of Nonlinearly Hardening Materials for Complex Loading," Acta Mechanica, Vol. 21, 1975, pp. 173-192.
37. Dafalias, Y.F., "The Concept and Application of the Bounding Surface in Plasticity Theory," Physical Non-Linearities in Structural Analysis, Eds. J. Hult and J. Lemaitre, IUTAM Symposium, Senlis, France, Springer Verlag, 1981, pp. 56-63.
38. Tseng, N.T., and Lee, G.C., "Simple Plasticity Model of the Two-Surface Type," ASCE Journal of Engineering Mechanics, Vol. 109, No. 3, June 1983, pp. 795-810.
39. Mroz, Z., "An Attempt to Describe the Behaviour of Metals Under Cyclic Loads Using a More General Workhardening Model," Acta Mechanica, Vol. 7, 1967, pp. 199-212.
40. McDowell, D. L., "A Two Surface Model for Transient Nonproportional Cyclic Plasticity: Part 1," ASME J. Applied Mechanics paper No. 85-APM-9, 1985.
41. McDowell, D. L., "A Two Surface Model for Transient Nonproportional Cyclic Plasticity: Part 2," ASME J. Applied Mechanics Paper No. 85-APM-10, 1985.
42. McDowell, D. L., Ho, K. I., and Stalley, J., "An Anisotropic, Damage-Coupled Viscoplastic Model for Creep-Dominated Cyclic Loading," presented at Third Int. Symp. on Nonlinear Fracture Mech., Knoxville, TN, Nov. 1986.
43. Nouailhas, D., "A Viscoplastic Modelling Applied to Stainless Steel Behavior, " in Constitutive Laws for Engr. Materials: Theory and Applications, Vol. II, Eds. Desai, Krempl, Kiousis and Kundu, Tucson, Arizona, USA, 1987, pp. 717-724.
44. McDowell, D. L., and Moosbrugger, J. C., "A Rate-Dependent Bounding Surface Model," work in progress, 1987.

45. Lowe, T. C., and Miller, A. K., "Improved Constitutive Equations for Modeling Strain Softening- Part I: Conceptual Development," ASME J. Engr. Materials and Technology, Vol. 106, 1984, pp. 337-342.
46. Lowe, T. C., and Miller, A. K., "Improved Constitutive Equations for Modeling Strain Softening- Part II: Predictions for Aluminum," ASME J. Engr. Materials and Technology, Vol. 106, 1984, pp. 343-348.
47. Cho, U.W., and Findley, W.N., "Creep and Creep Recovery of 304 Stainless Steel at Low Stresses with Effects of Aging on Creep and Plastic Strains," ASME J. Appl. Mech., Vol. 48, 1981, pp. 785-790.
48. Cho, U.W., and Findley, W.N., "Creep and Plastic Strains of 304 Stainless Steel at 593°C Under Step Stress Changes, Considering Aging," ASME J. Appl. Mech., Vol. 49, 1982, pp. 297-304.
49. Brown, M.W., and Miller, K.J., Low-Cycle Fatigue and Life Prediction, ASTM STP 770, ASTM, 1982, pp. 482-499.
50. Lohr, R.D., and Ellison, E.G., Fatigue of Engineering Materials and Structures, Vol. 3, 1980, pp. 1-17.
51. Lemaitre, J., and Plumtree, A., "Application of Damage Concepts to Predict Creep-Fatigue Failures," ASME J. Engr. Matls. Tech., Vol. 101, 1979, pp. 284-292.
52. Majumdar, S., and Maiya, P.S., "A Mechanistic Model for Time-Dependent Fatigue," ASME J. Engr. Matls. Tech., Vol. 102, 1980, pp. 159-167.
53. Priest, R.H., and Ellison, E.G., "An Assessment of Life Analysis Techniques for Fatigue-Creep Situations," Res Mechanica, Vol. 4, 1982, pp. 127-150.
54. Leckie, F.A., "Modelling of High-Temperature Microstructural Damage," presented at the 1987 ASME Applied Mech., Bioengr. and Fluids Engr. Conf., Cincinnati, OH, June 1987.
55. Ashby, M.F., and Raj, R., "Creep Fracture," Cambridge University, paper 16, 1975.
56. Kandil, F.A., Brown, M.W., and Miller, K.J., "Biaxial Low-Cycle Fatigue Fracture of 316 Stainless Steel at Elevated Temperatures," Book 280, The Metals Society, London, 1982, pp. 203-210.
57. Fash, J.W., Socie, D.F., and McDowell, D.L., "Fatigue Life Estimates for a Simple Notched Component Under Biaxial Loading," Multiaxial Fatigue, ASTM STP 853, ASTM, Philadelphia, 1985, pp. 497-513.

APPENDIX

In this appendix, the derivation leading to equation (27) is detailed. Consider first the case of a finite number, e.g. two, principal stress orientations in a given loading history. Also suppose that the damage is purely anisotropic, i.e. $\eta = 0$. For such cases in which a finite number of primary loading configurations are known a priori, we may analytically carry out the determination of Ψ. Define the two maximum principal stress directions as

$$\underset{\sim}{n}_I^{(1)} = a_I \, \underset{\sim}{e}_1 + b_I \, \underset{\sim}{e}_2 \tag{A1}$$

$$\underset{\sim}{n}_{II}^{(1)} = a_{II} \, \underset{\sim}{e}_1 + b_{II} \, \underset{\sim}{e}_2 \tag{A2}$$

where $\underset{\sim}{e}_1$ and $\underset{\sim}{e}_2$ are orthogonal unit vectors in the tube longitudinal and circumferential directions, respectively, as shown in Figure 2. Since $\eta = 0$, we may write $\omega(\underset{\sim}{n})$ as

$$\omega(\underset{\sim}{n}) = \underset{\sim}{n} \cdot [\, \omega(\underset{\sim}{n}_I^{(1)}) \, (\underset{\sim}{n} \cdot \underset{\sim}{n}_I^{(1)})^{2P} \, \underset{\sim}{n}_I^{(1)} \otimes \underset{\sim}{n}_I^{(1)} + \omega(\underset{\sim}{n}_{II}^{(1)}) \, (\underset{\sim}{n} \cdot \underset{\sim}{n}_{II}^{(1)})^{2P} \, \underset{\sim}{n}_{II}^{(1)} \otimes \underset{\sim}{n}_{II}^{(1)} \,] \cdot \underset{\sim}{n} \tag{A3}$$

and $\omega(\underset{\sim}{n}_\varsigma^{(1)})$ is given for ς = I, II by integration of equation (6) when the principal stress is in the ς orientation, i.e.

$$\dot{\omega}(\underset{\sim}{n}_{\varsigma}^{(1)}) = B\ (\sigma_1)^k \left[2 + \frac{1}{\left[1 - \omega(\underset{\sim}{n}_{\varsigma}^{(1)})\right]^2} \right]^{1/2} \qquad \text{(A4)}$$

The mean value of $\omega(\underset{\sim}{n})$ may be determined by a formal integration over the unit sphere carried out in spherical coordinates θ and ϕ (radius = 1) as

$$\Psi = \frac{2}{4\pi} \int_0^{2\pi} \int_0^{\pi/2} \omega(\hat{\underset{\sim}{n}}(\theta,\phi))\ \sin\phi\ d\phi\ d\theta \qquad \text{(A5)}$$

where $\underset{\sim}{n} = \hat{\underset{\sim}{n}}(\theta,\phi) = \cos\phi\ \underset{\sim}{e}_1 + \sin\phi\ \cos\theta\ \underset{\sim}{e}_2 + \sin\phi\ \sin\theta\ \underset{\sim}{e}_3$

Here, θ is taken positive counterclockwise from the positive $\underset{\sim}{e}_2$ direction to the projection of $\underset{\sim}{n}$ on the $\underset{\sim}{e}_2$- $\underset{\sim}{e}_3$ plane and ϕ is the angle between the $\underset{\sim}{n}$ and $\underset{\sim}{e}_1$ directions. By substitution of the two damage distributions indicated in equation (A4),

$$\Psi = \frac{1}{2\pi} \int_0^{2\pi} \int_0^{\pi/2} \sum_{\varsigma=1}^{2} W_{\varsigma}\ \sin\phi\ d\phi d\theta \qquad \text{(A6)}$$

where

$$W_{\varsigma} = \omega(\underset{\sim}{n}_{\varsigma}^{(1)})\ [a_{\varsigma}\cos\phi + b_{\varsigma}\sin\phi\cos\theta]^{2(P+1)} \quad , \qquad \text{(A7)}$$

we arrive, with the benefit of the identity $(a_{\varsigma}^2 + b_{\varsigma}^2) = 1$, at the simple recursion relation

$$\Psi(P) = (2P + 3)^{-1} \left[\omega(\underset{\sim}{n}_I^{(1)}) + \omega(\underset{\sim}{n}_{II}^{(1)}) \right] \qquad \text{(A8)}$$

which precludes the need for numerical integration to determine Ψ for any P in this case. It is interesting to note that if P = 0, the two ω distributions are each equivalent to that of a symmetric second rank tensor, and $\Psi(0)$ is simply the sum of the hydrostatic components of each tensor.

A great computational aid is offered if a general rate expression may be found for Ψ, the mean value of $\omega(\underset{\sim}{n})$ over the unit sphere. In particular, such an expression would eliminate the need to perform numerical integration at each time step over the surface of the unit sphere. In addition, the resolution of the discrete representation of $\omega(\underset{\sim}{n})$ on the unit sphere could be dramatically coarsened since the accuracy of numerical integration for Ψ would not be an issue; the discretization of the unit sphere (i.e. the finite number N of $\omega(\underset{\sim}{n}_N)$ values) would be left to consideration of the accuracy of the damage growth equation only.

This generalization is readily achieved by noting that the recursion formula stated in equation (A8) may be generalized by the superposition of an arbitrary number of anisotropic damage distributions for which $\eta = 0$, i.e.

$$\Psi(P) = (2P + 3)^{-1} \left[\omega(\underset{\sim}{n}_I^{(j)}) + \omega(\underset{\sim}{n}_{II}^{(j)}) + \ldots \right] \qquad \text{(A9)}$$

Recognizing that this relation applies to the anisotropic component of the damage rate distribution given in equation (6) and that the isotropic component of the distribution is equivalent to its mean value over the unit sphere, we may write the general expression which appears in equation (27).

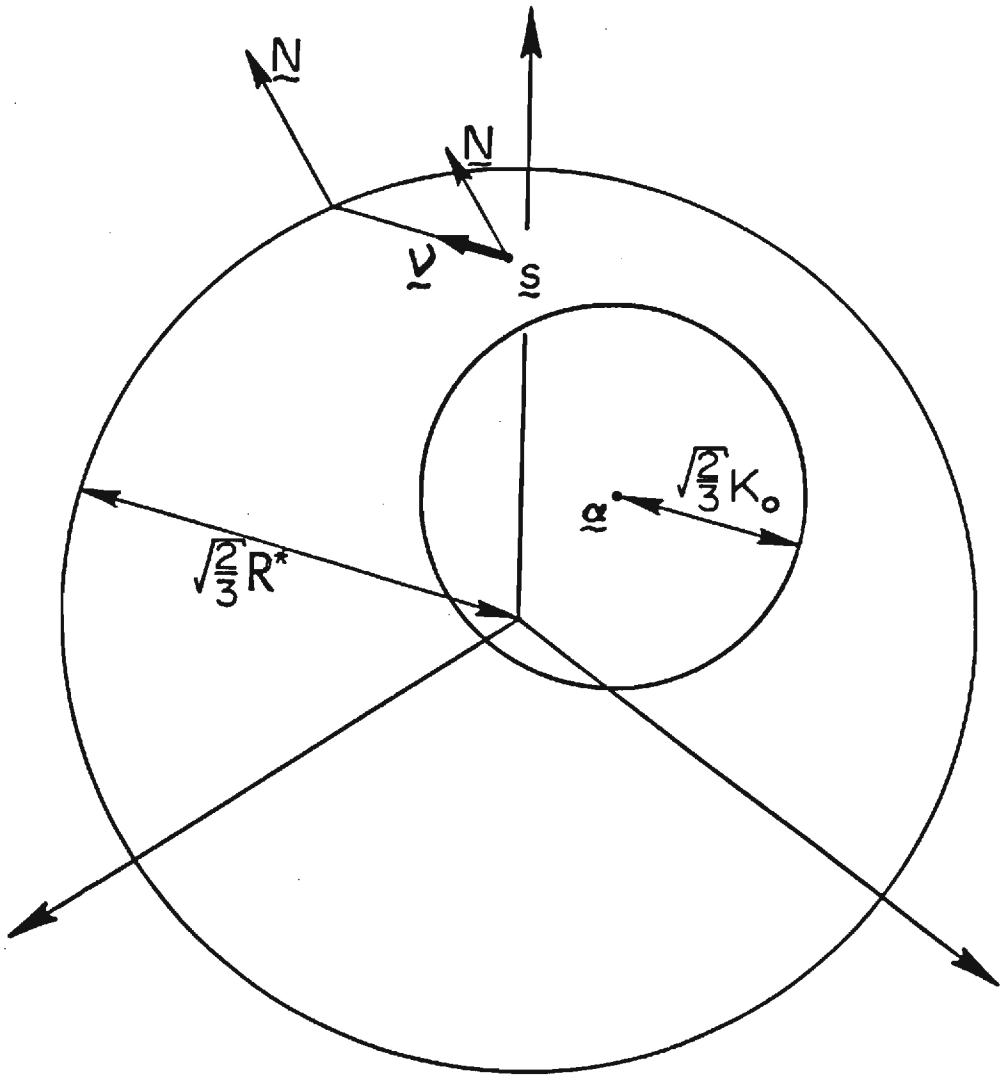

FIG. 1- Bounding and loading surfaces in deviatoric stress space.

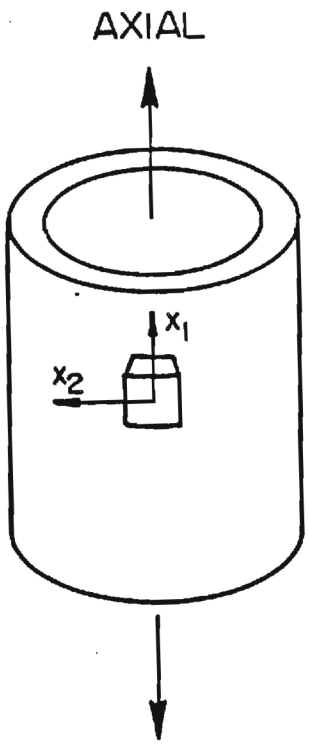

FIG. 2- Coordinate system for the thin-walled tubular tension torsion specimen; x_1 and x_2 are the axial and circumferential coordinates, respectively, at the specimen mid-plane.

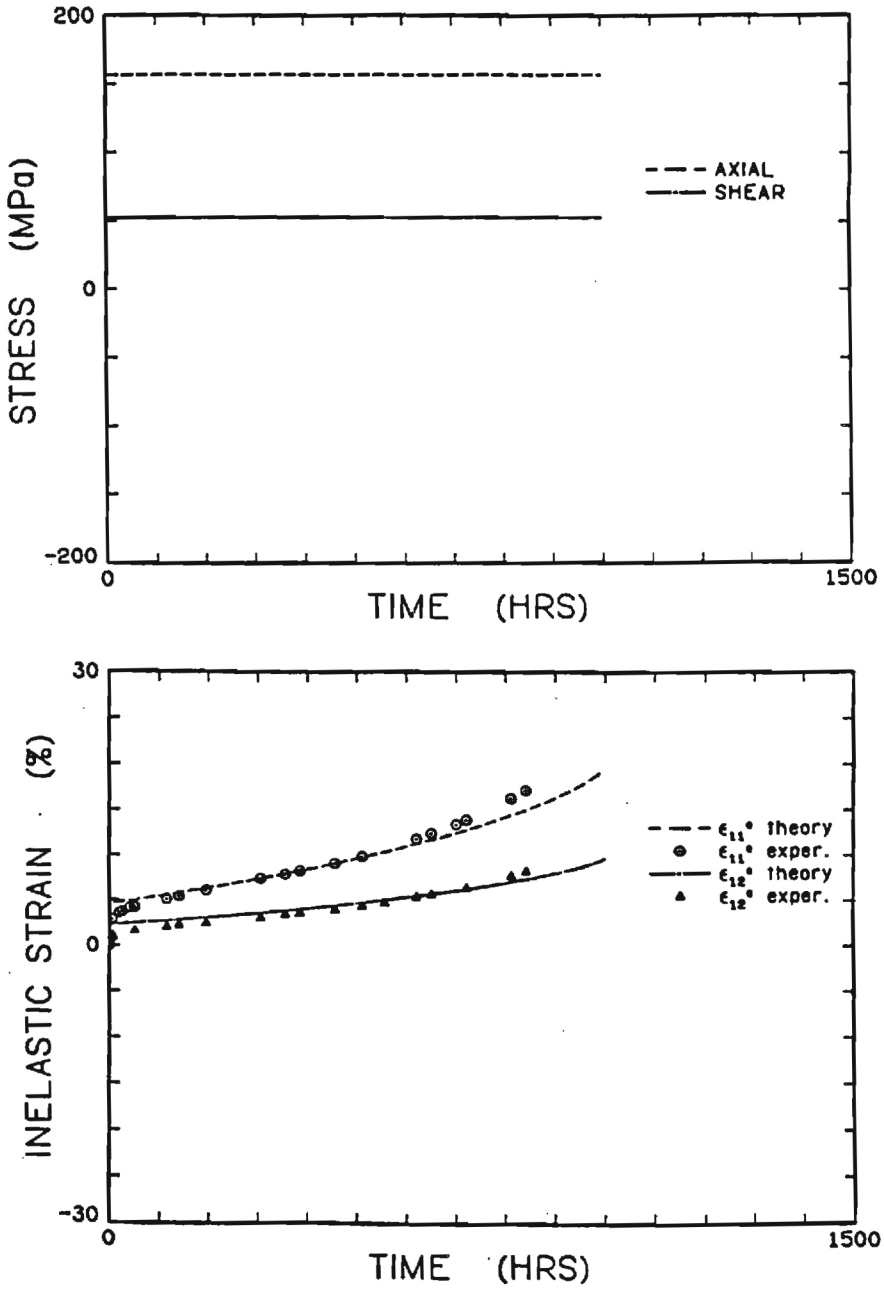

FIG. 3- Type 304 stainless steel at 593°C: applied biaxial nominal stress history (top) and predicted versus experimental inelastic strains (bottom) for specimen GT-1. Actual and predicted rupture times are 892 hr and 998 hr, respectively.

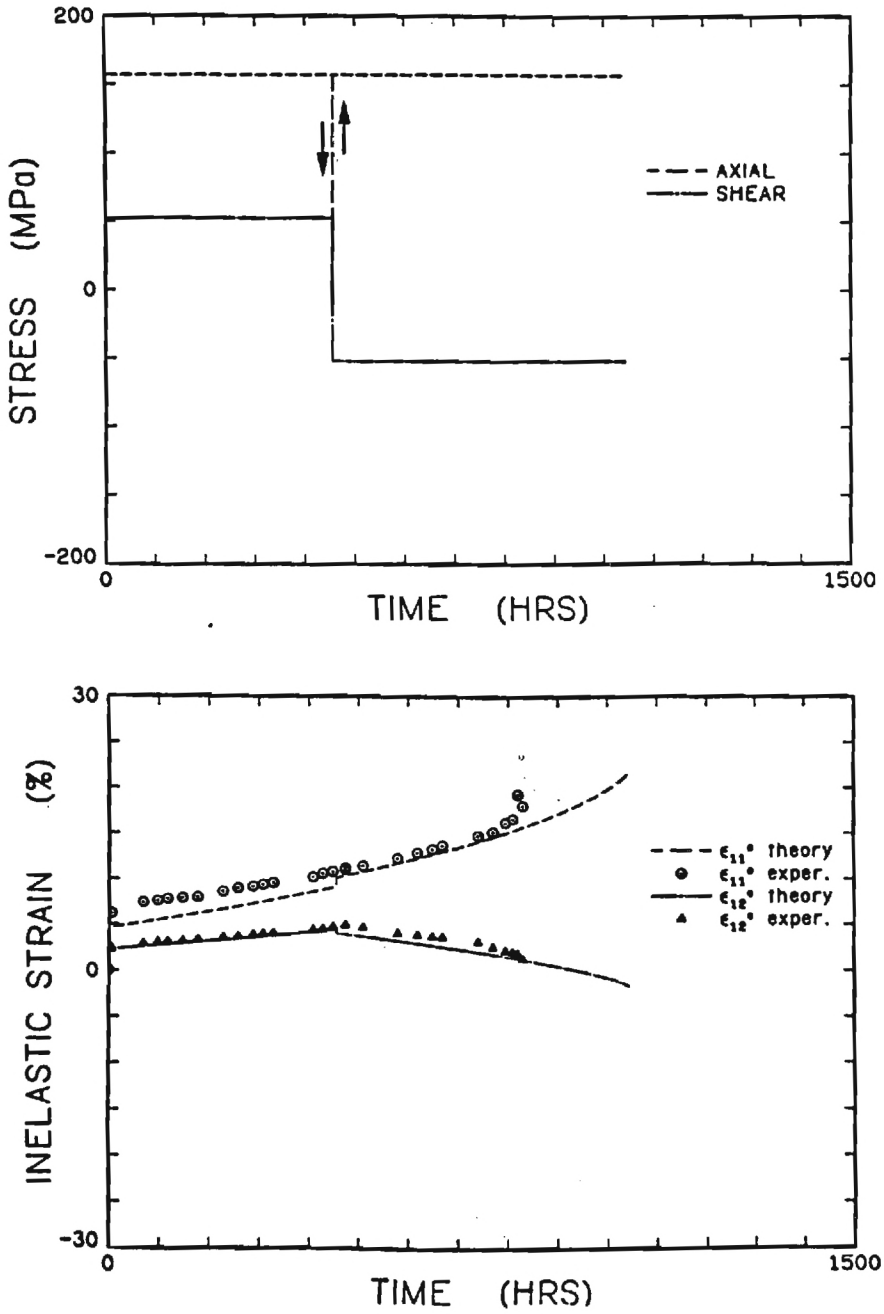

FIG. 4- Type 304 stainless steel at 593°C: applied biaxial nominal stress history (top) and predicted versus experimental inelastic strains (bottom) for specimen GT-4A. Actual and predicted rupture times are 851 hr and 1043 hr, respectively.

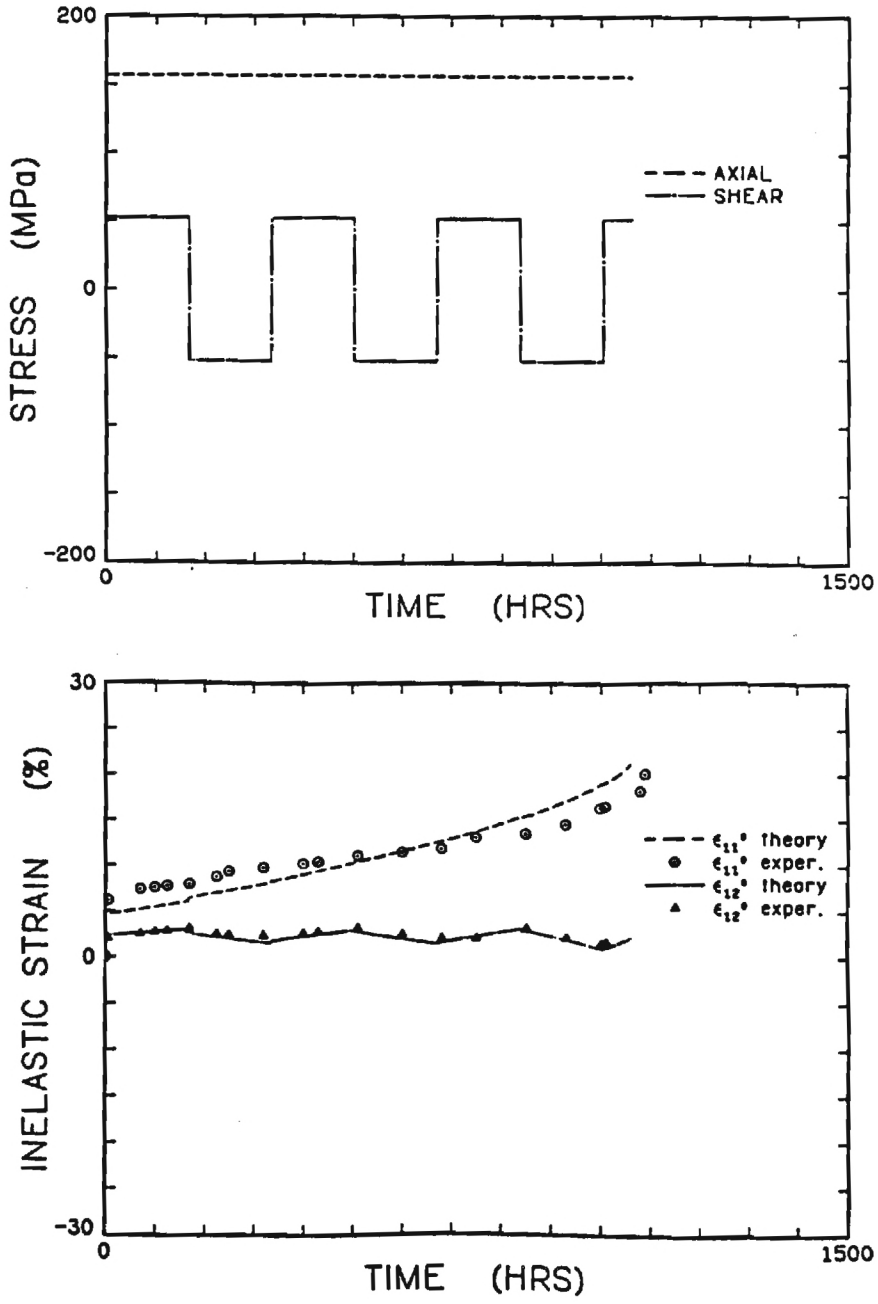

FIG. 5- Type 304 stainless steel at 593°C: applied biaxial nominal stress history (top) and predicted versus experimental inelastic strains (bottom) for specimen GT-6. Actual and predicted rupture times are 1088 hr and 1060 hr, respectively.

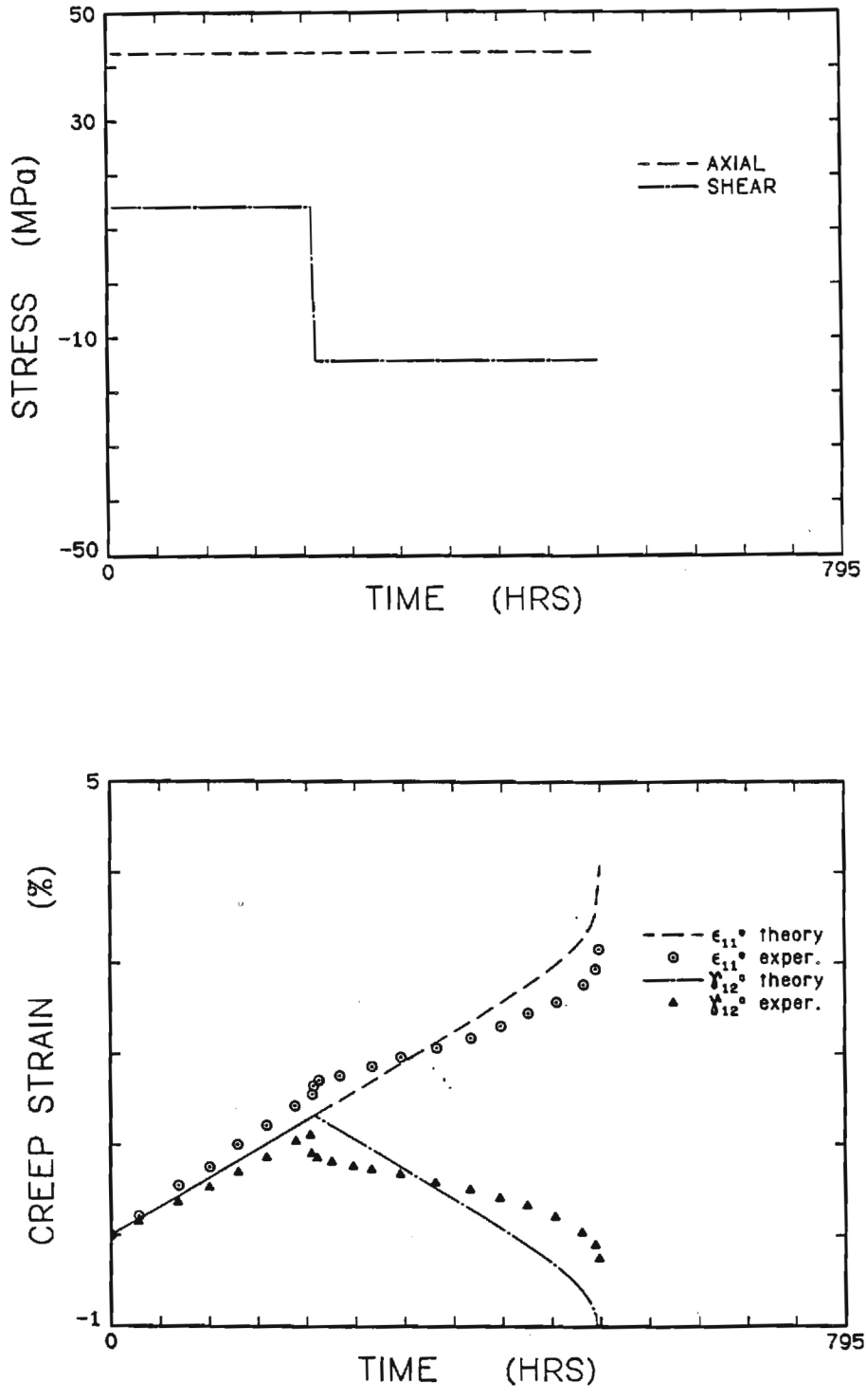

FIG. 6- Copper at 250°C: applied biaxial nominal stress history (top) and predicted versus experimental [3] creep strains (bottom) for a history with a single reversal.

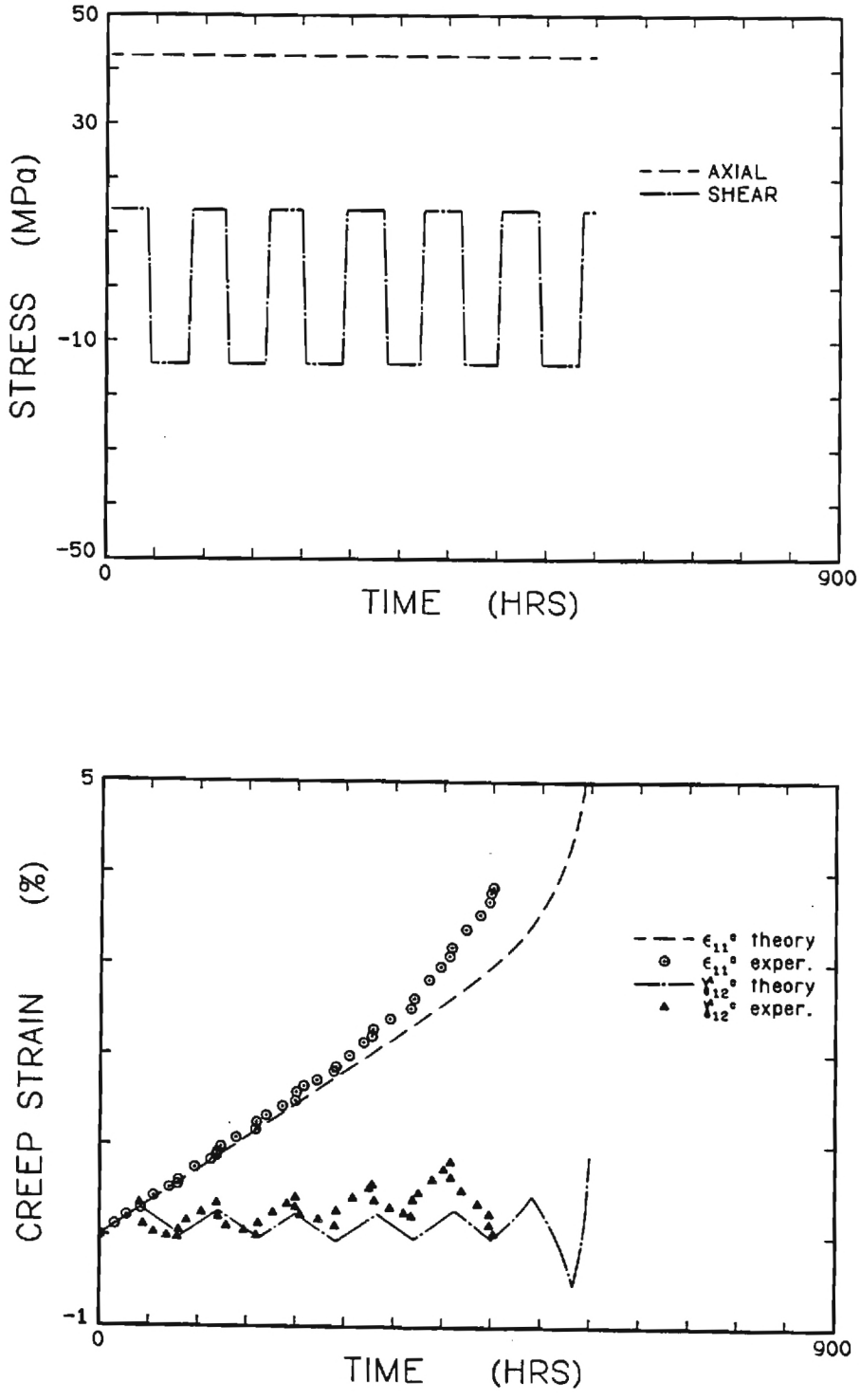

FIG. 7- Copper at 250°C: applied biaxial nominal stress history (top) and predicted versus experimental [3] creep strains (bottom) for a history with multiple reversals.

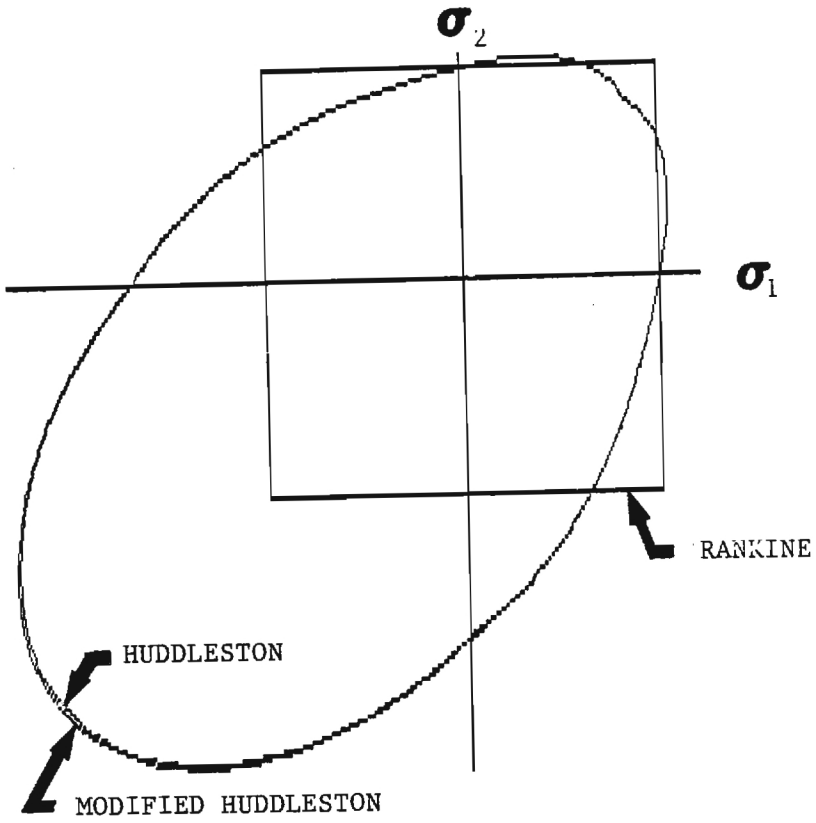

FIG. 8- Normalized plots of the isochronous stress surface of Huddleston [19] and the current formulation for type 304 stainless steel at 593°C in the biaxial σ_1-σ_2 space (σ_3 = 0).